THE UNIVERSITY OF MICHIGAN
COLLEGE OF ENGINEERING
Department of Engineering Mechanics ⌄

Final Report

WIDE-TEMPERATURE-RANGE SPRINGS

H. Gascoigne
J. H. Enns
P. Kessel

J. Ormondroyd, Project Supervisor

ORA Project 02879

FOREWORD

This report was prepared by The University of Michigan under USAF Contract No. AF 33(616)-6284. The contract was initiated under Project No. 9-(8-7360), "Study of Materials Criteria for Precision High Temperature Springs," Task No. 73605. The work was administered under the direction of the Directorate of Materials and Processes, Deputy for Technology, Aeronautical Systems Division, with Mr. Richard R. Rowland acting as Project Engineer.

This report covers work conducted from 1 February 1959 to 30 September 1961.

ABSTRACT

Bimetallic spring systems of 40% nickel-60% iron alloy combined with Inconel X and type 304 stainless steel exhibit characteristics suitable for applications from -65°F to 600°F. In this range the spring constant is held within ±0.25%.

The general theory of bimetallic, temperature independent helical coil and Belleville type springs is presented. The bimetallic systems tested show that a temperature independent spring is feasible although working stresses must be maintained at relatively low levels.

PUBLICATION REVIEW

This report has been reviewed and is approved.

FOR THE COMMANDER:

RICHARD R. ROWLAND
Chief, Applied Mechanics Section
Metals and Ceramics Laboratory
Directorate of Materials and Processes

TABLE OF CONTENTS

Page

TABLE OF CONTENTS (Concluded)

LIST OF ILLUSTRATIONS

LIST OF ILLUSTRATIONS (Continued)

LIST OF ILLUSTRATIONS (Concluded)

LIST OF SYMBOLS AND DEFINITIONS

k spring constant or spring rate usually expressed in pounds per inch of deflection (lb/in.)

k_O reference spring constant taken at 70°F, unless otherwise stated, lb/in.

k_e equivalent spring constant (lb/in.)

G shear modulus of material, lb/in.^{2}

G_O reference shear modulus taken at 70°F, unless otherwise stated, lb/in.^{2}

T temperature, °F

m_G thermoelastic coefficient based on shear modulus defined as

$$m_G = \frac{1}{G_O} \frac{\Delta G}{\Delta T}, \quad °F^{-1}$$

m_k thermoelastic coefficient based on spring constant of individual spring defined as

$$m_k = \frac{1}{k_O} \frac{\Delta k}{\Delta T}$$

α coefficient of linear thermal expansion defined as

$$\alpha = \frac{1}{l_O} \frac{\Delta l}{\Delta T}, \quad °F^{-1}$$

where l_O is a reference length, dimensionless length ratio.

σ normal stress, lb/in.^{2}

μ Poisson's ratio

τ shear stress, lb/in.^{2}

ϵ normal strain, in./in.

d coil spring wire diameter, in., derivative

n number of active coils in helical coil spring

P   force exerted on spring, lb.

δ   over-all spring compression, in.

$\overline{D}$ mean coil diameter of spring

$\overline{R}$ mean coil radius of spring = $\overline{D}/2$

c   spring index defined as c = $\overline{D}/d$

t   time, linear dimension

E   Young's modulus of elasticity

$e = \dfrac{1}{E}\dfrac{\Delta E}{\Delta T}$ thermoelastic coefficient of Young's modulus, $^\circ F^{-1}$

I. INTRODUCTION

The problem of the wide-temperature-range spring, of prime importance to the aircraft industry in fuel-control systems, has been a subject of research for many years. One of the early studies, supported by the National Advisory Committee for Aeronautics, by Keulegan and Houseman at the National Bureau of Standards (NBC Research Paper No. 531, 1933), was on thermoelastic coefficients of spring-type alloys. The temperature range that they covered was -60° to +120°F.

The temperature range proposed by the Aircraft Control Industry for this project was -65° to +1000°F, with an upper limit of +450°F as a first objective. These limits have been primary guides to this program, along with the understanding that, whatever the system, it must be simple and of a physical size within the realm of the usual coiled type of spring. Also, because elastic strain in general tends to change to plastic strain at elevated temperatures, the relaxation properties of the system must remain realistic.

Three main ideas were considered at the beginning of this study, all intended to counter the loss in material stiffness with temperature rise: (a) a change in the geometry of cross section of an elliptic tube due to thermal pressures created by the fluid within; (b) a bimetallic system utilizing differences in linear thermal expansion; and (c) a multi-material system utilizing positive and negative thermoelastic materials.

The geometric approach, (a), was considered analytically and turned out to be quite difficult. No satisfactory solution was derived which related the internal fluid pressure to dimension changes in the principal axes of tubular cross section. All experimental evidence indicated that the wall thickness required to give an effective change in cross section with the stipulated thermal pressure changes were too thin to support any appreciable load. Therefore this phase of the program was discontinued.

For (b), a simple, bimetallic-thermal expansion device in the form of a cantilever beam was analyzed. Such a system cannot result in a temperature-independent spring rate unless one of the two materials has a positive thermoelastic coefficient, because the thermoelastic coefficients for ordinary spring-type alloys are about ten times larger than their thermal expansion coefficients. The stiffening effect derived from thermal expansion is thus not sufficient to compensate for the loss in stiffness due to two materials with negative thermoelastic coefficients.

For (c), while for many years it has been known that certain iron-nickel alloys in the ferromagnetic state have a positive thermoelastic coefficient, nothing in the literature indicated that such alloys have been applied to the

problem of the wide-temperature-range spring. Certain alloys of this family, such as Ni-Span C, have been developed with a thermoelastic coefficient of zero over the temperature range -60° to +120°F. No spring-type alloy seems to be available whose isoelastic behavior goes past 200°F. However, in the above iron-nickel series, alloys with positive thermoelastic coefficients of a much wider temperature range are known. Thus the combination of plus and minus materials to achieve a constant spring rate over a wider temperature range seemed logical. The investigation of such systems in coiled and Belleville spring form became the major effort of this project.

Nonmetallic materials with anomalous thermoelastic properties, such as graphite, glasses, and ceramics were investigated as discussed in the next section. It was concluded that, while their thermoelastic behavior might be very promising, their structural properties are insufficient.

II. THERMOELASTIC PROPERTIES OF SPRING-TYPE MATERIALS

The elastic stiffness constants of solids vary inversely with atomic spacing, and almost all solid metals expand on heating; thus, roughly speaking, thermal expansion results because it is easier to increase interatomic spacing than to decrease it. The observed decrease in the elastic moduli with increasing temperature is hence to be expected for all such metals. These properties appear so basic that it is hard to conceive what could account for a vanishing or even negative expansion coefficient of some solid materials.

Materials known to vary from the above basic behavior of differing degrees are pure graphite, certain glasses, and the ferromagnetic alloys. The negative thermal expansion coefficients of graphite goes well beyond 1000°F, and from this standpoint graphite would be a most promising material. However, the maximum permissible stresses for pure graphite are far below those of the usual spring-type metals. Since the energy-storage capacity of springs is an important practical parameter, and the energy stored is proportional to the square of the stress, springs made from any known graphite material would be prohibitive in size. Future study of materials among which graphite is an important component may result in a practical spring material. This aspect was not considered further.

A. GLASS AND CERAMIC SPRINGS

The feasibility of glass or ceramic springs was investigated for this project by Dr. E. B. Shand, of Corning, New York. Dr. Shand is a technical consultant and author on this subject. The following is a short summary of his investigation.

The silica network in the glass structure tends to produce a modulus of elasticity which increases with temperature. As modifying ions are introduced into the composition, the modulus increasingly tends to droop with rising temperature. By suitable choice of composition, an aluminosilicate glass—Corning No. 1723—has been produced whose Young's modulus increases linearly from about 11.8×10^6 psi at 75°F to 11.9×10^6 psi at 1150°F. Over the same temperature range the rigidity modulus increases from about 4.7×10 to 4.8×10^6 psi. Poisson's ratio for this glass is given as 0.234 to 0.242.

The elastic moduli of ceramic materials tend to decrease with temperature. A particular ceramic called Mullite is the most stable. Its Young's modulus decreases from about 20.6×10^6 to 20×10^6 psi over the same 1000°F temperature rise.

From the structural standpoint, both materials are brittle and hence ex-

tremely notch-sensitive. Ordinarily reported working stresses are of little
value since the flow level is so important, and this differs widely for dif-
ferent specimens. Also, these materials are very sensitive to impact loading
because they are so brittle. The over-all effect results in a fairly low per-
missible working stress compared to the metal alloys.

Analysis shows that energy stored in a unit volume of spring is the prod-
uct of the specific resilience of the material and the efficiency of loading.
Specific torsional resilience is given by $\tau^2/2G$, and is the criterion of the
material for torsion-spring applications. τ is taken to be the permissible
working shear stress and G, the rigidity modulus. An approximate computation
shows that a coil spring, 1 in. OD and 3 in. long, made from a material of
specific resilience of 10 in.-lb/in.^{3}, can store roughly 4.5 in.-lb of energy.
For a spring rate of 40 lb per in. deflection, the maximum spring load will
be slightly under 20 lb.

For the above-mentioned aluminosilicate glass, a specific torsional re-
silience of 20 in.-lb/in.^{3} is considered reasonable up to about 750°F. At
1000°F (probably because of relaxation behavior), this value would have to
be greatly reduced.

For ceramics, available data on breaking stresses for the conditions
here considered are entirely inadequate, according to Dr. Shand. He estimates
that the specific resilience may range from 12 to 20 in.-lb/in.^{3}

At room temperature the specific resilience of good metal springs is
about 160 in.-lb/in.^{3} However, this too has to be decreased according to the
maximum operating temperature, and so the 8:1 unfavorable volume ratio of
metal to glass quoted by Dr. Shand would actually become much less. A basic
materials study of glasses and ceramics with the intent of gaining in spring-
like properties should be considered in any new program on wide-temperature-
range springs.

B. FERROMAGNETIC ALLOY SPRINGS

The thermoelastic properties of the Ni-Fe system has been reported by W.
Koster (1) from 100% Ni down to 28% Ni, with the remainder as Fe. A number
of Young's modulus E vs. temperature T curves from his paper are shown in
Fig. 1. The range of positive thermoelastic coefficient ($e = \frac{1}{E}\frac{dE}{dT}$) below the
Curie temperature (the temperature at which a ferromagnetic material becomes
paramagnetic, indicated by arrow) is to be noted. The Ni-Fe alloys whose
spring data are reported on below were selected with Fig. 1 as a guide.

The region of positive slope in these curves is generally explained as
due to the fact that here ferromagnetic contraction exceeds thermal expansion.
The known isoelastic alloys derived from the Ni-Fe system by the addition of
minor constituents fails to meet the isoelastic temperature range of present
interest. An example of this is Ni-Span C, of composition 42% Ni, 2.5% Ti,

4

5.5% Cr, .03% C and the rest Fe. The manufacturer of this material considers its isoelastic range only between -58°F and +122°F. By comparison the 40% Ni-60% Fe curve of Fig. 1 shows a region of positive slope extending over about 450°F. Achieving an effective isoelastic range of 450°F from this material combined with an ordinary spring-type alloy with negative thermoelastic properties seems to be a direct possibility. Nothing in the literature indicates that this approach has been investigated. Bimetallic spring systems of this type, both in helical and Belleville form, were studied in this program and the results are reported in III-D and IV-F.

III. HELICAL COIL COMPRESSION SPRINGS

A. INTRODUCTORY DISCUSSION

To use the positive thermoelastic coefficient of the ferromagnetic alloys previously mentioned, the type of mechanical spring best suited to experimental studies had to be selected. Although torsion-bar springs are easy to test using a torsion pendulum with an associated furnace for elevated-temperature and a cold chamber for low-temperature testing, we wanted to use a more common type of spring: either or both helical coil and Belleville-type springs. The BGR Division of the Associated Spring Corporation, located in Plymouth, Michigan, agreed to fabricate any springs which might be required, and to give technical assistance during the duration of the project.

We found the existing literature insufficient, and in some cases contradictory, regarding thermoelastic data (modulus variation with temperature), and therefore decided to determine experimentally the variation in shear modulus with temperature of materials possibly suited to spring applications. Since the spring constant of coil springs with relatively low coil pitch angle is proportional to the shear modulus, such data are necessary for proper analysis of a bimetallic spring system. The dynamic shear modulus-temperature variation of 15 materials was determined using a torsion pendulum, with the results reported in this section.

As a result of the torsion-pendulum tests, 40% nickel-60% iron alloy, Inconel X and 304 stainless steel were the materials selected for detailed evaluation. Next, several coil springs were fabricated and tested statically to see if the results agreed with those previously obtained by a dynamic test. The general trend of modulus variation was the same with the exception that the thermoelastic coefficients were substantially different. This result has been found in previous work (2), and although not at first considered critically important, came to be regarded very seriously as the work progressed.

To determine the thermoelastic coefficient required in coil-spring calculations, several sets of springs were tested in which the spring index and number of active coils were varied to see if there was a dependence on the geometry of the spring. One possible reason for such a dependence is that the stress distribution in the cross section of the wire varies with the spring index. This dependence was substantiated only in the 40% nickel alloy and it is relatively slight.

Finally, on the basis of the results of tests on individual springs, coaxial (parallel) spring systems were designed, fabricated, and tested. Each spring combination tested resulted in a system in which the spring con-

7

stant remained essentially constant over a temperature range far greater than any single-alloy spring presently commercially available. The limited amount of relaxation testing indicated no serious problems below 500°F, but considerably more relaxation testing should be done.

B. DYNAMIC SHEAR MODULUS OF SELECTED MATERIALS

The dynamic shear moduli of the materials proposed for use in a bimetallic system were measured in a conventional manner using a torsion pendulum. The results of this work are shown in Figs. 2 and 3. The nominal chemical composition and heat treatment for these materials is given in Table I. The materials that show an <u>increase in shear modulus with increasing temperature</u> are 36% nickel alloy, 39% nickel alloy, and 40% nickel alloy. The 49% nickel alloy tested exhibited nearly constant modulus until about 600°F, rising until approximately 750°F, and then decreasing. Of these materials in the iron-nickel family, 40% nickel was considered to show the most promise of utility in a bimetal system, due to the somewhat higher temperature possible until a decrease in shear modulus results. This material was selected for detailed investigation, but another member of the iron-nickel family could have been selected just as well. For example, 39% nickel alloy appears to have a greater temperature range in which the slope is constant and hence a constant thermoelastic coefficient over a wider range. Also, the so-called "Iso-Elastic" material has constant modulus to slightly over 200°F. This material exhibited the most constant modulus of the materials tested but had a very limited range of temperature independence. Note also in Figs. 2 and 3 that all the conventional spring materials have shear moduli which decrease with increasing temperature. The increasing shear modulus of one material coupled with the decreasing shear modulus of another will possibly result in a system in which the spring constant is insensitive to temperature over a relatively wide temperature range.

Several comments are in order regarding Figs. 2 and 3. The absolute values of the moduli as calculated by Eq. (25) (see Appendix III) agreed with most of those in the literature with the exception of 304 stainless steel. As a result of testing and subsequent calculation by Eq. (25), a shear modulus of 9.80×10^6 lb/in.^{2} was found at room temperature. Most of the published data give a room-temperature shear modulus of between 11×10^6 and 11.5×10^6 lb/in.^{2}. The data and calculations were rechecked with no indication of error. Apparently some mistake had been made in experiment (probably in period measurement of the oscillations), resulting in an erroneous value. In all the calculations that follow the room-temperature shear modulus for 304 stainless steel was taken as 11.5×10^6 lb/in.^{2}.

The 40% nickel alloy tested also resulted in a room-temperature modulus somewhat lower than that published by the International Nickel Company. However, an independent check was made since tension test stress-strain data were available (see Fig. 10). Using the equation $G = \dfrac{E}{2(1+\mu)}$ and assuming

8

TABLE I

CHEMICAL COMPOSITION OF MATERIALS USED IN DYNAMIC SHEAR-MODULUS TESTS

Material	Composition	Condition
1. 430 stainless steel	Cr 18	---
2. Hy Mu 80	Ni 79, Mo 4 Fe 18 + Si, Mn, etc.	Annealed at 1200°F
3. Iso Elastic Special	Ni 35-37, Cr 7, C .05-.15 Mo .35-.75, Mn .45-.75	---
4. 49% Nickel (Simonds)	49 Ni, 50 Fe + Si, Mn, etc.	Annealed at 1200°F
5. "Hy Per 49" 49% Nickel (Hy Per)	48 Ni, 50 Fe + Si, Mn, etc.	Annealed at 1200°F
6. 40% Ni Alloy	40 Ni, 60 Fe nominal	Unaged
7. 39% Ni Alloy	39% Ni, 61 Fe nominal	Unaged
8. S-816 National Standard Co.	Co 40-44, Cr 19-21 Ni 19-21, Fe 5 Mo 3.5-4.5, Cb 3-4.5 W 3.5-5	Annealed
9. NS-25 National Standard Co	Co 50, Cr 19-21 Ni 9-11, W 14-16 Fe 3	Annealed
10. Inconel X National Standard Co.	Co 1, Cr 14-17 Ti 2-2.5, Ni 69 Fe 5.9	Annealed
11. Haynes 25	Ni 10, Cr 20, W 14-15 Mn 1.4, Si 0.5, Ti 0.15 Bal Co	---
12. Tantaloy	Ta 92.5, W 7.5	20% cold-drawn
13. NS-A-286 National Standard Co.	Cr 13.5-16, Ni 24-27 Mo 1-1.75, Ti 1.75-2.25 V .1-.5, Al .35, Bal Fe	Annealed
14. 304 stainless steel	Cr 19, Ni 9	---

$\mu = 0.28$, the room-temperature value of the shear modulus was calculated to be 6.93×10^6 lb/in.^{2} which agreed with the torsion-pendulum result.

C. ANALYSIS OF TEMPERATURE-COMPENSATED BIMETALLIC COIL-SPRING SYSTEMS

1. Geneeral Considerations.—Since spring elements may be combined in two basic ways, series and parallel arrangements (with the possibility of further combinations of these basic schemes), it is of interest to discuss the utilization of such systems. For a multi-spring system the series combination is one in which the same force is exerted on each component. When more springs are added in series to an existing system the over-all stiffness, or force per unit deflection, is reduced. Excluding problems of mechanical stability when the system, or some part of the system, is under a compressive force, any stiffness, or spring constant, is possible simply by the addition of more springs in series. Of course, the more springs added, the softer is the resultant system.

In a parallel arrangement the over-all deformation of each spring element is the same and adding more springs in parallel to an original system increases the system stiffness. Here mechanical stability is usually not a consideration so that in some ways the parallel arrangement may be more satisfactory. The stability mentioned here is in the sense of mechanical buckling as a result of some slenderness index (perhaps the ratio of length to over-all transverse dimension) being too large. But there are other stability problems having to do with nonlinear softening springs that are acting as part of an oscillating system. Here one can get unstable motions in which the amplitude of motion grows prohibitively large due to nonlinear spring characteristics. Fortunately, conventional coil springs do not show this softening character and hence this oscillatory stability is not an issue.

When some form of internal or external guide is provided to prevent buckling or when the external dimension perpendicular to the axis of the spring is limited due to space restrictions, the series arrangement may be quite useful. If these conditions do not prevail or if quite a stiff spring is required, a parallel arrangement may prove most beneficial. When conditions limit the volume occupied by the spring, a parallel coaxial system may be considered, as one spring sits inside another, having common axial center lines. For example, see Figs. 19 and 20.

Several types of problems involve the effect of temperature. First, there is the elevated-constant-temperature spring problem. Whatever the temperature may be, the spring must function properly, depending on the application. Usually a high-temperature spring must be free of "load loss" or relaxation at a relatively high stress, have good fatigue properties if cycling is incurred, and have a prescribed spring constant at the elevated temperature in question. Further, in many high-temperature spring applica-

10

tions the spring constant should be the same over quite a wide range in temperature. The initial objective of this project was to develop a constant-stiffness spring to operate from -65°F to 450°F with 1000°F as a prospective goal. As previously pointed out, the shear moduli of all the common high-temperature spring materials, Inconel X, A-286, S-816, Haynes 25, and NS-25, decreasing as temperature increases. There is thus no hope that these materials alone can compose a system of constant stiffness for variable temperatures. Combining a material which has a stiffening characteristic with increasing temperature with one which decreases in stiffness is one solution to this problem. Of course, the ideal situation would be to have both materials increasing or decreasing linearly in stiffness over a temperature range sufficient to cover the desired temperature range. Looking at Figs. 2 and 3, it will be noted that most of the materials decreasing in stiffness do so in a relatively linear fashion. The 36%, 39%, and 40% nickel ferromagnetic alloys increase in stiffness linearly over a temperature sufficient to be of considerable interest. One would probably select the ferromagnetic alloy that has the greatest linear modulus-temperature characteristic so that, when combined with a material that decreased linearly in stiffness, the result could be a temperature-independent system.

2. <u>Bimetallic Series System</u>.—Let a system composed of two, small-pitch-angle, helical coil springs arranged in series (placed end to end) be subjected to an axial compressive force. The ratio of the applied force to the corresponding deflection of the individual springs is commonly called the spring constant. For the series arrangement consisting of two springs, the equivalent spring constant can be written as

$$\frac{1}{k_e} = \frac{1}{k_1} + \frac{1}{k_2} \quad \text{or} \quad k_e = \frac{k_1 k_2}{k_1 + k_2} \tag{1}$$

where

k_1 and k_2 are the spring constants of the individual springs, and k_e is the equivalent spring constant.

The temperature characteristic slope is found by taking the first derivative with respect to temperature, which is, after some reduction,

$$\frac{dk_e}{dT} = \frac{k_1^2 \frac{dk_2}{dT} + k_2^2 \frac{dk_1}{dT}}{(k_1 + k_2)^2} \tag{2}$$

From elementary spring theory (3),

$$k = \frac{Gd}{8nc^3}$$

11

where

G = shear modulus of material,
d = spring wire diameter,
n = number of active coils, and
c = spring index; ratio of mean coil diameter to wire diameter.

$$\frac{dk}{dT} = \frac{1}{8nc^3}\left[\frac{dG}{dT}\,d + G\,\frac{dd}{dT}\right]$$

$$\frac{dk}{dT} = \frac{G_0 d_0}{8nc^3}\left[\frac{1}{G_0}\,\frac{dG}{dT} + \frac{1}{d_0}\,\frac{dd}{dT}\right]$$

When n = number of actual turns (assumed constant)

$$c = \frac{\overline{D}}{d} \text{ (assumed constant)}$$

But

$$\frac{1}{G_0}\,\frac{dG}{dT} = m_G = \text{thermoelastic coefficient of } G$$

$$\frac{1}{d_0}\,\frac{dd}{dT} = \alpha = \text{coefficient of expansion.}$$

Therefore

$$\frac{dk}{dT} = k_0\left[\alpha + m_G\right] \tag{3a}$$

For a spring constant, k_e, independent of temperature

$$\frac{dk_e}{dT} = k_{10}^2 k_{20}\left[\alpha_2 + m_{G2}\right] + k_{20}^2 k_{10}\left[\alpha_1 + m_{G1}\right] = 0$$

Therefore

$$k_{10}\left[\alpha_2 + m_{G2}\right] + k_{20}\left[\alpha_1 + m_{G1}\right] = 0$$

If

$$d_{10} = d_{20}$$

$$\overline{D}_{10} = \overline{D}_{20}$$

$$c_1 = c_2$$

12

$$\frac{G_{10}}{n_1} \left[\alpha_2 + m_{G_2} \right] = - \frac{G_{20}}{n_2} \left[\alpha_1 + m_{G_1} \right]$$

and

$$\frac{n_2}{n_1} = - \frac{G_{20}}{G_{10}} \frac{(\alpha_1 + m_{G_1})}{(\alpha_2 + m_{G_2})} \qquad (4)$$

This equation relates the material properties to system geometry. Note in Eq. (4) that if both materials have positive coefficients of linear expansion, and if the thermoelastic coefficients are larger in magnitude than the expansion coefficients (which are assumed positive), then one material must have a positive thermoelastic coefficient and one a negative thermoelastic coefficient. Also, if the thermoelastic coefficients m_{G_1} and m_{G_2} are constant as well as the thermal expansion coefficients α_1 and α_2, the ratio n_2/n_1 is constant. This is highly desirable as it would be very difficult to vary the number of active coils as a function of temperature.

Some experimental work was done with series bimetallic springs. But most of the results were not encouraging because, during the early stages of the work, accurate information on the thermoelastic coefficients was not available. There was no time for experimental work to validate the theory presented above; more work in this area is definitely needed.

3. Bimetallic Parallel System.—Instead of placing two coils end to end, let one be nested inside the other to form a parallel arrangement where both springs are of the same free length. Making the springs coaxial decreases the volume required for the bimetallic system and is done here for that purpose. The springs could be placed side by side. For this arrangement, the equivalent spring constant is

$$k_e = k_1 + k_2 \qquad (5)$$

Again taking the derivative with respect to temperature,

$$\frac{dk_e}{dT} = \frac{dk_1}{dT} + \frac{dk_2}{dT} = \frac{d}{dT} \left(\frac{G_1 d_1}{8 n_1 c_1^3} \right) + \frac{d}{dT} \left(\frac{G_2 d_2}{8 n_2 c_2^3} \right) \qquad (6)$$

After considerable reduction, one can show that for a temperature-independent spring, with the same approximations as in the series analysis,

$$\left(\frac{\overline{D}_{20}}{\overline{D}_{10}} \right)^3 = - \left(\frac{d_{20}}{d_{10}} \right)^4 \frac{(\alpha_2 + m_{G_2})}{(\alpha_1 + m_{G_1})} \cdot \left(\frac{G_{20}/G_{10}}{n_2/n_1} \right) \qquad (7)$$

where $\overline{D}_{20}$ and $\overline{D}_{10}$ refer to the mean coil diameters of the two springs. Equation (7), while more involved than Eq. (4) has the same structure, one re-

lating material properties to geometry. Once the particular materials are selected, one can vary the number of active coils, wire diameter, and mean coil diameters for the combination until the equation is satisfied. There is no theoretical restriction on the number of different combinations that can satisfy Eq. (7). Physically, certain combinations satisfying Eq. (7) will not be possible due to interference of the two coils if a coaxial arrangement is used. Figures 19 and 20 show two combinations tested. An interesting parallel combination is one shown in Figs. 61 and 62. Here a coil spring is fabricated from a material with negative thermoelastic coefficient in very-thin-walled tube form with the inside filled with a material with positive thermoelastic coefficient. The analysis for this system appears in Appendix I. This scheme has the advantage of stressing the tube to a higher level (usually the negative thermoelastic materials have much higher stress capacity than the ferromagnetic materials) than the central core, providing a protective jacket for the temperature-corrosion-sensitive nickel alloy as well as a convenient spring package. The results of the tests for this spring are given in Appendix I.

D. EXPERIMENTAL PROCEDURE AND RESULTS

1. Selection of Test Springs.—The most promising materials appeared to be 40% nickel alloy, Inconel X, and AISI type 304 stainless steel. The former is of the ferromagnetic class with positive thermoelastic coefficient, and the latter two materials have negative thermoelastic coefficients. The thermoelastic coefficients of Inconel X and 304 stainless steel were different enough so that, when combined with the 40% nickel, most sizing problems could be solved by either a series or parallel combination.

Several sets of springs were fabricated and preliminary tests were conducted. Here the coil springs were tested essentially statically using the test apparatus described in Section E. The shear moduli of the materials tested were calculated using Eq. (3) and the coil-spring static shear modulus versus temperature was plotted. Calculations of the thermoelastic coefficients were made from these data; comparison showed that the thermoelastic coefficient based upon the coil spring data was consistently less, in an algebraic sense, than that calculated on the basis of the dynamic shear modulus tests. One of the first 40% nickel alloy springs tested is shown in Fig. 4.

At this point it was decided to fabricate a set of springs of each material to be investigated with the spring index and the number of active coils as parameters. By this it could be determined if the thermoelastic data were dependent on a spring-size parameter. Here the 40% nickel alloy springs had nominal spring indices of 7, 9, and 11 with several different numbers of active coils. The Inconel X springs had nominal indices of 7 and 9 and different numbers of active coils. Some of these springs are shown in Figs. 5-8. Since the 304 stainless steel was considered to be an alternate neg-

ative thermoelastic material, no new springs of this material were fabricated in this phase of the program.

With few exceptions, the springs fabricated were made with two solid turns on each end so as to eliminate end effects (see definition sketch in Fig. 64).

The 40% nickel alloy was secured in bar stock and drawn into wire form by the Hoskins Manufacturing Co., Detroit, Michigan. The Inconel X spring temper wire was obtained from National Standard Co., Niles, Michigan. This material has good strength and relaxation properties up to a maximum of 650°F to 750°F. See Ref. 4 for information about this material.

2. Method of Testing and Determination of Spring Constants.—Since heat treatment has a pronounced effect on the behavior of springs, a standard heat treatment was given to each of the test springs before testing. All coil springs tested, unless otherwise stated, were heated to 1000°F and held at that temperature for a period of two hours and slowly cooled in air.

As can be seen from Figs. 26 and 28, the load-carrying components of the testing apparatus, namely, the load cell, pull rod, and holding fixtures, act as a spring in series with the test spring. It was therefore necessary to consider several problems associated with the determination of the spring constant of the test spring. First, since one has essentially two springs in series, the testing apparatus and the test spring, the load-deformation output shown on the recorder (see Fig. 28) is a measure of the over-all response of the two mentioned components. It is therefore necessary, if one is concerned with the absolute value of the spring constant of the test spring, to know the response of the testing apparatus individually so that this can be taken into account. Secondly, if the apparatus response varies with the test temperature, the variations should also be known. If the test apparatus response does not significantly vary with temperature, then one may display the data in dimensionless form, for example, comparing the gross output elevated- or reduced-temperature data to that at room temperature. But if there is a significant variation in test apparatus behavior with temperature, then the nondimensional scheme will not be convenient.

Figure 9 shows the room temperature load-deformation response of the two machines used for both 5- and 10-lb full chart scale. Next, several tests were made to see if temperature had an effect on these data. No significant variation in the testing apparatus response with temperature was determined. Two individual checks were made where load-deformation data were taken in increments of 100°F to a maximum of approximately 800°F in the test furnace. Since no temperature dependence was noted, one could make a nondimensional display of the gross output of the recorder to reflect the behavior of the test spring accurately. This procedure was used in displaying the data obtained.

15

A stress calculation was made on each spring to determine the maximum permissible load so as not to exceed the proportional limit of the material. The 40% nickel alloy was most critical in this respect, as the proportional limit in tension at 700°F was approximately 25,000 lb/in.[2] as determined by a simple tension test. Figure 10 shows stress-strain diagrams at 70°F and 700°F for this material. Taking one-half this value for the proportional limit in shear as a basis for calculation, the maximum load for each spring was determined. The Inconel X and 304 stainless steel maximum spring loads were calculated similarly. See Appendix II for stress calculations.

The test spring in question was gradually loaded from free height with the deformation being linear with time to a peak value below the calculated maximum value, and then unloaded. For any given temperature, several loading-unloading cycles were produced to obtain an average condition. With each loading-unloading cycle, an associated load-deflection curve was traced out on the recorder chart, shown in Figs. 11 and 12. The spring constant for the spring in question was calculated by taking two convenient, well-spaced points on the loading curve and calculating the slope of a chord line formed by these two points. In almost every spring tested, the load-deflection curve was very nearly linear. The test temperature was varied in convenient increments and the above procedure repeated until enough data were obtained to plot a spring constant-temperature curve. Typical spring constant-temperature curves are shown in Figs. 13 and 14.

To consolidate the data into a convenient display, a dimensionless plot was made by forming the ratio of the spring constant at a particular temperature to the room temperature value and plotting versus temperature. In most cases, at least two complete temperature cycles of an individual spring were run to determine if the behavior was reproducible. Variations between the results were very small.

3. Results for Individual Springs.—The results for the individual springs tested are shown in Fig. 15, plotted in nondimensional form versus temperature. Figure 16 shows the same plot with fitted lines through the average of the data of Fig. 15. Note that Fig. 16 shows a dependence on spring index of the 40% nickel-60% iron alloy. The thermoelastic coefficient based on the coil-spring data is very easily calculated from these nondimensional plots by the equation

$$m_k = \frac{1}{k_0} \frac{\Delta k}{\Delta T} = \frac{\Delta(\frac{k}{k_0})}{\Delta T} \tag{8}$$

where the Δ refers to a difference between two points on the curve. The values of m_k calculated in this manner are given below and were constant over the temperature range indicated.

Material	m_k	Temp. Range
40% nickel alloy, spring index < 9	$+155 \times 10^{-6}/°F$	-110°F to +550°F
40% nickel alloy, spring index > 9	$+135 \times 10^{-6}/°F$	-110°F to +550°F
Inconel X, spring temper	$-165 \times 10^{-6}/°F$	-110°F to +700°F
304 stainless steel	$-275 \times 10^{-6}/°F$	70°F to +700°F

For the purpose of this investigation, testing was restricted to the range of from -110°F to approximately 700°F. Since the 40% nickel alloy thermoelastic coefficient becomes less positive after approximately 550°F and becomes negative at about 625°F to 650°F, higher temperatures were thought unnecessary.

The 40% nickel alloy springs exhibited moderate scaling as a result of the elevated-temperature environment as shown in Figs. 5 and 6.

As shown by Fig. 2, the 49% nickel alloy seemed to have possibilities because of the relatively constant dynamic shear modulus. The results for a 49% nickel (Hy-Per 49) spring are shown in Fig. 17. As can be seen the spring constant decreased until about 600°F, with indications of a rise starting at 700°F. Since the 40% nickel alloy is not suitable past about 600-700°F, a 40%-49% nickel bimetallic system did not appear suitable for further study.

4. **Results for Bimetallic Spring Systems.**—On the basis of the thermoelastic data obtained from the coil-spring tests, it was concluded that Eq. (7) should be modified by replacing m_G by m_k, so as to reflect the actual coil-spring behavior. With this change, Eq. (7) becomes

$$\left(\frac{\overline{D}_{20}}{\overline{D}_{10}}\right)^3 = - \left(\frac{d_{20}}{d_{10}}\right)^4 \frac{(\alpha_2 + m_{k_2})}{(\alpha_1 + m_{k_1})} \cdot \left(\frac{G_{20}/G_{10}}{n_2/n_1}\right) \tag{9}$$

Using this equation, calculations were made for several parallel spring combinations designed to be temperature-independent relative to the spring constant. Appendix II gives several sample calculations that were the basis for spring fabrication. Figure 18 shows a dimensionless display of the spring constant versus temperature for these combinations.

Of the five bimetal combinations reported in Fig. 18, none varied more than 1.5% in spring constant over the temperature range of from -110°F to 525°F. The second and third combinations shown in Fig. 18 (see also Fig. 19) had less than 0.5% variation in spring constant in the range of from -65°F to 600°F. Figure 18 shows one combination which was slightly stiffening with increasing temperature. All the bimetal spring systems resulted in spring constants in the range of from 34-43 lb/in.

5. Time Effects.—It should be recalled that all the work mentioned has been done for nonrelaxation conditions. Relaxation is generally regarded as the inability of a spring to remain at a fixed height under a specified load at a specified temperature for relatively long periods of time. The conventional relaxation test involves loading the spring to a fixed height, resulting in a maximum wire stress (to be predetermined), subjecting the spring to an elevated temperature, and at a specified elapsed time releasing the spring to free length and measuring the resulting free length. Knowing the starting free length, one can calculate the "loss in stress" resulting from the reduced free height after exposure to the elevated temperature for the period of time in question. Making a plot of maximum wire stress versus time at constant temperature with stress as a parameter is the normal way to display data of this nature (see Fig. 21). For "fixed distance" applications where a mechanical spring must hold a constant distance between two components, the above method of test and representation appears to be adequate. But sometimes the force per unit deflection is to be held constant, with absolute distances not being a critical consideration. Then a representation as shown in Fig. 22 could be used to judge the time-temperature characteristic of a particular spring or spring system. The spring is stressed to a particular level and held. At convenient intervals of time, the spring is loaded and unloaded and the spring constant is determined. An indication of the ability of the particular spring or spring system to maintain its spring constant would be determined.

We planned to obtain considerable time effects, but the intial aspects of the coil-spring program took more time than we anticipated. Only an indication of time effects is given here, along with the results from very limited time-temperature testing.

The method described above, resulting in the representation shown in Fig. 22, was followed in testing the bimetallic spring system composed of 40% nickel alloy $c = 6.95$ and Inconel X $c = 9.18$ parallel combination. The results for a 12-hour test at 500°F with a maximum wire stress of approximately 10,000 lb/in.^{2} for the 40% nickel alloy indicated no reduction of spring constant. Further work in this area should be considered for any future program.

E. EXPERIMENTAL APPARATUS USED FOR TESTING

Figures 23 and 24 show the testing machines used for the experimental work done. Figure 23 shows the Instron textile testing machine type TTCLM1; Fig. 24 shows the table model type TM machine. Figure 23 shows the larger unit with furnace in place. The esential features of both test set-ups are as follows: starting at the top (see Figs. 23 and 26) is a heavy steel extension tube with associated cooling fans, the purpose of which was to keep the load cells at a constant temperature. Since the load cell is an electrical strain gauge, it is quite important that the temperature remain

constant throughout testing. Next comes a 1/2-in.-diameter round rod, which extends through the machine crosshead, and a fixture assembly consisting of a stainless-steel pipe. The rod runs through the inside diameter of the test spring and is accommodated with a thread end for the purpose of a spring holding plug (see Fig. 27). All components of test fixtures were made of stainless steel to reduce corrosion problems as well as heat conduction.

The Instron machine is commonly used in industrial research. Its basic functioning is shown in Fig. 28. The advantage here over the normal testing machine or a dead weight system is one of extreme force-measuring accuracy as well as continuous permanent recording on the associated Leeds and North-rup high-speed potentiometer recorder embodying a synchronous drive.

For the elevated-temperature work, an electrically heated furnace controlled by a Wilson-Maeulen controller with on-off relays was used (see Fig. 29). Chromel-Alumel thermocouples were used to measure the temperature in close proximity of the spring both in an angular and longitudinal distribution so as to get an accurate indication of the test temperature (see Fig. 27). For the low-temperature work, a mixture of solid carbon-dioxide and methyl alcohol was used. The entire lower portion of the fixture assembly was submerged in a container of the mixture, and temperature stability was maintained throughout all tests at -110°F.

A Leeds and Northrup portable millivolt potentiometer was used to measure the millivolt differences for the determination of the test temperature.

F. CONCLUSIONS

A feasible bimetallic coil-spring system can be constructed in which the spring constant is independent of temperature within approximately 0.5% over the temperature range of from -65°F to 600°F. A temperature-independent system is possible within 2.0% over the range of from -100°F to 700°F.

G. RECOMMENDATIONS

More testing is recommended to insure the reliability and reproduc-ibility of bimetal spring systems such as studied in this program.

Also, since very little relaxation work was done during this project, extensive experimental work should be done in this area to determine fully the relaxation characteristics of such bimetal systems.

The possibility of a coating, to be applied to the nickel alloy materials to prevent elevated-temperature scaling revealed during the course of this project should be investigated.

More work should be done on springs in series.

IV. ANALYSIS OF BELLEVILLE SPRING WASHERS AS A MEANS OF PRODUCING A SPRING HAVING A CONSTANT SPRING-RATE VERSUS TEMPERATURE

A. INTRODUCTION

The motivation behind the analysis of Belleville spring washers is basically that behind the analysis of coil springs, namely, to combine materials possessing positive and negative thermoelastic coefficients. Two additional important reasons for investigating Belleville spring washers are (1) their immense versatility in producing from a given material and thickness a spring of any desirable characteristics simply by a slight variation of the spring height, and (2) that the combinations of materials can easily be effected by simple substitution in their stacking, either series or parallel as indicated in Fig. 30.

The method of stacking used for all tests throughout the project was that of series, mostly because of the greater friction present in parallel combinations. The series combination of washers were effected by two means: (1) stacking by use of spacer plates; (2) stacking by means of welding washers together. The latter method makes possible the use of the temperature-dependent bimetallic effects to increase spring stiffness versus temperature. Methods of stacking and bimetallic effects will be further explored below.

Five basic materials were used in all tests, namely, 304 and 430 stainless steels and 31%, 42% and 50% Ni-balance Fe alloys. All materials were heat-treated at 1200°F for 2 hours and air-cooled.

B. THEORETICAL CONSIDERATIONS

The basic theory for Belleville spring washers has been known for quite some time. Several papers about, and refinements of, their analysis have been written. One of the most complete and best known is that by Almen and Laszlo (5). The analysis of the washers considered here will be based entirely on their results.

The geometrical notation used here is indicated in Fig. 31.

On the basis of the investigations by Almen and Laszlo (5), the load-deflection equation for a simply supported washer, loaded uniformly around the inside diameter in compression, may be written as

$$P = \frac{E\delta}{(1-\mu^2)Ma^2} [(h-\delta)(h-\frac{\delta}{2})t + t^3] \tag{10}$$

The maximum stress in the upper edge is

$$\sigma = \frac{E\delta}{(1-\mu^2)Ma^2} [c_1(h-\frac{\delta}{2}) + c_2 t] \tag{11}$$

The maximum stress in the lower edge is

$$\sigma = \frac{E\delta}{(1-\mu^2)Ma^2} [c_1(h-\frac{\delta}{2}) - c_2 t] \tag{12}$$

where P = applied load, σ = stress, δ = deflection, E = modulus of elasticity, μ = Poisson's ratio, a = outside radius, h = free height, and t = thickness. M, c_1, and c_2 are functions of the outside-to-inside diameter ratio α as follows:

$$\frac{1}{M} = \left[\frac{\alpha+1}{\alpha-1} - \frac{2}{\ln \alpha}\right] \pi \left(\frac{\alpha}{\alpha-1}\right)^2 \tag{13}$$

$$c_1 = \left(\frac{\alpha-1}{\ln \alpha} - 1\right) \frac{b}{\pi \ln \alpha} \tag{14}$$

$$c_2 = \frac{3(\alpha-1)}{\pi \ln \alpha} \tag{15}$$

where $\alpha = \frac{a}{b}$ and b = inside radius.

The stress equations (11) and (12) above have often been observed to result in considerable error. A more exact analysis of Belleville spring washers by Wempner (6) has substantiated the load-deflection equation (10) given here and greatly improved the stress equations. However, time did not permit their application to this investigation. To insure use in the elastic range, all washers investigated were tested for yield data.

Considering Eq. (10), letting $A = E/(1-\mu^2)Ma^2$, and differentiating with respect to δ to obtain the slope of a load-deflection curve, or the spring constant k, one obtains

$$k = \frac{\partial P}{\partial \delta} = A \left\{\left[(h-\delta)(h-\frac{\delta}{2})t + t^3\right] - \delta t\left[\frac{3h}{2} - \delta\right]\right\} \tag{16}$$

Letting k_0 = the slope of the load-deflection curve at room temperature, the ratio of k at any temperature to k_0 becomes

$$\frac{k}{k_0} = \frac{A}{A_0} \frac{\{[(h-\delta)(h-\frac{\delta}{2})\,t + t^3] - \delta t[\frac{3h}{2} - \delta]\}}{\{[(h-\delta)(h-\frac{\delta}{2})\,t + t^3] - \delta t[\frac{3h}{2} - \delta]\}} \tag{17}$$

Now if we calculate the slopes of a load-deflection curve at a corresponding deflection for the same h and t values, then

$$\frac{k}{k_0} = \frac{A}{A_0} = \frac{E(1-\mu_0^2)}{E_0(1-\mu^2)} \tag{18}$$

This relation excludes any changes in h or t due to thermal expansion which are extremely small.

Equation (18) indicates that the dimensionless ratio k/k_0 versus temperature is independent of spring geometry and a function of material properties only. This is as expected. But Eq. (18) also indicates a very basic difference between the temperature behavior of a Belleville spring washer and a coil spring. The temperature behavior of a coil spring is a function of only one elastic constant, G, the shear modulus, whereas the temperature behavior of a Belleville spring washer is a function of two elastic constants, E and μ (or G).

Considering Eq. (18) again, it will be noted that, if E decreases with temperature, the effect is to lower the ratio k/k_0. At the same time, the k/k_0 ratio will tend to increase with temperature if μ increases with temperature. For the materials investigated here, on the basis of comparison of the curves for the elastic constants, Fig. 33 and those of the ratios k/k_0 versus temperature, Figs. 34 and 35, it appears that if the thermoelastic coefficients m and e are positive, the thermal coefficient of Poisson's ratio is negative, and for materials of negative m and e, the thermal coefficient of Poisson's ratio is positive. This cannot be said of all materials, however, and must be determined in each individual case.

This effect is substantiated by Figs. 36 and 32 where E/E_0 and k/k_0 versus temperature are plotted for 430 stainless steel and 50% Ni-balance Fe. Note from these curves that wherever the thermoelastic coefficients are negative, the Poisson effect is to increase the k/k_0 ratio, and whenever the thermoelastic coefficients are positive, the Poisson effect is to decrease the k/k_0 ratio.

Mathematically, this can be explained by considering a biaxial state of stress (Fig. 37) of an element, which is the state of stress in Belleville spring washers. Considering the strain in an arbitrary direction, say the x-direction, then the strain from generalized Hooke's Law may be written as

$$\epsilon_x = \frac{1}{E}(\sigma_x - \mu \sigma_y).$$

Thus, although a decreasing strain, an increasing Poisson's ratio tends to decrease the strain.

Physically this means that it is possible to obtain optimum performance from a given material in a Belleville spring washer. Thus if a single material could be found, although possessing a decreasing modulus versus temperature, whose slope of a modulus versus temperature curve was small, and if the thermal coefficient of Poisson's ratio was positive, it might be possible to make a spring out of a single material to withstand temperature effects. This effect certainly should be further investigated.

The above point is fairly well illustrated by the dimensionless ratio of k/k_O versus temperature for 50% Ni-balance Fe (Fig. 32). As previously mentioned, where the thermoelastic coefficients are negative, the k/k_O ratio is increased, and where the thermoelastic coefficients are positive, the ratio is lowered. The net effect is a flattening of the curve to a reasonably constant value. Through the temperature range of approximately 75-850°F, the maximum deviation of k/k_O is less than 1.5%. Thus this particular Ni-Fe alloy certainly demands consideration as a single material for springs to withstand temperature effects.

The remainder of the analysis of Belleville spring washers was carried out entirely experimentally. First, the dimensionless ratios k/k_O versus temperature were determined for each of the five materials available. Second, the individual curves of load versus deflection for each of the washers available with various h and t values were determined at room temperature. On the basis of these two sets of curves and the expression for the equivalent spring constant of series combinations of springs

$$\frac{1}{k_e} = \sum_{i=1}^{n} \frac{1}{k_i} \text{ , where i = 1,2,...n,}$$

washers of different materials were put together and tested versus temperature.

C. ELASTIC MODULI

For completeness, the three elastic moduli versus temperature which were determined are included in Fig. 33. In any future work of this type, the static values of E, G, μ should be one of the first things determined. These values would allow a close check between theory and experiment. These values were not determined for this report because we did not have the equipment available to determine the static values of elastic moduli. The work had to be done by an outside source which was unable at the time to determine these data.

D. DIMENSIONLESS RATIOS k/k_O VERSUS TEMPERATURE FOR 304 AND 430 STAINLESS STEELS AND 31%, 42%, 50% NICKEL-BALANCE IRON ALLOYS

The dimensionless ratios of k/k_O versus temperature for each of the five materials used in tests are included in Figs. 34 and 35. The curves for the two stainless steels were determined on the basis of Eq. (18) from the experimentally determined values of the elastic moduli. The values of Possion's ratio were determined from available data in the literature. The curves of the three iron-nickel alloys were determined directly by experiment.

E. INDIVIDUAL WASHER DATA

Each washer available was tested at room temperature for individual load-deflection data. The resulting curves are included in Figs. 38, 39 and 41-50. All washers used throughout the project were of a standard 1.50-in. OD and 0.75-in. ID. Washers of various h/t ratios and of different stock thickness were tested for each material. The values of stock thickness and h/t ratios are listed on each figure.

The washers were simply supported and loaded uniformly around the inside diameter in compression.

It was necessary to correct experimental data for deflections of the test fixtures. All values plotted are corrected. The calibration curve for the load cell and fixtures used in tests is included in Fig. 40.

Some of these load-versus-deflection curves for the individual washers exhibit an irregular behavior in the initial loading period because the base of the washers was not perfectly flat. This effect can be eliminated by pre-loading.

Friction was present in the loading due to the method of support. To eliminate the effect of friction the loop curves of load versus deflection for loading and unloading were obtained. A mean value was then used, as the friction effect would be in opposite directions for loading and un-loading.

In any future work it would be desirable to design a support which would minimize friction.

F. COMBINATIONS OF WASHERS

Combinations of washers will be discussed on the basis of their method of stacking, either (1) by use of spacer plates, or (2) by welding washers together.

1. Stacking by Use of Spacer Plates.—This method of stacking is il-
lustrated in Fig. 51. Results of tests of combinations effected by this
method are included in Figs. 52 and 53.

It is to be noted from these graphs that the experimental values are
within approximately 1% of the predicted values determined on the basis of
the load-deflection curves for the individual washers, the k/k_O ratios versus
temperature for the individual materials, and the expression for the equiv-
alent spring constant in series

$$\frac{1}{k_e} = \sum_{i=1}^{n} \frac{1}{k_i} \text{ , where } i = 1,2,\ldots n.$$

Figure 52 further indicates that both the experimental and predicted
values of k/k_O versus temperature are within 1% deviation over the temperature
range 72-800°F. Figure 53 substantiates that it is possible to obtain a k/k_O
ratio versus temperature greater than one over the entire temperature range 72-
1000°F. Thus a constant k/k_O ratio over this entire range of temperature is
entirely possible. Time did not permit further investigation of what, exactly,
should be the combination of washers.

This particular method of stacking produces considerable friction. As
previously pointed out, loop curves of load versus deflection for loading and
unloading were obtained to eliminate the friction effect. A proper choice
of lubricants and spacer material would certainly minimize this effect and
should be carefully considered for any future work. No lubricant was used
in these tests. Further, the spacer material, which was hardened tool steel,
scaled considerably at high temperatures. Some type of glass might be quite
useful for spacer material to minimize the above-mentioned effects.

2. Stacking by Welding Washers Together.—This method of stacking is
illustrated in Figs. 54 and 55. Results of tests of combinations effected by
this method are included in Figs. 56-59. It cannot be said for this method
of stacking that the load-deflection equation (10) is valid, since of course
the boundary conditions of the washer support are changed. But elastic con-
stants would probably enter in the exact relation in the same manner. If
so, then the dimensionless ratio k/k_O would be of the same form. This seems
to be substantiated in Fig. 56, where the predicted values of the k/k_O ratio
on the basis of free supports are plotted against experimental results of
the welded combination.

If Eq. (18) for k/k_O versus temperature for free supports is true for
welded supports, then Fig. 56 further shows the advantage of bimetallic ef-
fects in welded combinations. The thermal coefficients of expansion versus
temperature for the materials used in the combination of Fig. 56 are plotted
in Fig. 57. Figure 56 shows that the experimental value is greater than the
predicted value at all times. But the agreement between experimental and

predicted values is very close at the temperature when the thermal coefficients of expansion are equal, and the deviation is the greatest of the highest temperature where the thermal coefficients of expansion differ considerably. Although the difference of these thermal coefficients is quite large at lower temperatures also, their absolute values are considerably less. Since the load-deflection equation is nonlinear the deflections due to the bimetallic effects should be greatest when their magnitudes are maximum, which is at the highest temperature. This is substantiated by Fig. 56.

A major effect of welding to be considered in design is that it increases the initial stiffness of the spring k_O. For the springs fabricated by welding, k_O was increased by approximately 100%. This of course could be varied considerably either way, depending on fabrication since the initial stiffness of the spring k_O can be adjusted accordingly.

Many combinations of washers can accomplish a constant k/k_O ratio versus temperature. In contrast to the individual washers whose behavior is a function of the thermoelastic coefficients only, combinations have two variables: (1) the number of each kind of washer, and (2) the individual values of k_O to weigh in these effects.

G. TEST APPARATUS

All fixtures and equipment used for tests of Belleville spring washers were the same as those used for tests of coil springs. Fixtures and equipment involved have been discussed thoroughly in Section III.

27

APPENDIX I

ANALYSIS OF TUBE-CORE BIMETALLIC SYSTEM

Consider a system composed of a thin walled tube in which the inside is filled to a snug fit with a second material. For the analysis to follow the tube is composed of a material with a negative thermo-elastic coefficient and the core of a material with positive thermo-elastic coefficient. Using Eq. (3a) one may express the independence of spring on temperature as

$$k_{10}(\alpha_1 + m_{k_1}) + k_{20}(\alpha_2 + m_{k_2}) = 0 \tag{19}$$

where

$$k_{10} = \frac{G_{10}\, d_{10}^4}{64 \bar{R}_1^3 n_1} \tag{20}$$

for a solid round wire cross section, and

$$k_{20} = \frac{G_{20}(d_{20}^4 - d_{10}^4)}{64 \bar{R}_2^3 n_2} \tag{21}$$

for a tubular round wire cross section. (Refer to Ref. 3 for derivation of these spring constants.)

Equation (21) has presumed the inside diameter of the tube and the wire diameter of the coil to be equal. For a configuration of this nature $n_1 = n_2$, $\bar{R}_1 = \bar{R}_2$ so Eq. (19) after substitution of Eq. (20) and Eq. (21) and rearrangement becomes

$$\left(\frac{d_{20}}{d_{10}}\right)^4 = -\frac{G_{10}}{G_{20}}\frac{(\alpha_1 + m_{k_1})}{(\alpha_2 + m_{k_2})} + 1 \tag{22}$$

For a specific case taking Inconel X as the tube material and 40% nickel-60% iron alloy as the core material,

$$\left(\frac{d_{20}}{d_{10}}\right)^4 = -\frac{(6.90 \times 10^6)\ (3 + 155)}{(11.5 \times 10^6)\ (10 - 165)} + 1$$

$$\left(\frac{d_{20}}{d_{10}}\right)^4 = (0.60) \frac{158}{155} + 1$$

$$\left(\frac{d_{20}}{d_{10}}\right)^4 = 1.61, \quad \frac{d_{20}}{d_{10}} = 1.126$$

Taking $d_{10} = 3/32$ in., $d_{20} = 0.106$ in.

EXPERIMENTAL RESULTS OF TUBE-CORE BIMETALLIC SYSTEM

Inconel X tubing of outside diameter 0.119 in. and inside nominal diameter of 3/32 in. was used with 40% nickel-60% iron alloy to experimentally check the feasibility of such a composite spring. Figs. 61 and 62 shows this spring and Fig. 63 shows the test results. Note that although the diameter ratio is incorrect as demanded by Eq. (22) the temperature variation is relatively slight with the variation at 500°F being approximately 2%.

APPENDIX II

SAMPLE CALCULATIONS FOR BIMETAL COIL SPRING SYSTEMS

(a) 304 stainless steel-40% nickel alloy.

Using Eq. (9), one can size the individual springs for the system. Taking for 304 stainless steel $m_k = -275 \times 10^{-6}/°F$ and assuming a 40% nickel alloy spring with $c < 9$, where $m_k = +155 \times 10^{-6}/°F$, one has for $\alpha_2 \cong 10 \times 10^{-6}/°F$, $\alpha_1 \cong 3 \times 10^{-6}/°F$

$$\left(\frac{\overline{D}_2}{\overline{D}_1}\right)^3 = -\left(\frac{d_2}{d_1}\right)^4 \frac{(10-275)}{(3+155)} \frac{(11.5/6.9)}{(n_2/n_1)}$$

Now assuming $d_2 = d_1$ and $n_2 = n_1$ the above reduces to

$$\left(\frac{\overline{D}_2}{\overline{D}_1}\right)^3 = +(1.68)(1.67) = 2.80$$

$$\frac{\overline{D}_2}{\overline{D}_1} = 1.41$$

Choosing D_{1O} (outside diam of inner coil) = 13/16 in. or 0.81, $\overline{D}_1 = 0.72$ in.

$$\overline{D}_2 = (1.41)(0.72) = 1.015$$

$$D_{2O} = 1.015 + .094 = 1.11; \quad c_2 = 10.85$$

So the sizing would be with 8 active turns in each spring, 40% nickel, OD = 0.81, n = 8, d = 3/32; 304 stainless steel, OD = 1.11, n = 8, d = 3/32, with both springs having the same pitch.

(b) Inconel X spring temper-40% nickel alloy.

Again assuming $c < 9$ for the 40% nickel spring, one may write Eq. (9) as

$$\left(\frac{\overline{D}_2}{\overline{D}_1}\right)^3 = -\left(\frac{d_2}{d_1}\right)^4 \frac{(10-165)}{(3+155)} \frac{(11.5/6.9)}{(n_2/n_1)}$$

Assuming $d_2 = d_1$ and $n_2 = n_1$ as before

$$\left(\frac{\overline{D}_2}{\overline{D}_1}\right)^3 = + (0.98)(1.67) = 1.64$$

$$\frac{\overline{D}_2}{\overline{D}_1} = 1.18$$

Choosing as before $D_{1O} = 0.81$ so that $\overline{D}_1 = 0.72$, $\overline{D}_2 = 0.85$. The outside diameter of the inner coil is 0.81 and the inside diameter of the outer coil is 0.766 in. This is not possible because there would be interference of the two coils.

If one restricts the wire diameter and the number of active coils to be the same, the coil diameters of the two springs becomes impractically large. At this point one may make several choices. For example, let

$$d_2 = 0.112, \quad d_1 = 0.09375$$

$$n_2 = 9, \quad n_1 = 10$$

Then

$$\left(\frac{\overline{D}_2}{\overline{D}_1}\right)^3 = \left(\frac{0.112}{0.09375}\right)^4 (0.98) \frac{(1.67)}{(9/10)}$$

$$\left(\frac{\overline{D}_2}{\overline{D}_1}\right)^3 = (2.04)(0.98)(1.85) = 3.70$$

$$\frac{\overline{D}_2}{\overline{D}_1} = 1.545$$

Letting $D_{1O} = 0.75$ so that $\overline{D}_1 = 0.656$, $c_1 = 7.0$,

$$\overline{D}_2 = (1.545)(0.656) = 1.01$$

$$D_{2O} = 1.01 + 0.112 \cong 1.12; \quad c_2 = 9.00$$

STRESS CALCULATION

To stay within the proportional limit during testing, the total spring loads were calculated as follows:

$$\tau_{max} = \frac{16P\overline{R}}{\pi d^3} K$$

where

    P - total spring load, lb.
    $\overline{R}$ - mean coil radius, in.
    d - wire diameter, in.
    K - Wahl stress factor, nondimensional

Solving for the total allowable load in case (a) above, using 12,500 lb/in.^{2} as the allowable shear stress,

$$P = \frac{(12,500)(\pi)(3/32)^3}{(16)(0.36)(1.19)} = 4.7 \text{ lb}$$

The specific torsional resilience for 40% nickel alloy, as mentioned in the introduction, is at room temperature

$$S.R. = \frac{\tau^2}{2G} = \frac{(12,500)^2}{(2)(6.9 \times 10^6)} = 11.3 \text{ in.-lb/in.}^3$$

and at 600°F is approximately 10.0 in.-lb/in.^{3}

APPENDIX III

ANALYSIS AND EXPERIMENTAL PROCEDURES FOR
DETERMINATION OF DYNAMIC SHEAR MODULUS

The basic idea is that through use of a torsional vibratory system, the shear modulus will be reflected in the frequency of vibration. For a torsional system assuming (a) no damping, end effects or cross-coupling vibration, (b) perfect elasticity and no geometry variations, and (c) infinitely rigid support for hanging wire, the linearized equation of motion for a circular wire spring is:

$$I\ddot{\Theta} + \frac{JG}{L}\Theta = 0 \qquad (23)$$

where

   I - moment of inertia of end mass about axis of rotation
       (in.-lb$_f$-sec^2)
   Θ - angular displacement (radians)
   J - polar moment of inertia of wire (in.^{4})
   G - wire shear modulus (lb/in.^{2})
   L - free length of wire (in.)
   $\cdot$ - time derivative (sec^{-1})

(a) can be written as

$$\ddot{\Theta} + p^2\Theta = 0 \qquad (24)$$

where

$$p^2 = \frac{JG}{IL}$$

From the above, the shear modulus may be calculated as

$$G = \frac{128\pi IL}{d^4} \cdot \frac{I}{\tau^2} \qquad (25)$$

where

   d - wire diameter (in.)
   τ - period of oscillation of pendulum (sec)

Hence, by measurement of the period of oscillation and by measurement or calculation of the moment of inertia of the effective oscillating mass, the shear modulus may be calculated.

The experimental set-up (see Figs. 65 and 66) consisted of a vertical tubular furnace heated by electric current passing through Nicrome coil windings. The ceramic tube which enclosed the pendulum suspension wire was insulated and the furnace proper was suspended from an aluminum framework.

The pendulum with associated holding fixtures for gripping the suspension wire was suspended and secured against any movement to a heavy torsion plate by use of a steel taper pin. The torsion plate was part of the furnace-suspension framework; hence the supporting frame of great torsional rigidity.

The pendulum with associated gripping fixtures consisted of the following (from top to bottom):

   a.   A steel tube approximately 1-1/2-in. OD 2ft long, one
        end of which fastens to the torsion plate by use of a
        taper pin. At the other end is a special expansion-
        contraction insert which slides inside the tube and is
        secured by a threaded holding collar.

   b.   The expansion-contraction insert is used to grip the
        material specimen (in wire form) which has in some suit-
        able way been imbedded in cylindrical plugs which slip
        snugly into the cylindrical central portion of the insert.
        The top expansion-contraction insert has on the inner
        cylindrical portion a shallow groove to secure a wire to
        which thermocouples are attached for sensing the tem-
        perature in close proximity. Naturally, thermocouples
        could not be applied to the pendulum suspension wire for
        fear of changing the natural frequency. The thermo-
        couple supports were made out of stainless-steel welding
        rod approximately 1/16 in. in diameter. Three Chromel-
        Alumel thermocouples were used to sense the temperature
        in close proximity of the pendulum wire.

   c.   Next is the pendulum suspension wire made of the mate-
        rial for which the shear modulus is desired. The spec-
        imens had a free length of approximately 10-12 in. and
        a diameter of not greater than 3/16 in. Most of the
        work done was with 1/8-in.-diam wire and smaller. Forced
        onto both ends of the wire are stainless-steel (type
        304) plugs, .75-in.-diam by .75 in. long, cylindrical
        in form.

   d.   Next is the lower expansion-contraction insert with
        threaded holding collar and tube much like the upper
        portion. The major difference between the top and

bottom tube sections is 3 thermocouple-wire access
holes in the top assembly. The thermocouple wires
run centrally through the upper tube from the thermo-
couple holding wire and out to a potentiometer for
measuring millivolt differences. A circularly sym-
metric mass is attached by a taper pin to the bottom
tube assembly.

The furnace was heated by a 220-v, a-c, single-phase supply in conjunc-
tion with a temperature controller and on-off relay.

For low-temperature work, the furnace was replaced by a special copper
cylinder with seals adequate to contain a mixture of solid carbon dioxide
and methyl alcohol. By using this mixture a temperature of approximately
-110°F was obtained. Figure 66 shows testing at this temperature.

A Leeds and Northrup portable millivolt potentiometer was used to read
the millivolt differences and was accurate to within ±3°F at 1000°F.

The period of torsional vibration was obtained by taking the total
time for 50 complete oscillations by means of a stop-watch and dividing the
total time by 50.

REFERENCES

1. Köster, W., _Ztsch. Metallkde_, _35_, 194-199 (1943).

2. Vosteen, L. F., NACA Technical Report 4348, August, 1958.

3. Wahl, A. M., Mechanical Springs, Peyton Publishing Company, 1944.

4. International Nickel Co. Tech. Bull. T-35.

5. Almen, J. O., and Laszlo, A., "Uniform-Section Disk Springs," _ASME_, _58_, 305-14 (1936).

6. Wempner, G. A., "The Conical Disk Spring," _Proc. U.S. National Cong. Appl. Mech._, 473-78 (1958).
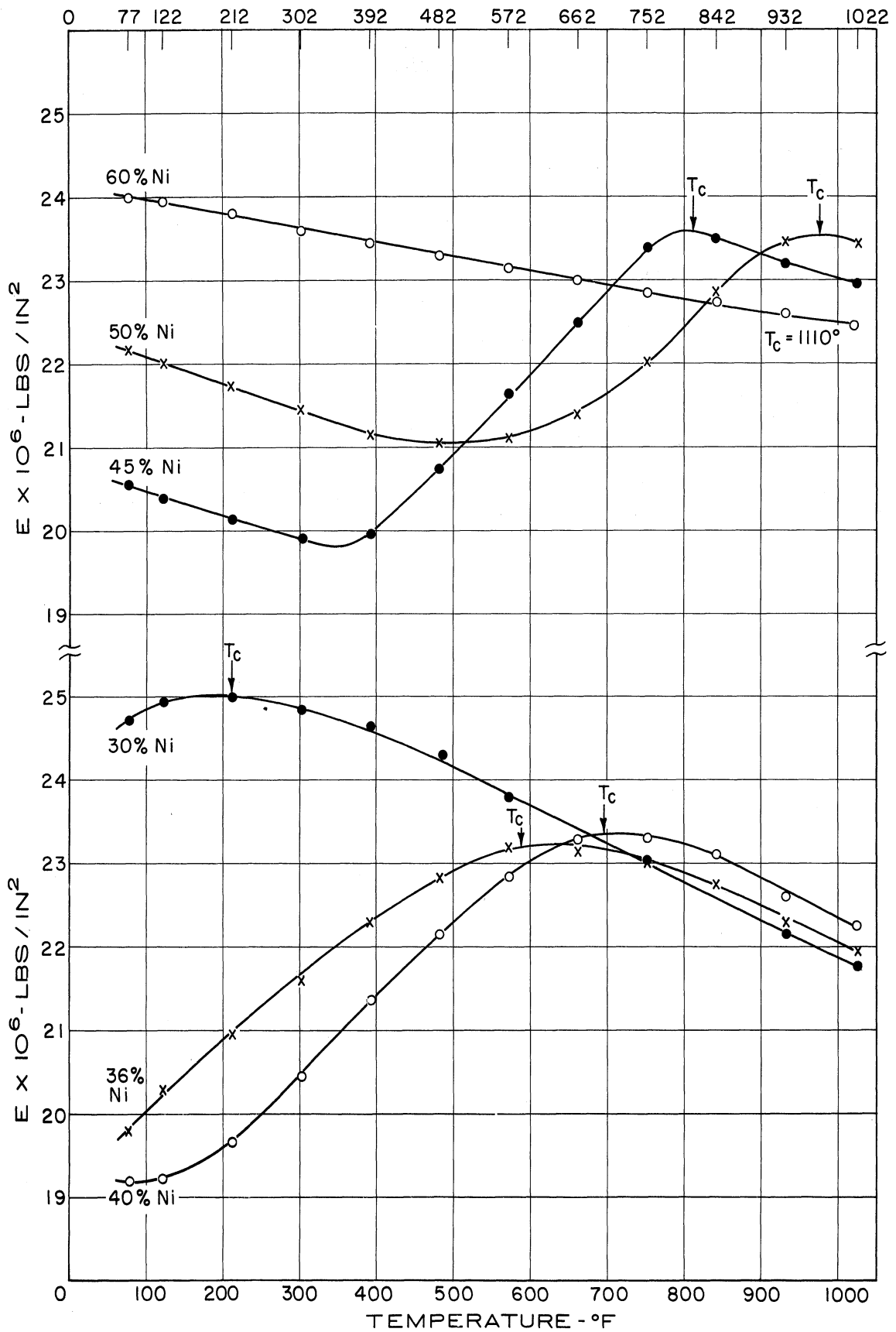
Fig. 1. Young's modulus versus temperature for iron-nickel family between 30% and 60% nickel.

40
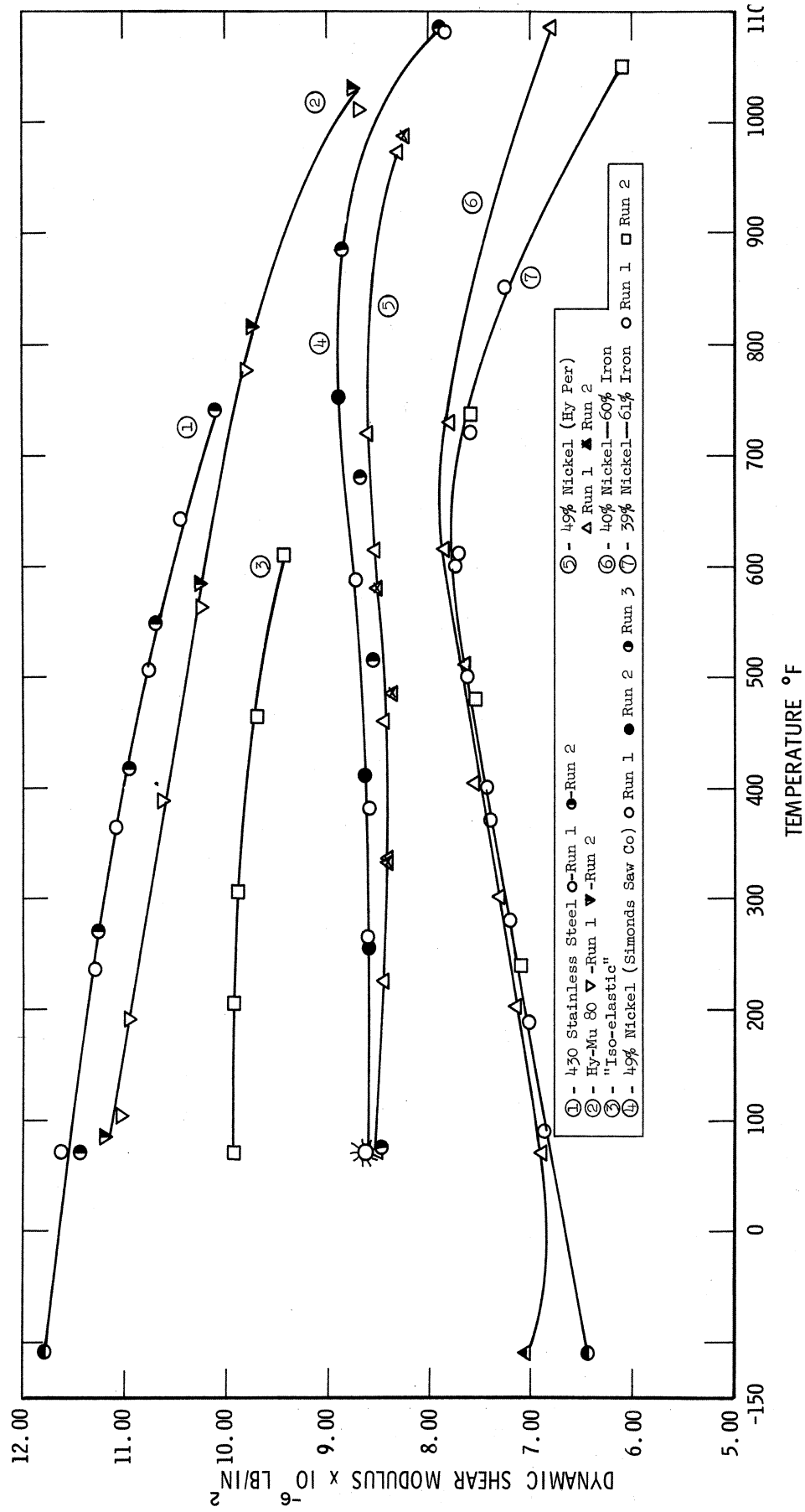
Fig. 2. Dynamic shear modulus versus temperature.

41
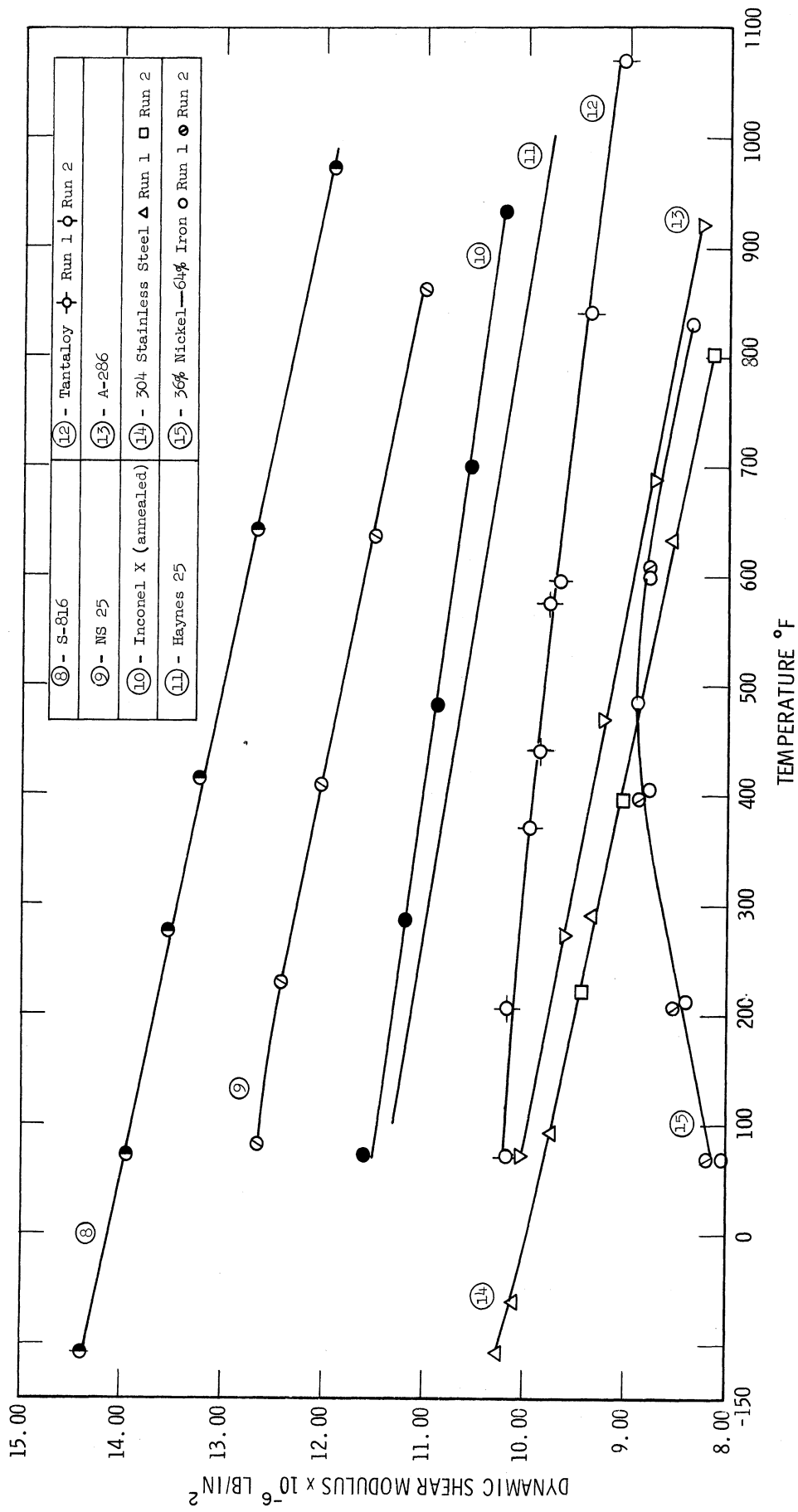
Fig. 3. Dynamic shear modulus versus temperature.
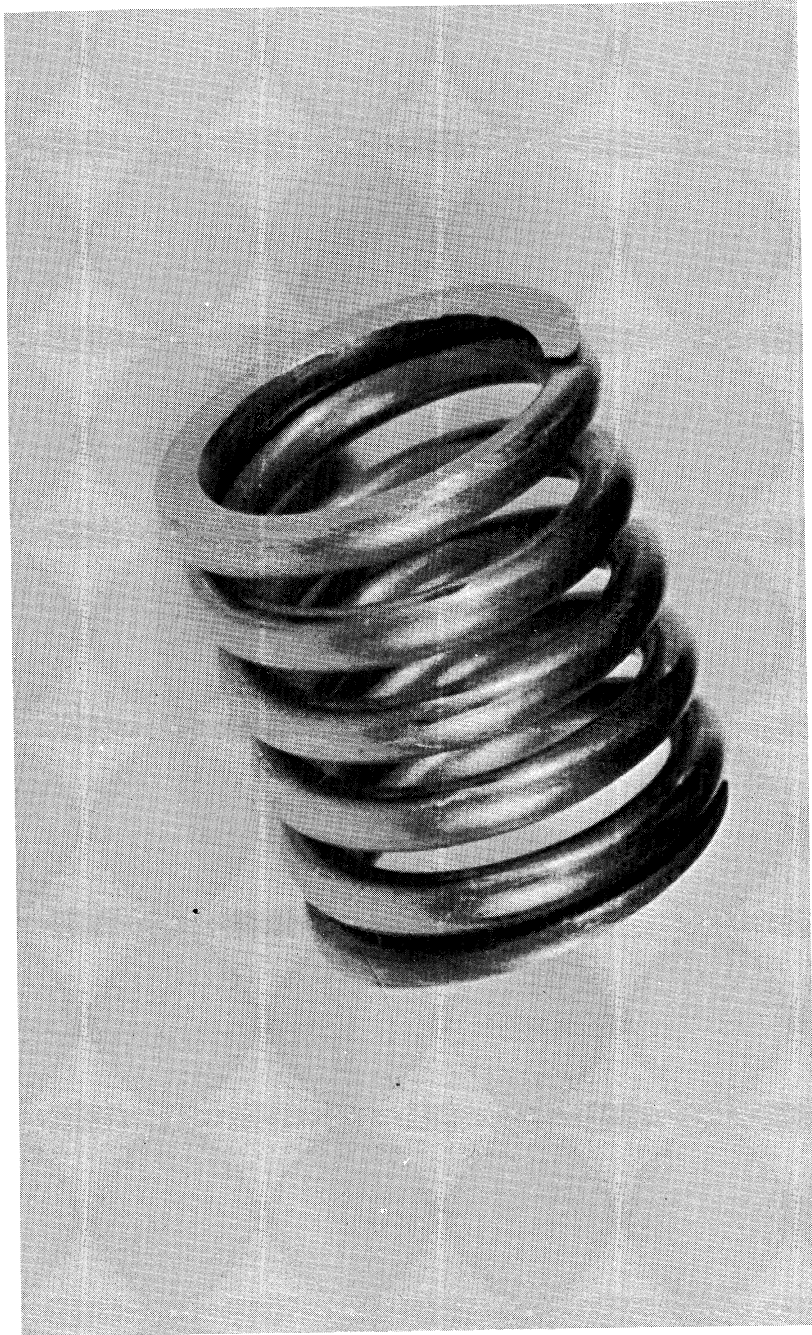
Fig. 4. 40% nickel alloy compression spring. Wire diameter 0.125 in., outside diameter 0.98 in.
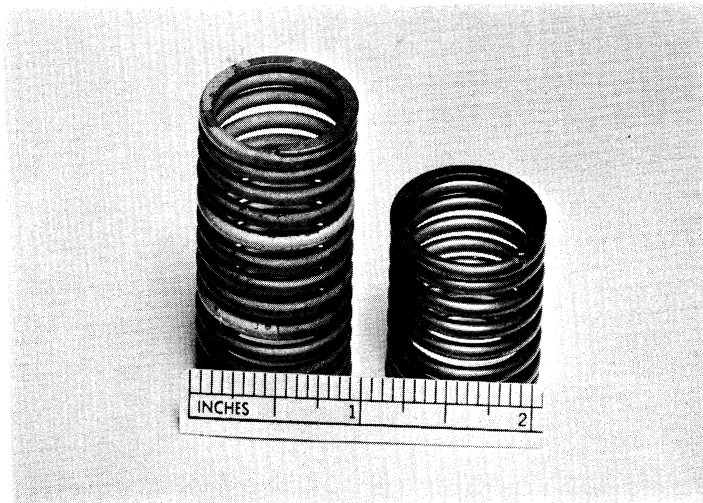
Fig. 5. 40% nickel alloy coils. Wire diameter 3/32 in., c = 9.0, n = 9-1/2, p = 9/64 in. (on left); wire diameter 3/32 in., c = 9.0, n = 4-2/3, p = 9/64 in. (on right). Note surface scaling.

Fig. 6. 40% nickel alloy coils. Wire diameter 3/32 in., c = 7.0, n = 15, p = 9/64 in. (on left); wire diameter 3/32 in., c = 6.95, n = 10, p = 9/64 in (on right).
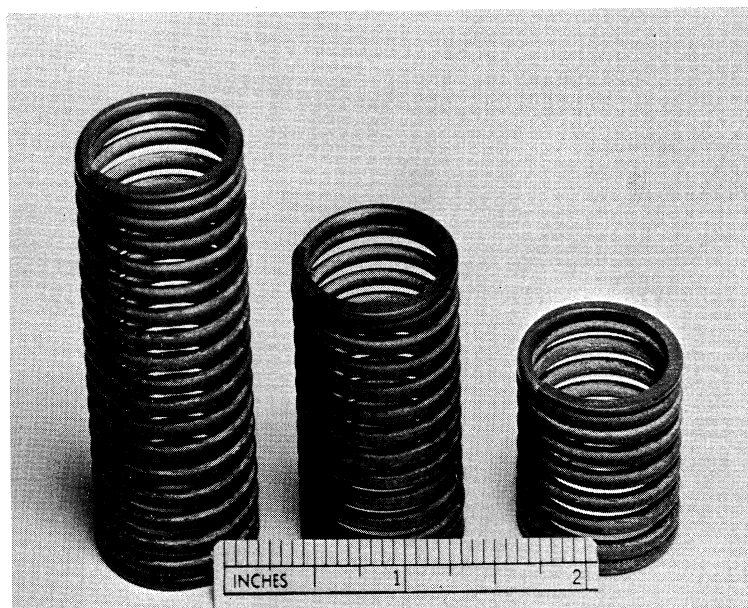
Fig. 7. Inconel X spring temper coils. Wire diameter 3/32 in., c = 9.0, n = 15, p = 9/64 in. (on left); wire diameter 3/32 in., c = 9.0, n = 9-1/2, p = 9/64 in. (middle); wire diameter 3/32 in., c = 9.0, n = 6, p = 9/64 in. (on right).
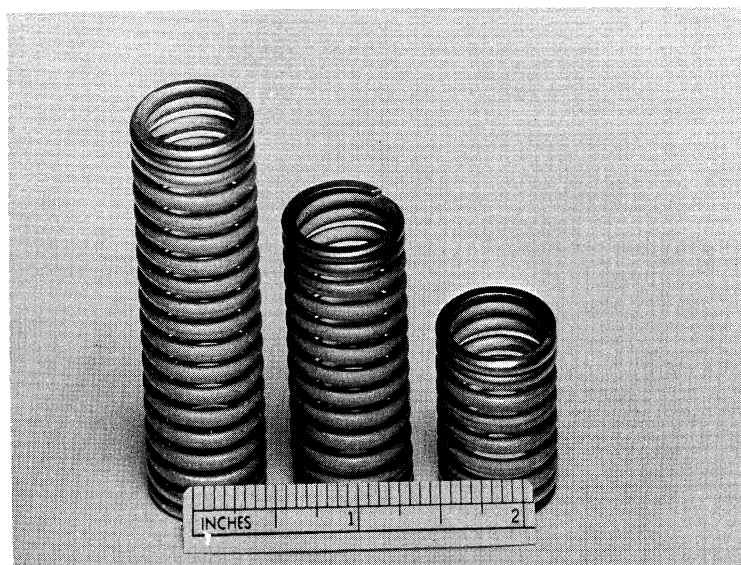
Fig. 8. Inconel X spring temper coils. Wire diameter 3/32 in., c = 7.0, n = 15, p = 9/64 in. (on left); wire diameter 3/32 in., c = 7.0, n = 10, p = 9/64 in. (middle); wire diameter 3/32 in., c = 7.0, n = 5, p = 9/64 in. (on right).
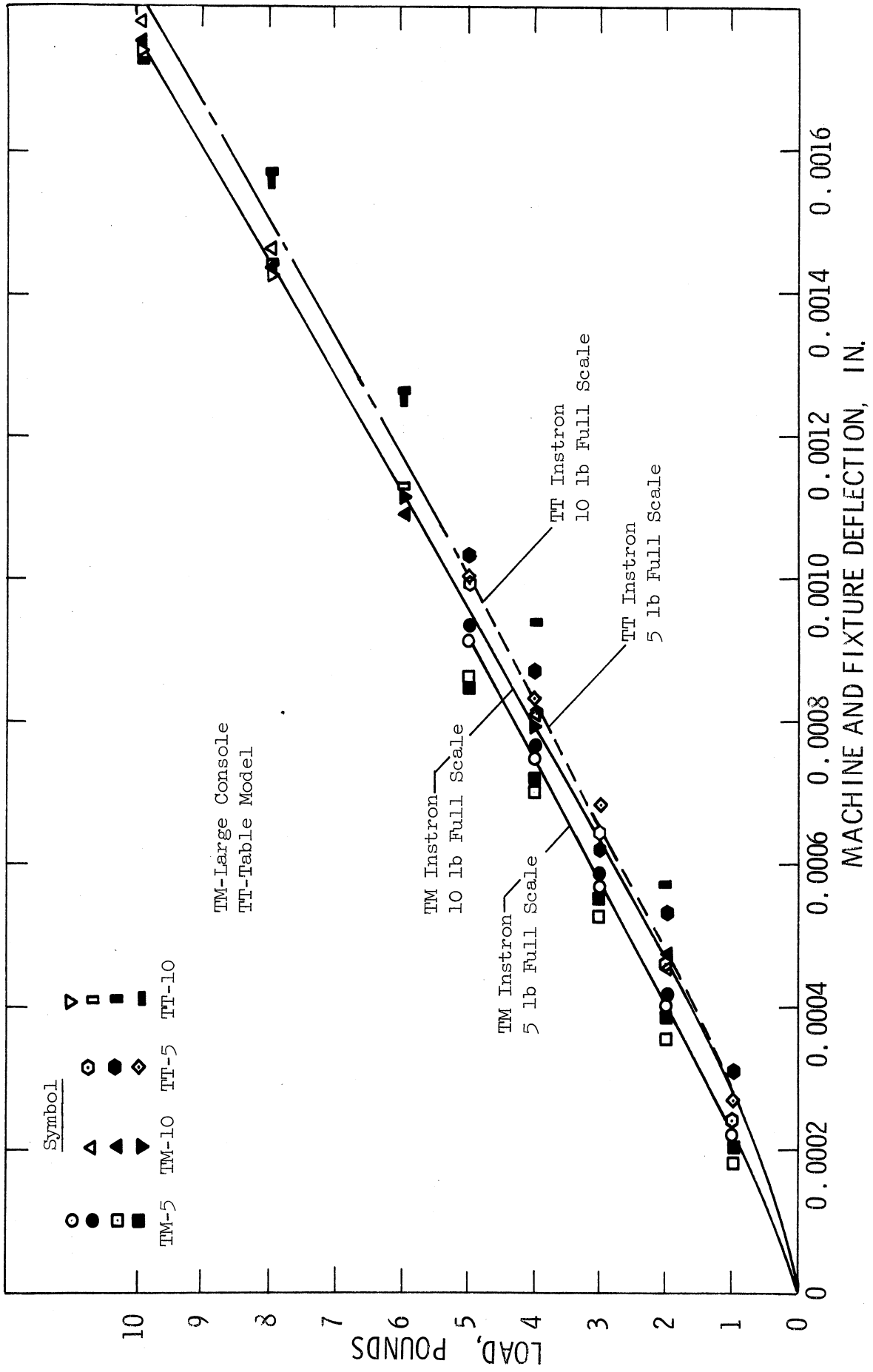
Fig. 9. Load versus deformation for Instron testing machines with test fixtures.
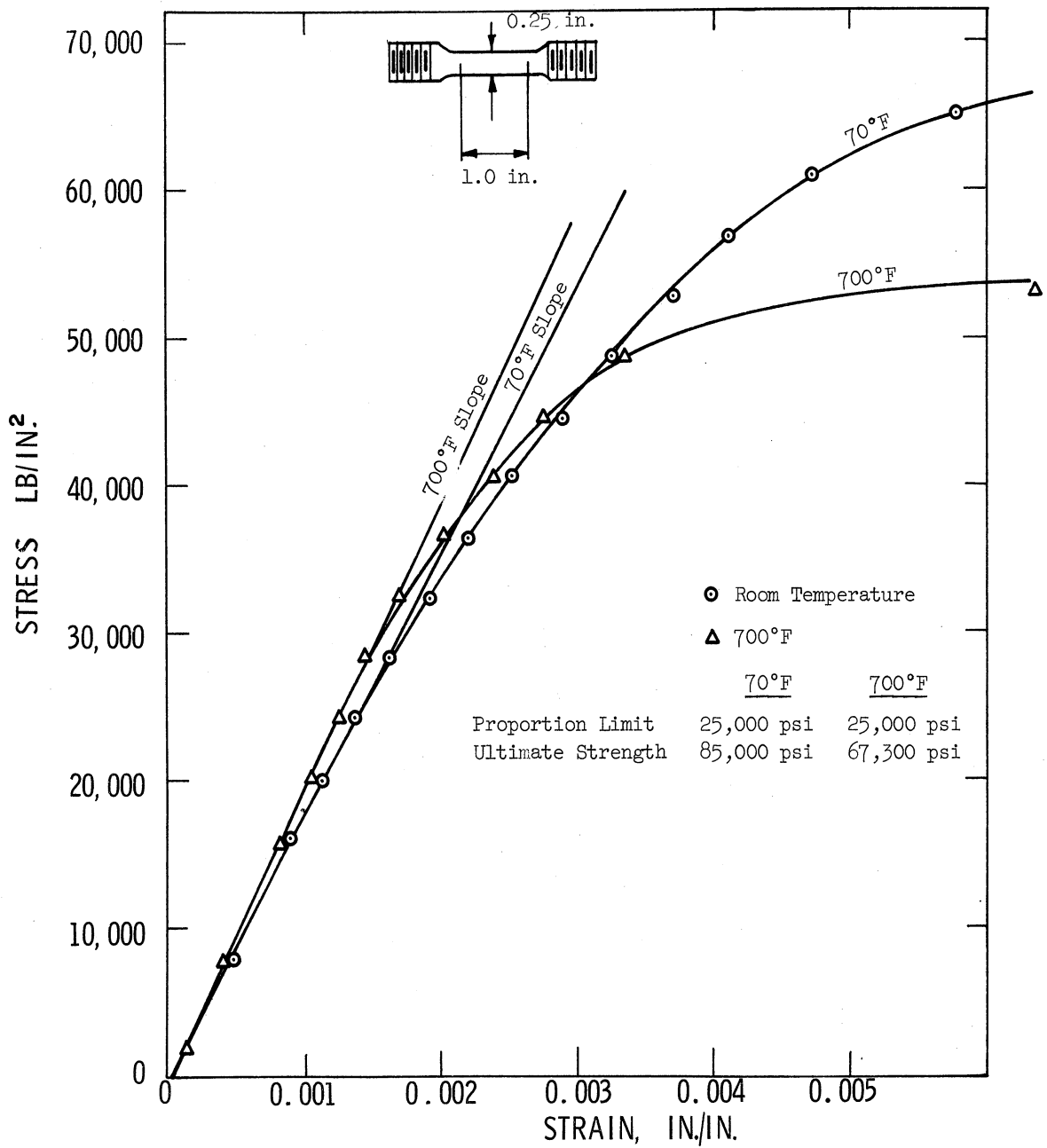
Fig. 10. Stress-strain diagrams for 40% nickel—60% iron alloy at 70 and 700°F. Material annealed before tests at 1200°F for 2 hours.

Deflection vs Load @ 440°F
for
40% Nickel-60% Iron Helical Coil Spring

Outside diameter	0.98
Wire diameter	0.125
Free length	1.01
Horizontal Scale	1 pound per div.
Vertical scale	0.01 inch per div.
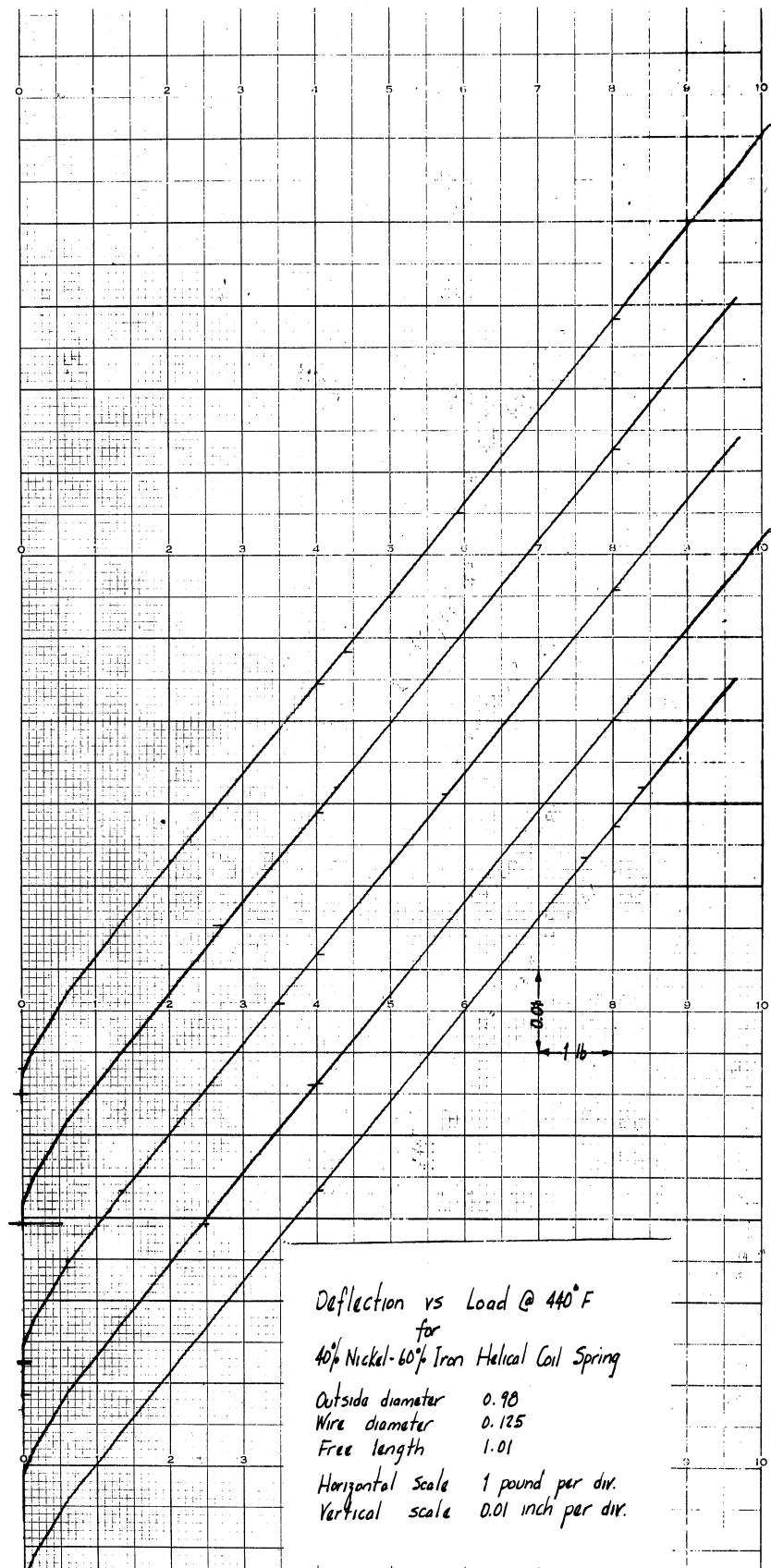
Fig. 11. Load-deflection output of coil spring as traced by recorder. 40% nickel alloy at 440°F.

Deflection vs Load @ 695°F
for
40% Nickel·60% Iron Helical Coil Spring

Outside diameter   0.98
Wire diameter   0.125
Free length   1.01
Horizontal scale   1 pound per div.
Vertical scale   0.01 inch per div

Note hysterisis loop
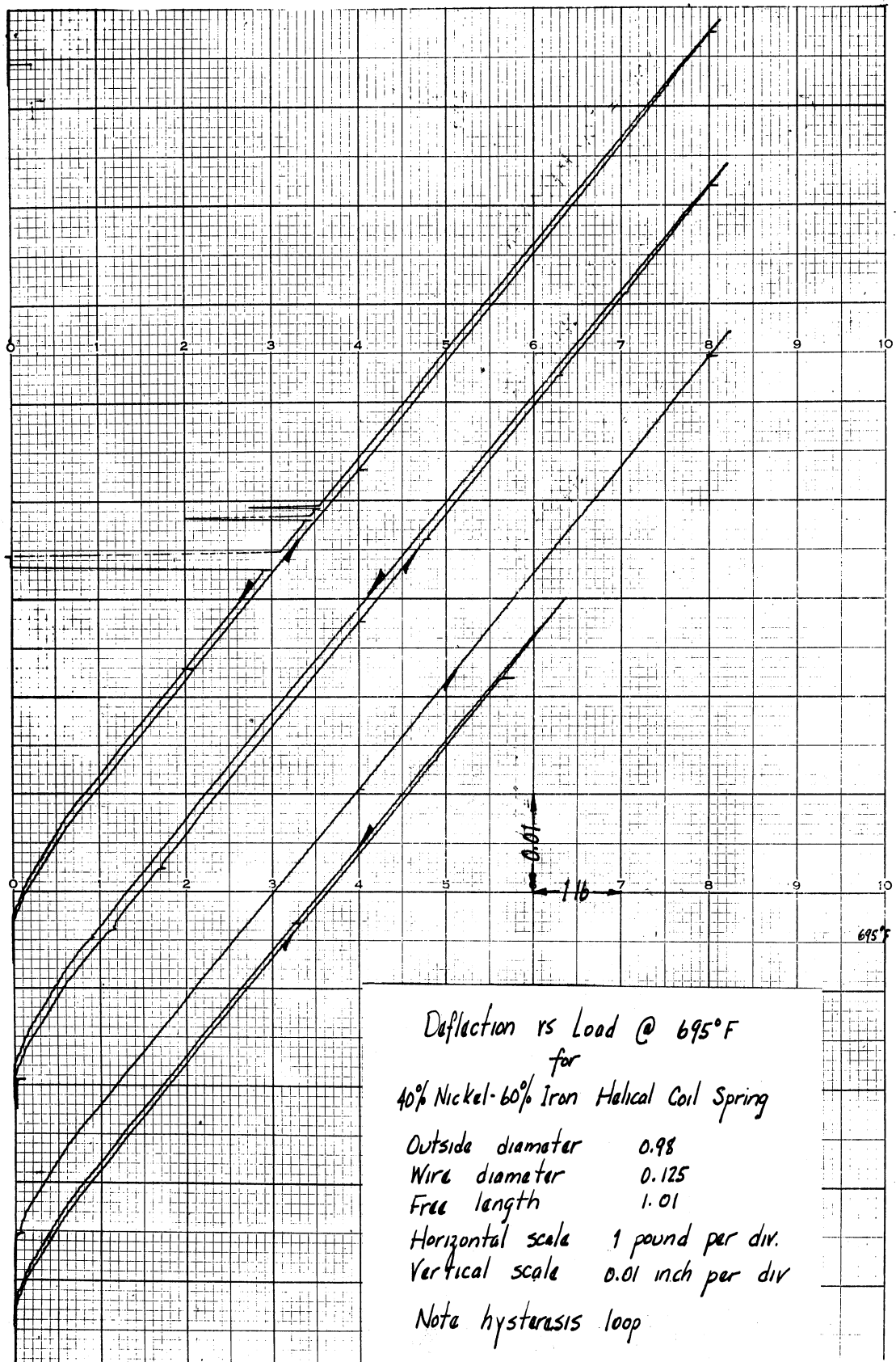
Fig. 12. Load-deflection output of coil spring as traced by recorder. 40% nickel alloy at 695°F.
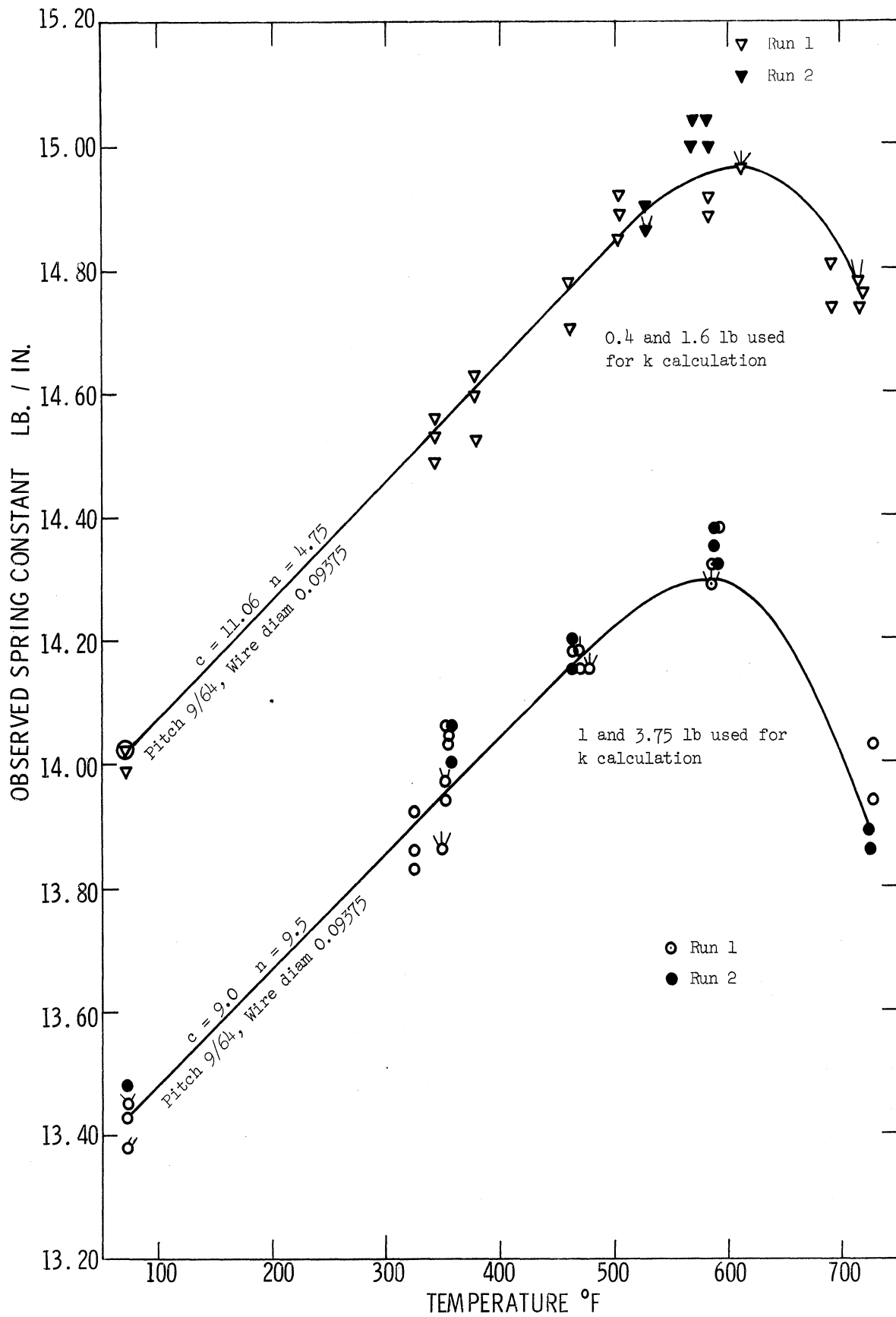
Fig. 13. Spring constant-temperature diagram for 40% nickel alloy coil springs.

Spring Index   9.00
Active Coils   4-2/3
Wire Diam   0.09375
Pitch   9/64
Outside Diam   0.938
c = 9.0, n = 4-2/3

OBSERVED SPRING CONSTANT LB./IN.

27.60   27.20   26.80   26.40   26.00   25.60

TEMPERATURE °F

0   100   200   300   400   500   600   700

○ Run 1
□ Run 2

1 and 4 lb used for k calculation
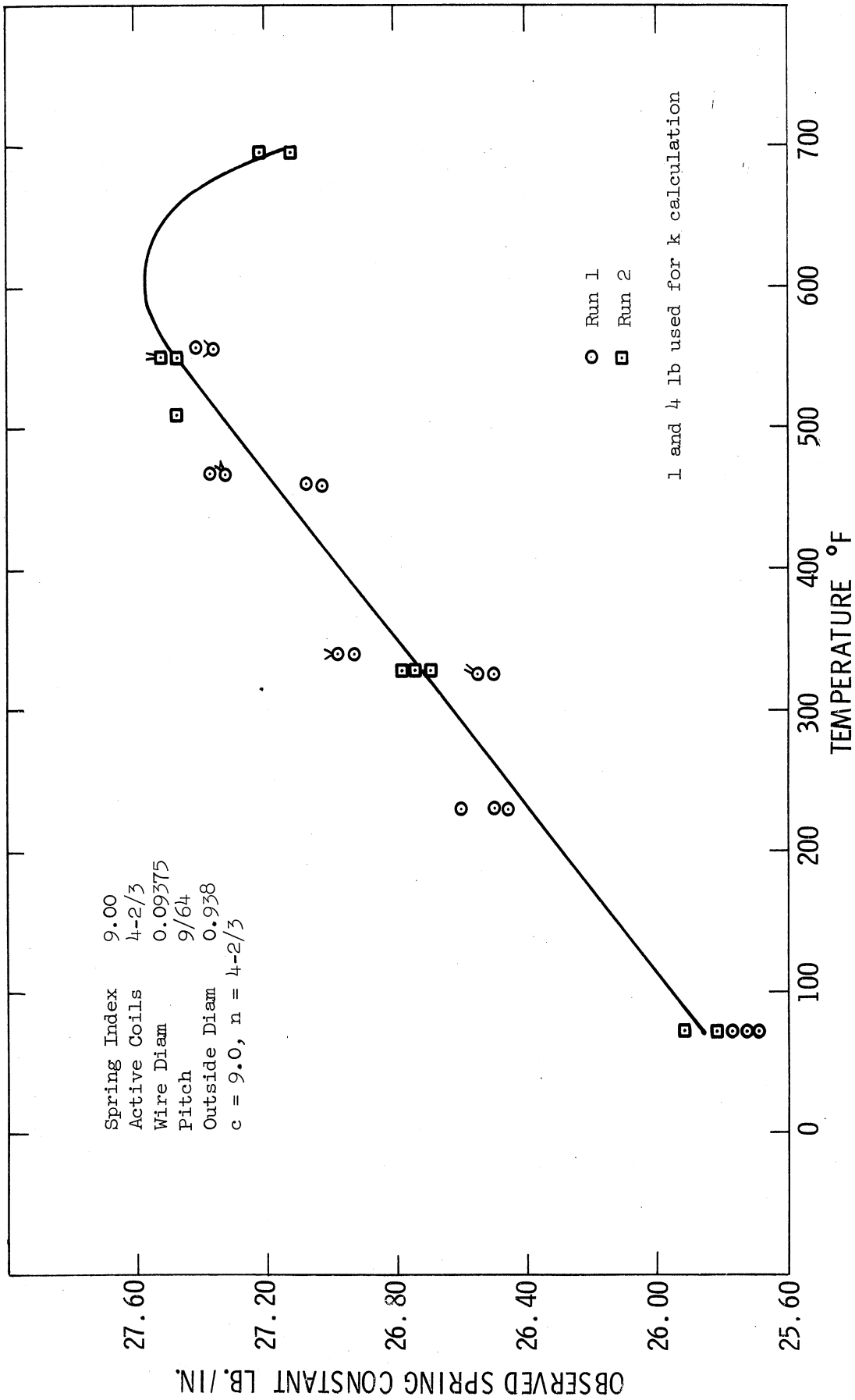
Fig. 14. Spring constant-temperature diagram for 40% nickel alloy coil spring.

51
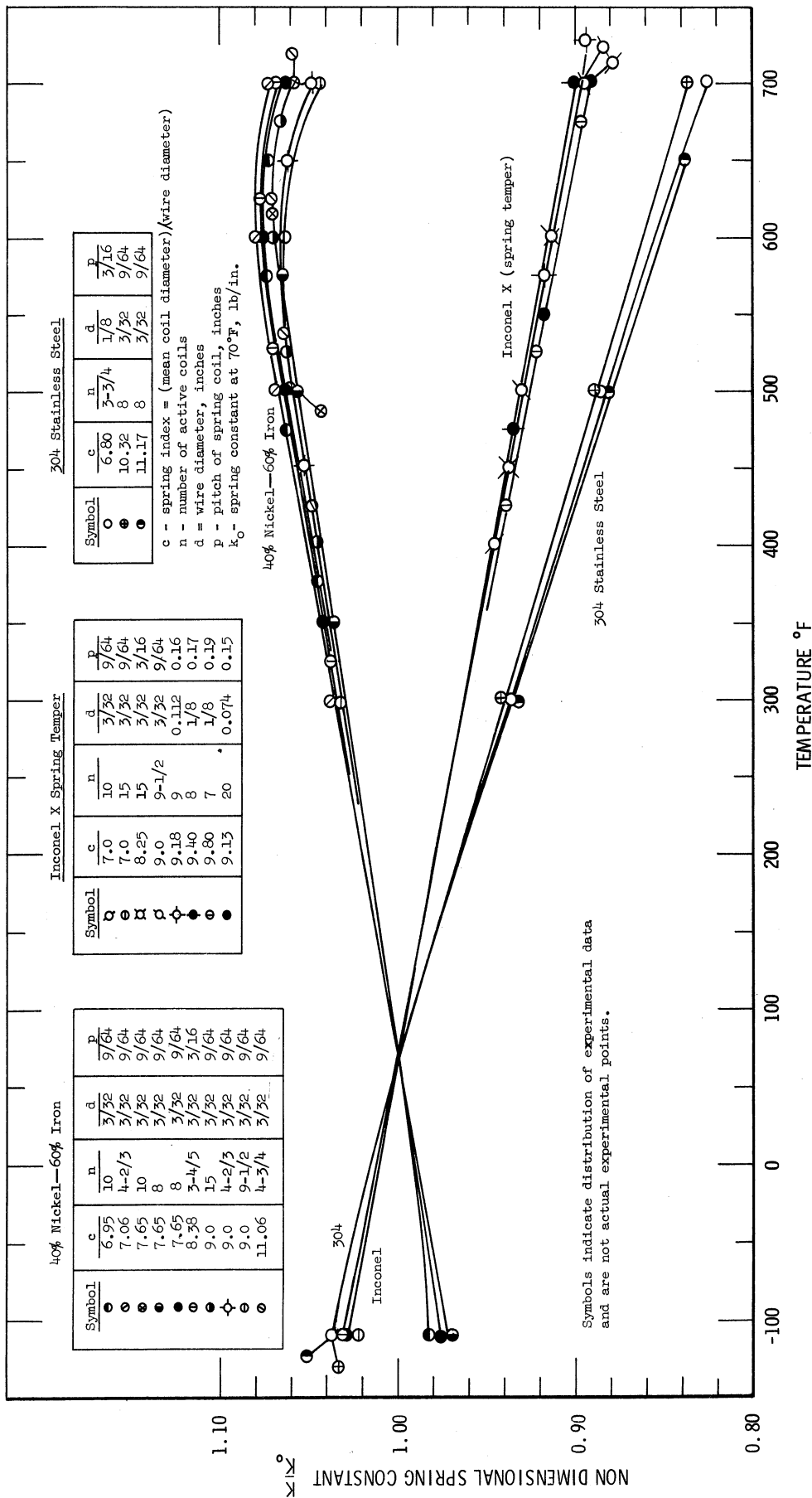
Fig. 15. Nondimensional spring constant versus temperature for 40% nickel alloy, Inconel X spring temper and 304 stainless-steel coil springs.
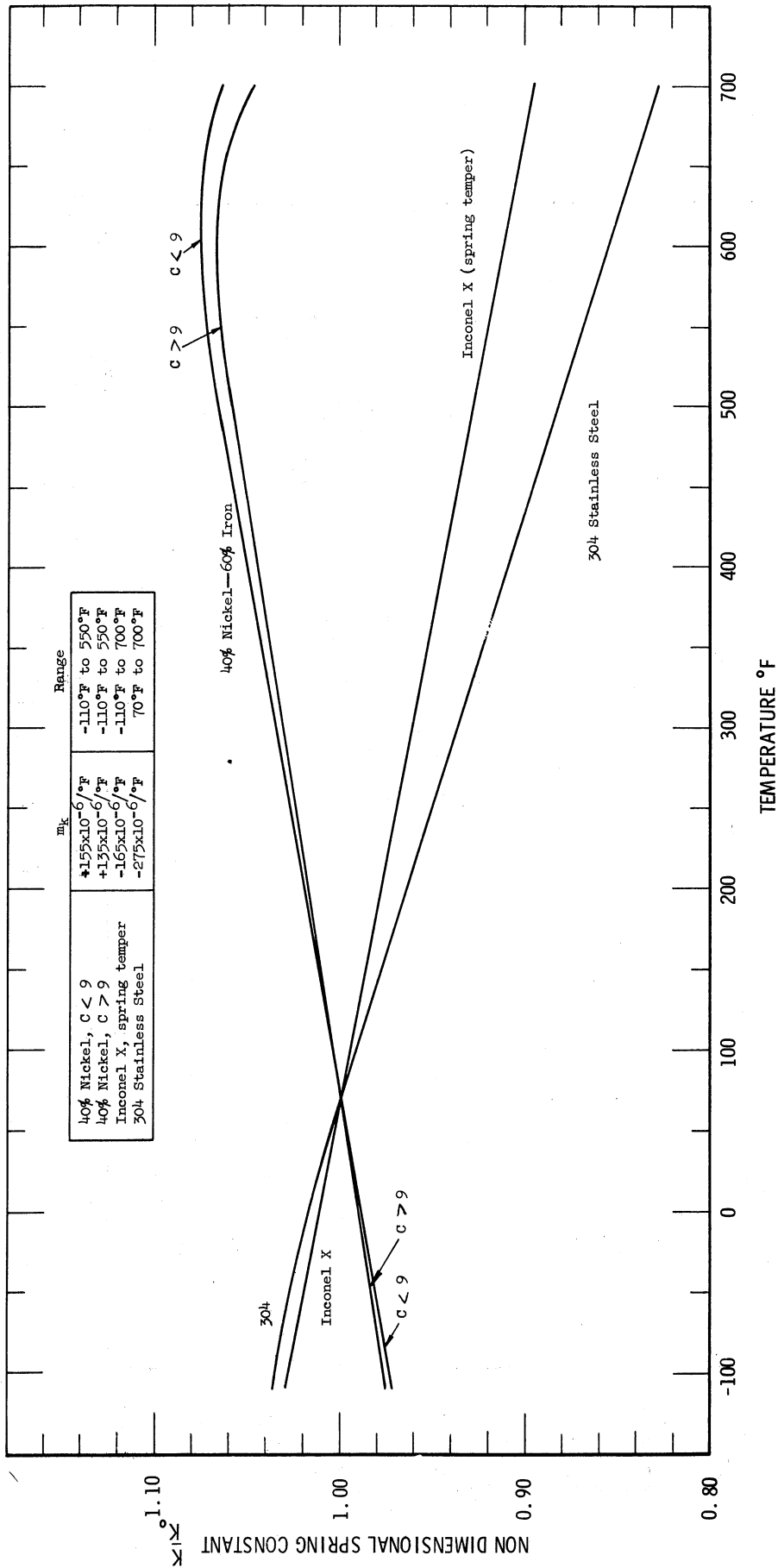
Fig. 16. Nondimensional spring constant versus temperature for 40% nickel alloy, Inconel X spring temper and 304 stainless-steel coil springs. Lines indicate average of data shown in Fig. 15.

53
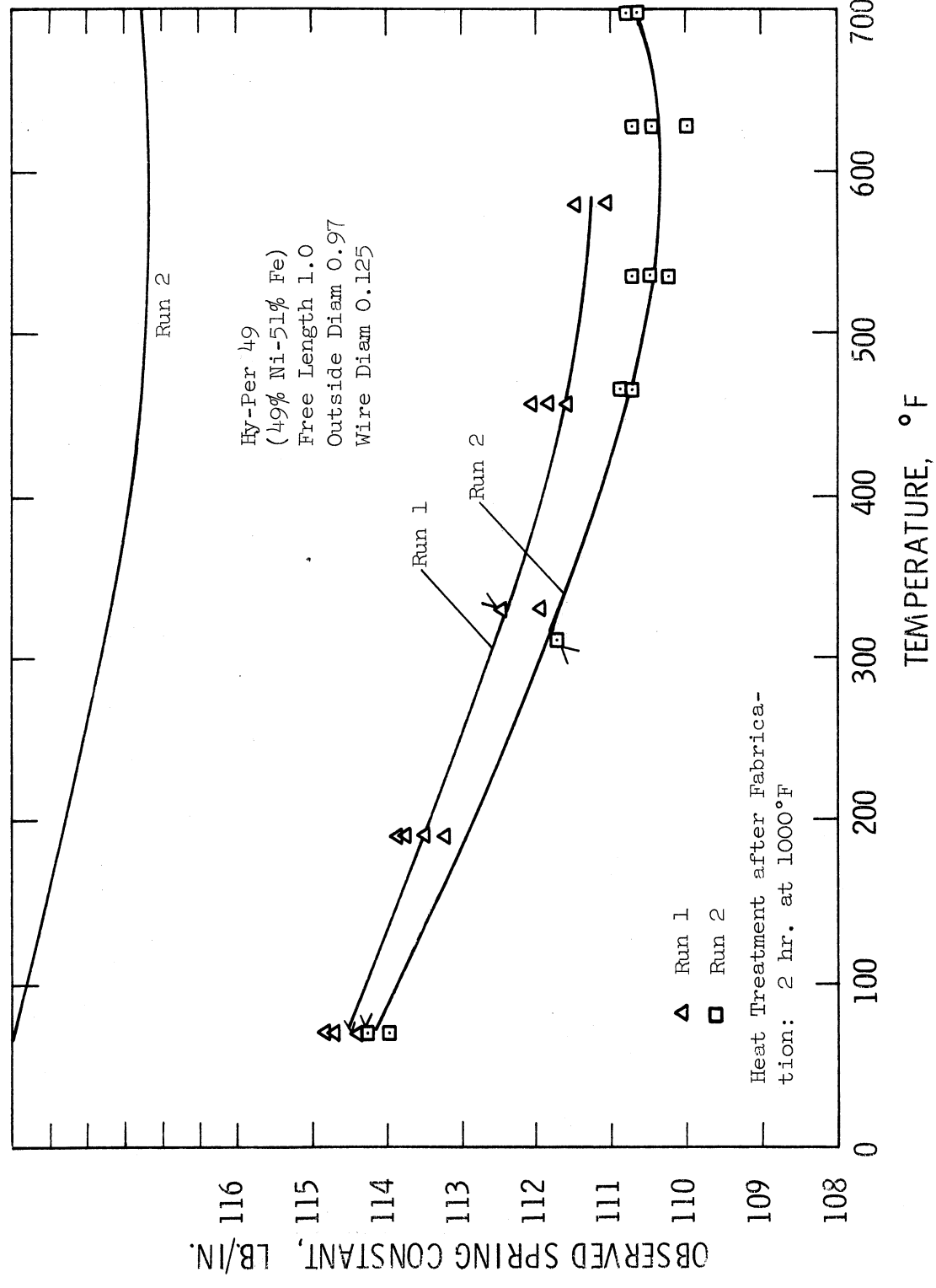
Fig. 17. Plot of spring constant and nondimensional spring constant versus temperature for 49% nickel-balance iron coil spring.
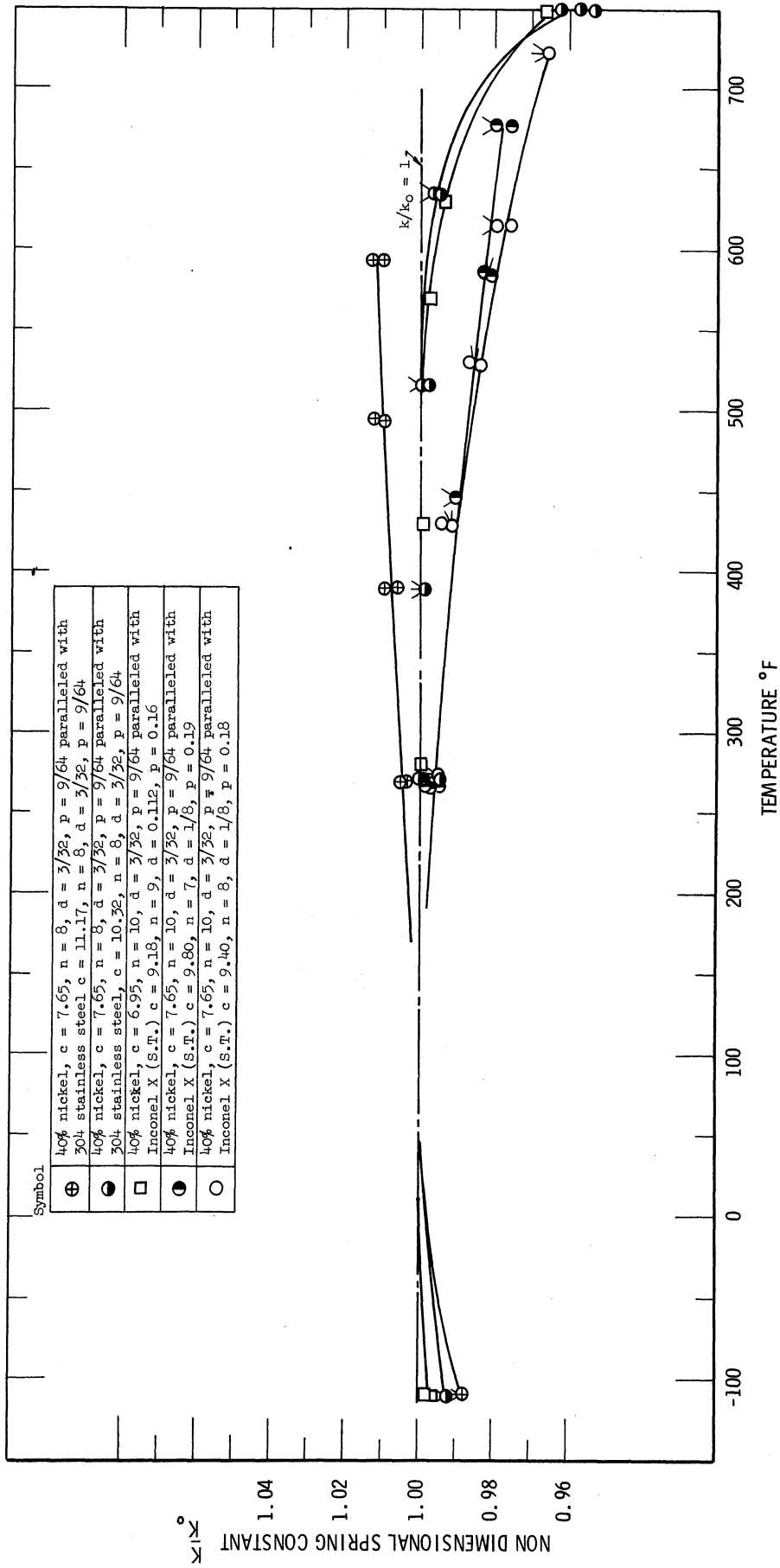
Fig. 18. Nondimensional spring constant versus temperature for bimetal coil spring systems tested.
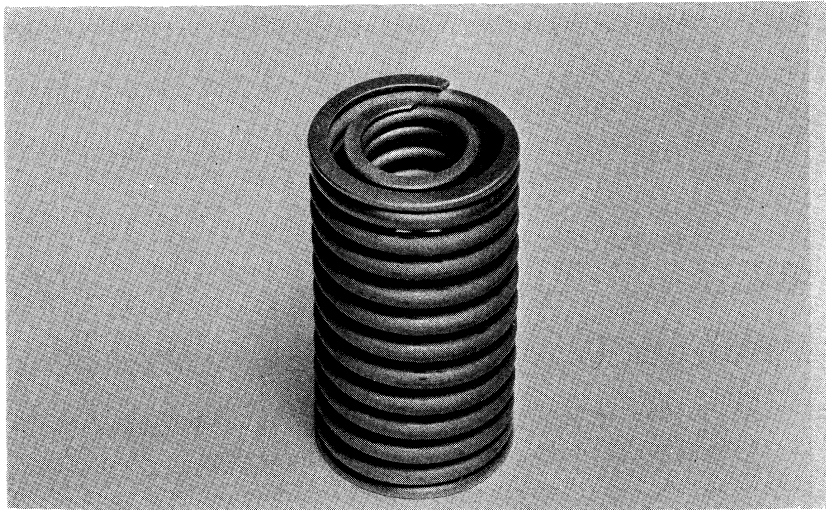
Fig. 19. 40% nickel alloy c = 6.95, n = 10, d = 3/32 in., p = 9/64 in. paralleled with Inconel X spring temper c = 9.18, n = 9, d = 0.112 in., p = 0.16 in.
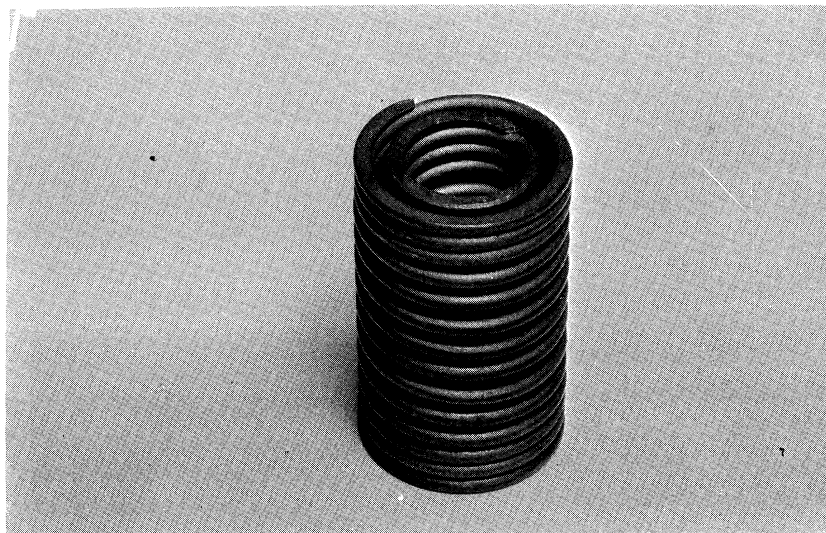
Fig. 20. 40% nickel alloy c = 7.65, n = 8, d = 3/32 in., p = 9/64 paralleled with 304 stainless steel c = 11.17, n = 8, d = 3/32 in., p = 9/64 in.
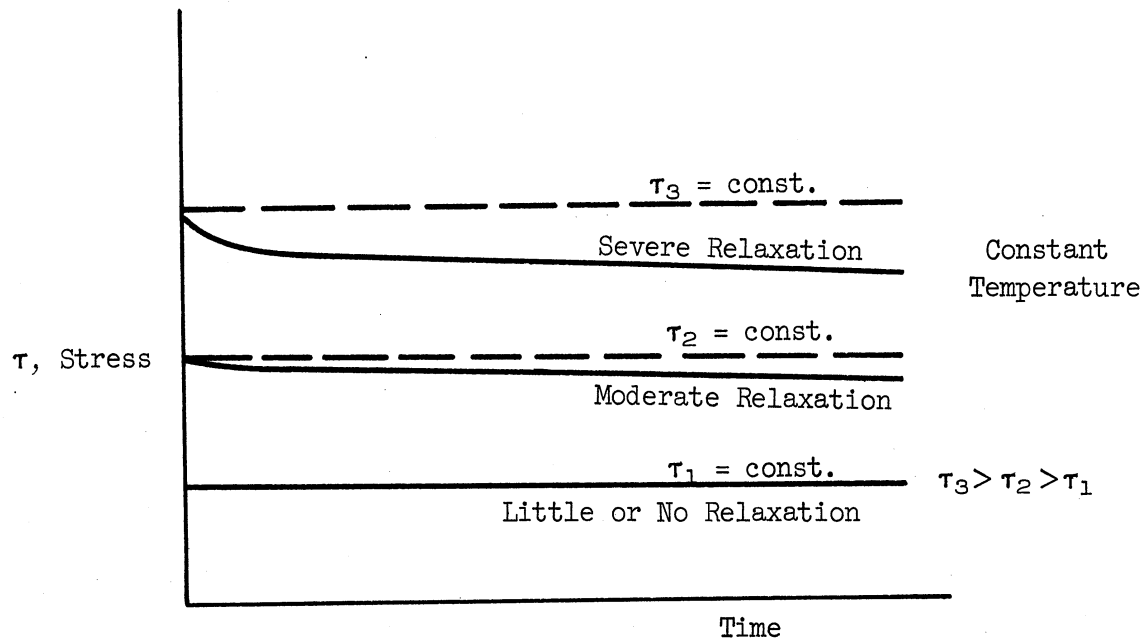
Fig. 21. Stress relaxation diagram.
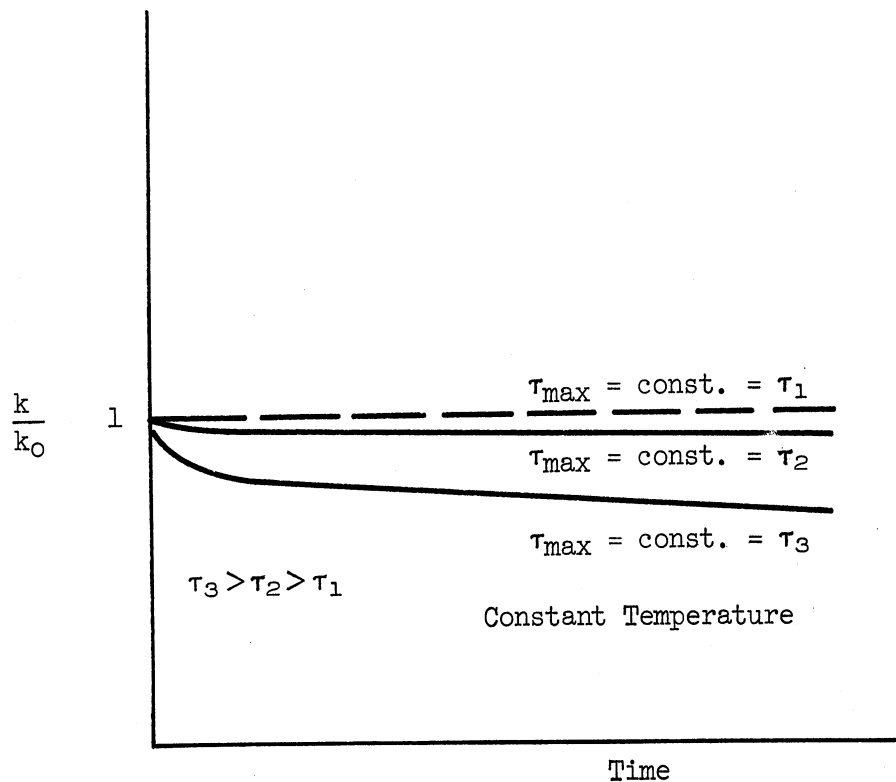
Fig. 22. Spring constant "relaxation" diagram.
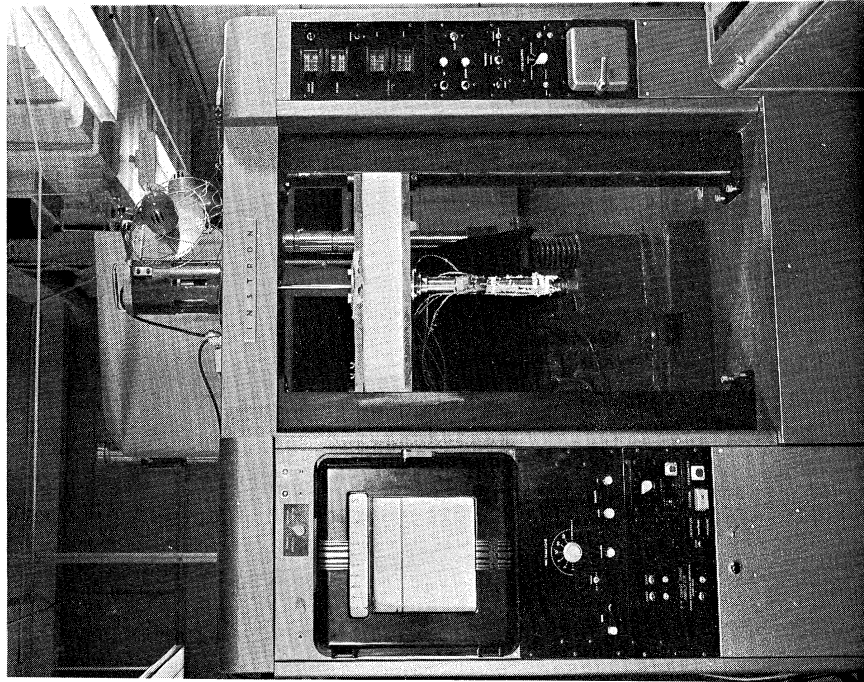
Fig. 23. Instron testing machine type TTCIML.
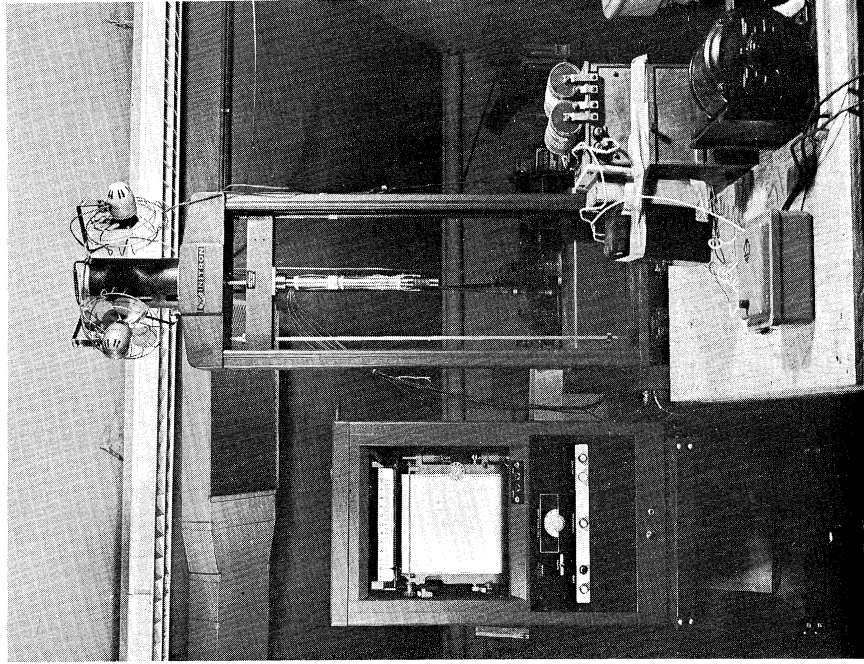
Fig. 24. Instron testing machine table model Type TM with associated furnace and control equipment.
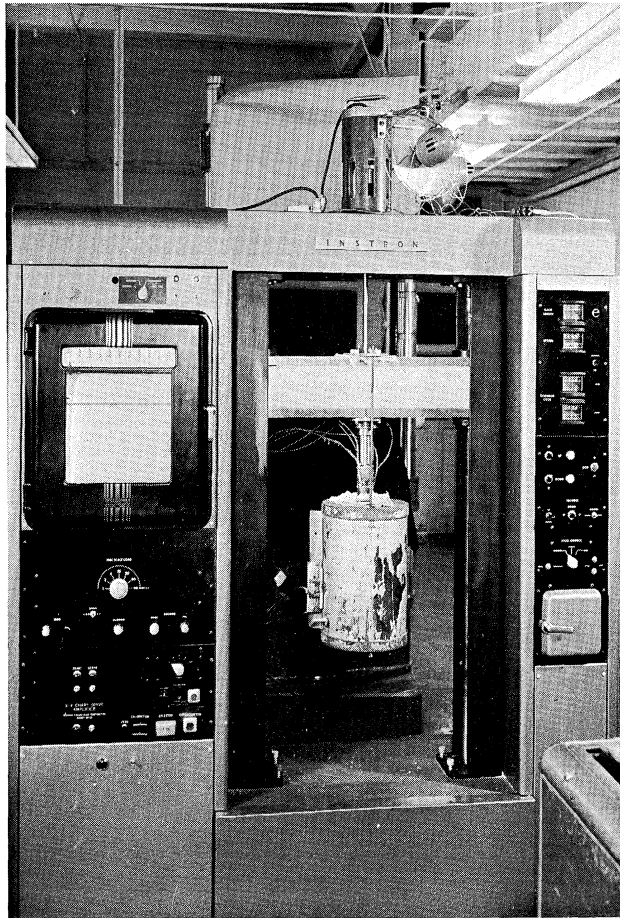
Fig. 25.   Instron testing machine TTCLM1 with furnace and test
fixtures in place.
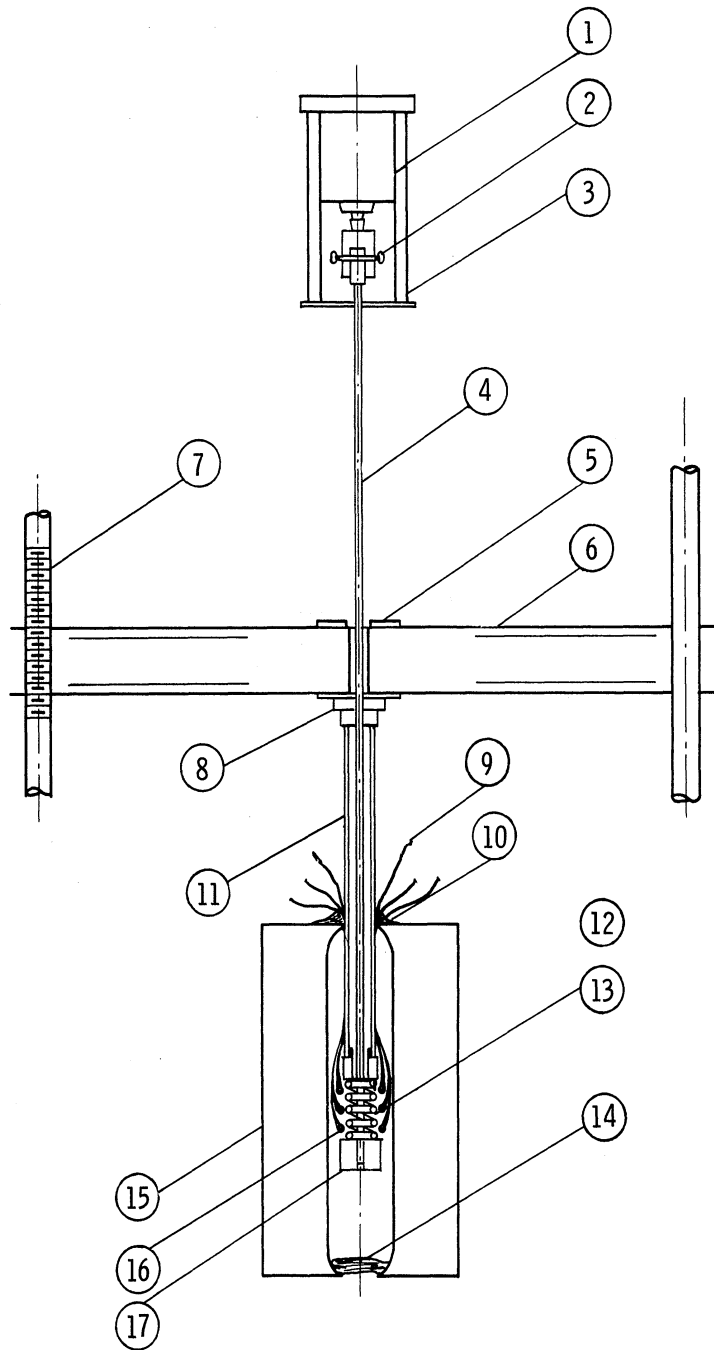
Fig. 26. Spring loading apparatus.

1.	Load cell.	9.	Thermocouple leads.
2.	Securing pin on load cell to pull rod coupling.	10.	Asbestos packing.
		11.	Compression pipe.
3.	Extension jacket.	12.	Upper spring bearing piece.
4.	Pull rod.	13.	Test spring.
5.	Furnace hangar support.	14.	Asbestos packing.
6.	Machine cross head.	15.	Furnace.
7.	Drive screw.	16.	Thermocouple heads.
8.	Compression pipe head piece.	17.	Spring holding plug.
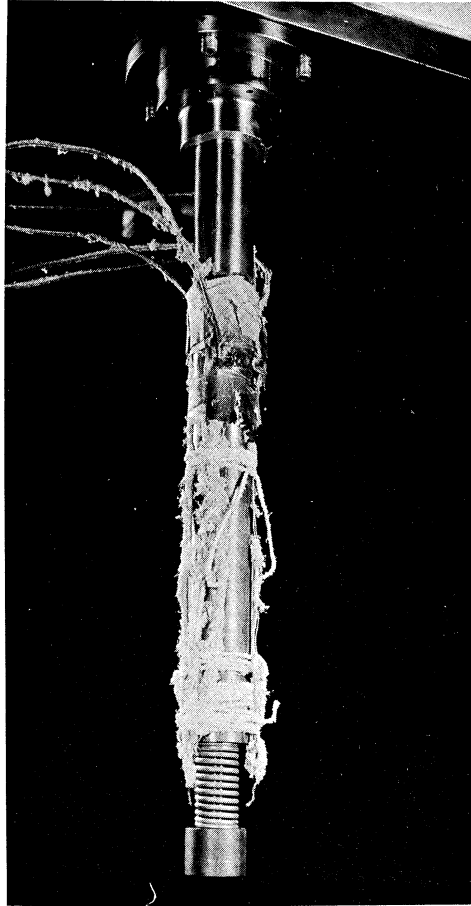
Fig. 27. Lower test fixtures showing spring.
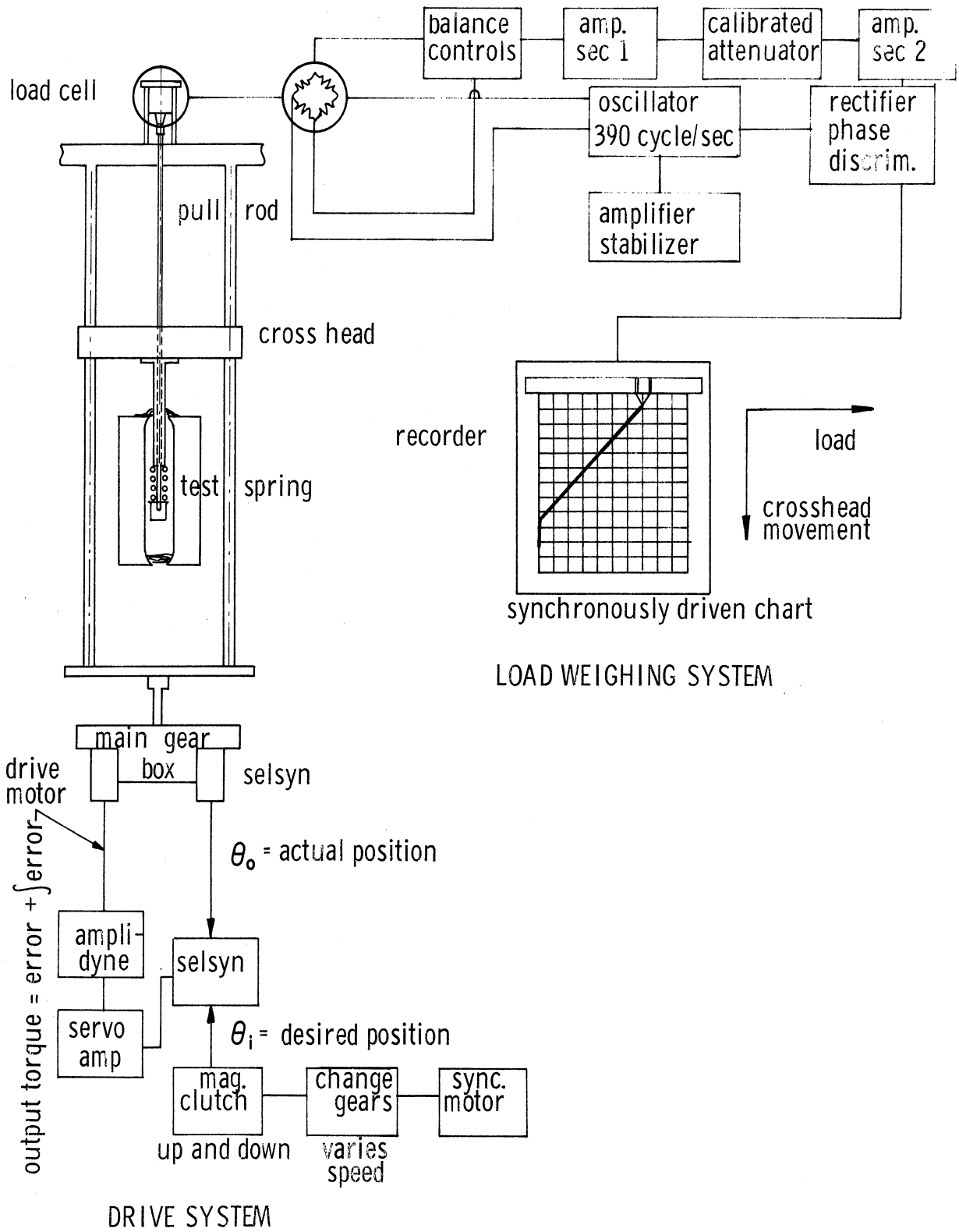
Fig. 28. Schematic diagram of testing apparatus.

230v a.c. 1 ph

Motor

Gear
Box

Maeulen
Controller

+
−

L   C   H

Furnace Temperature
Sensing Thermocouple

GE Relay
Cat. 3656063-GR3

2   1   H

2

4

3   C   L

2   L1   L2

230v a.c. 1 ph

T3   T4

Furnace

Allen Bradley Automatic Motor Starter
Bulletin 709SP, Size 0, Form 2, Type 1
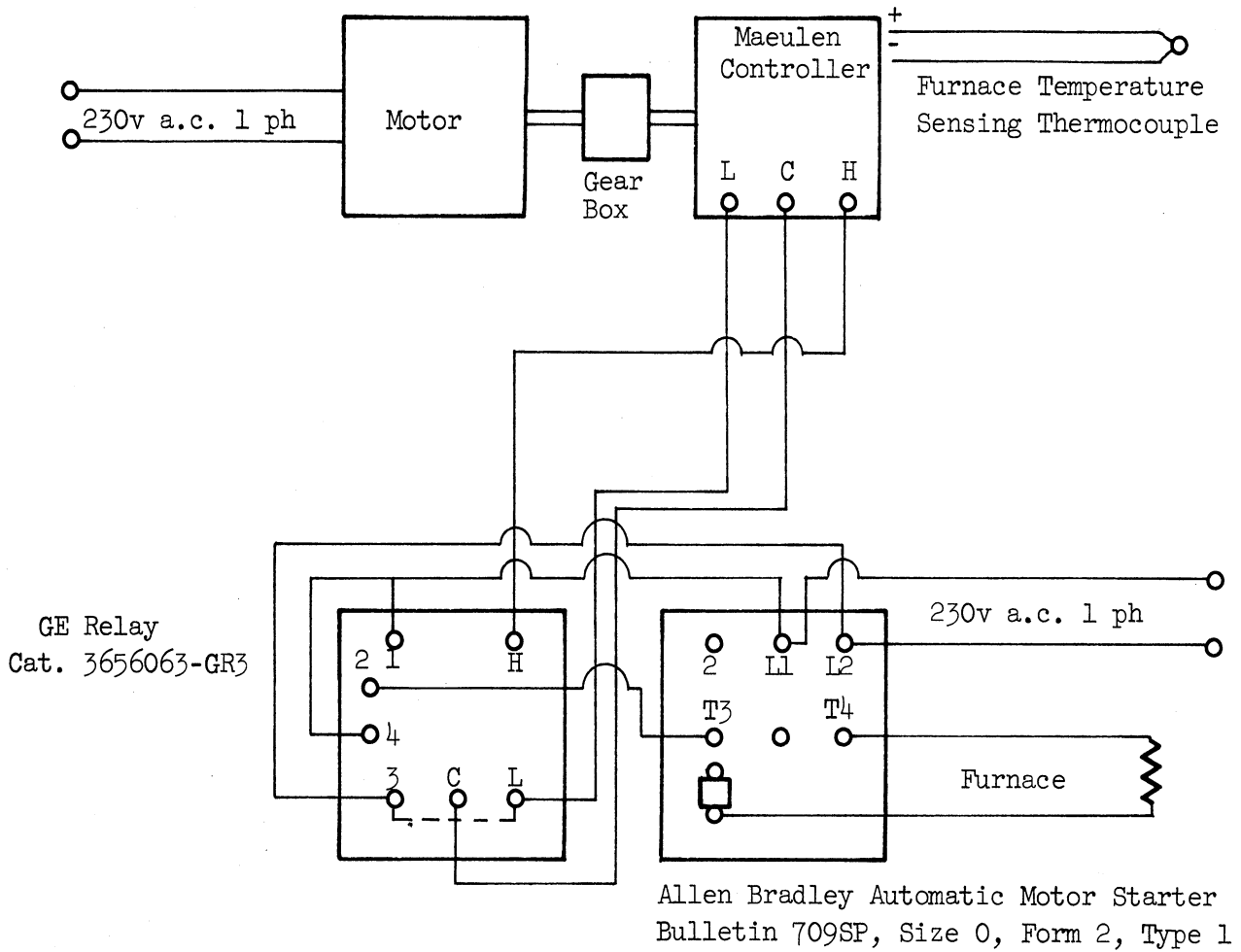
Fig. 29.   Schematic diagram of furnace control.

63
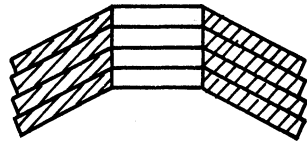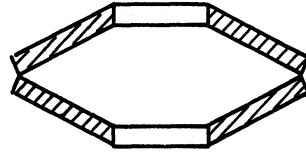
Parallel   Series

Fig. 30. Parallel and series stacking of Belleville spring washers.
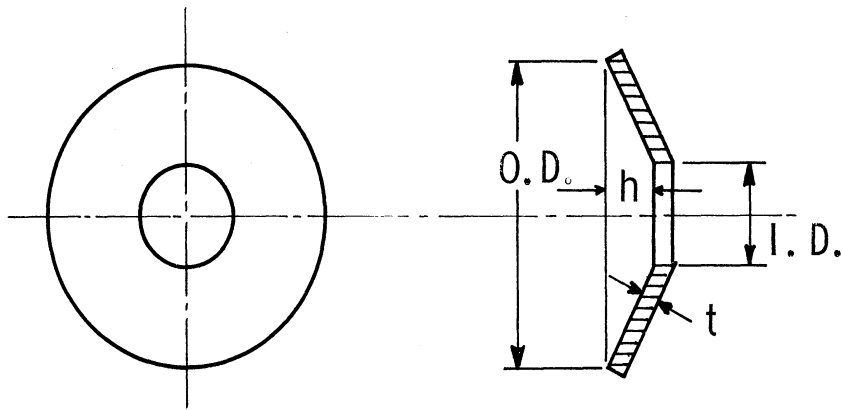
Fig. 31. Geometrical notation of Belleville spring washers.
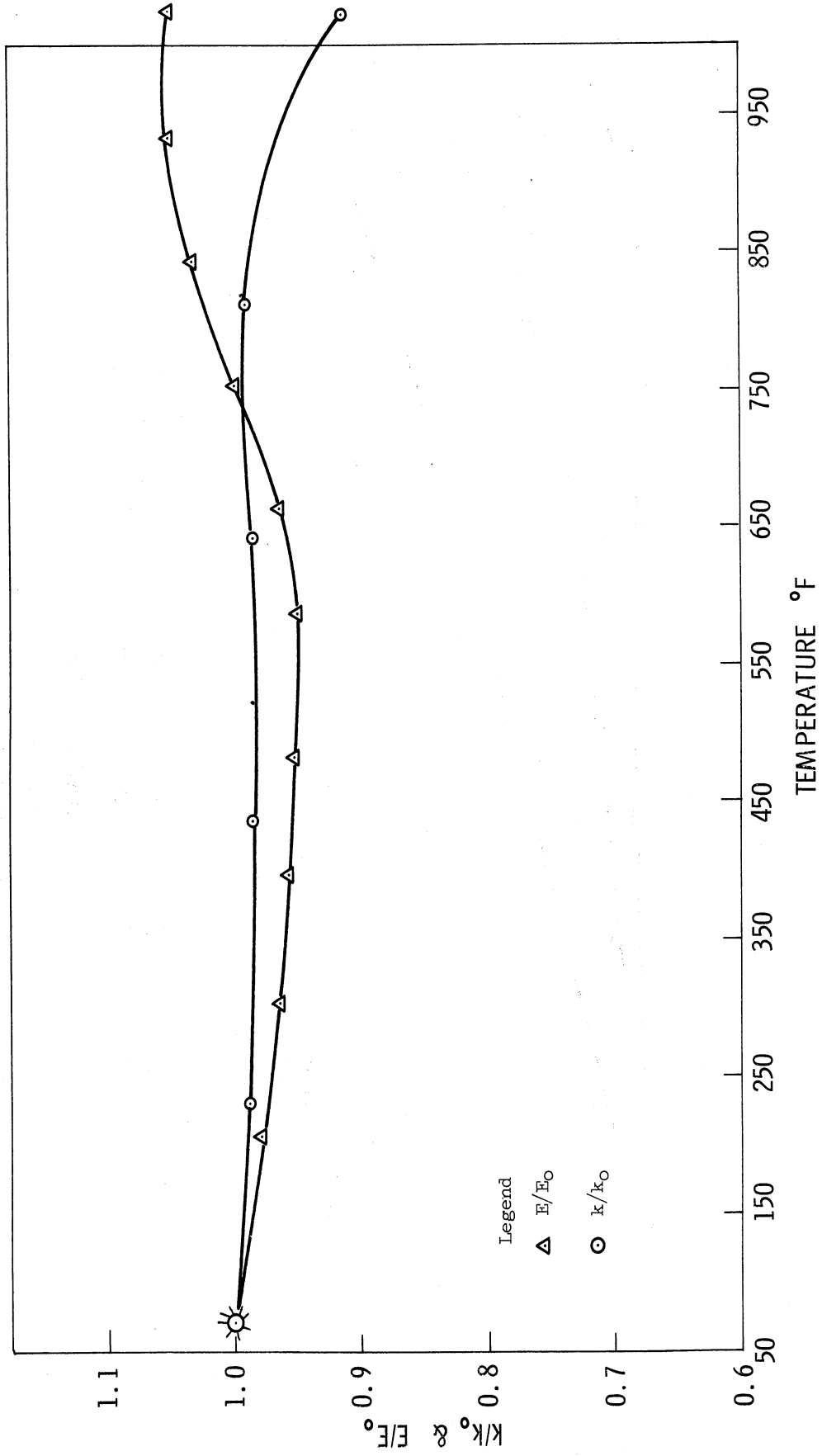
Fig. 32. Dimensionless ratios k/k_O and E/E_O versus temperature for 50% nickel-balance iron alloy where k_O and E_O are values of spring constant and elastic modulus at 70°F.
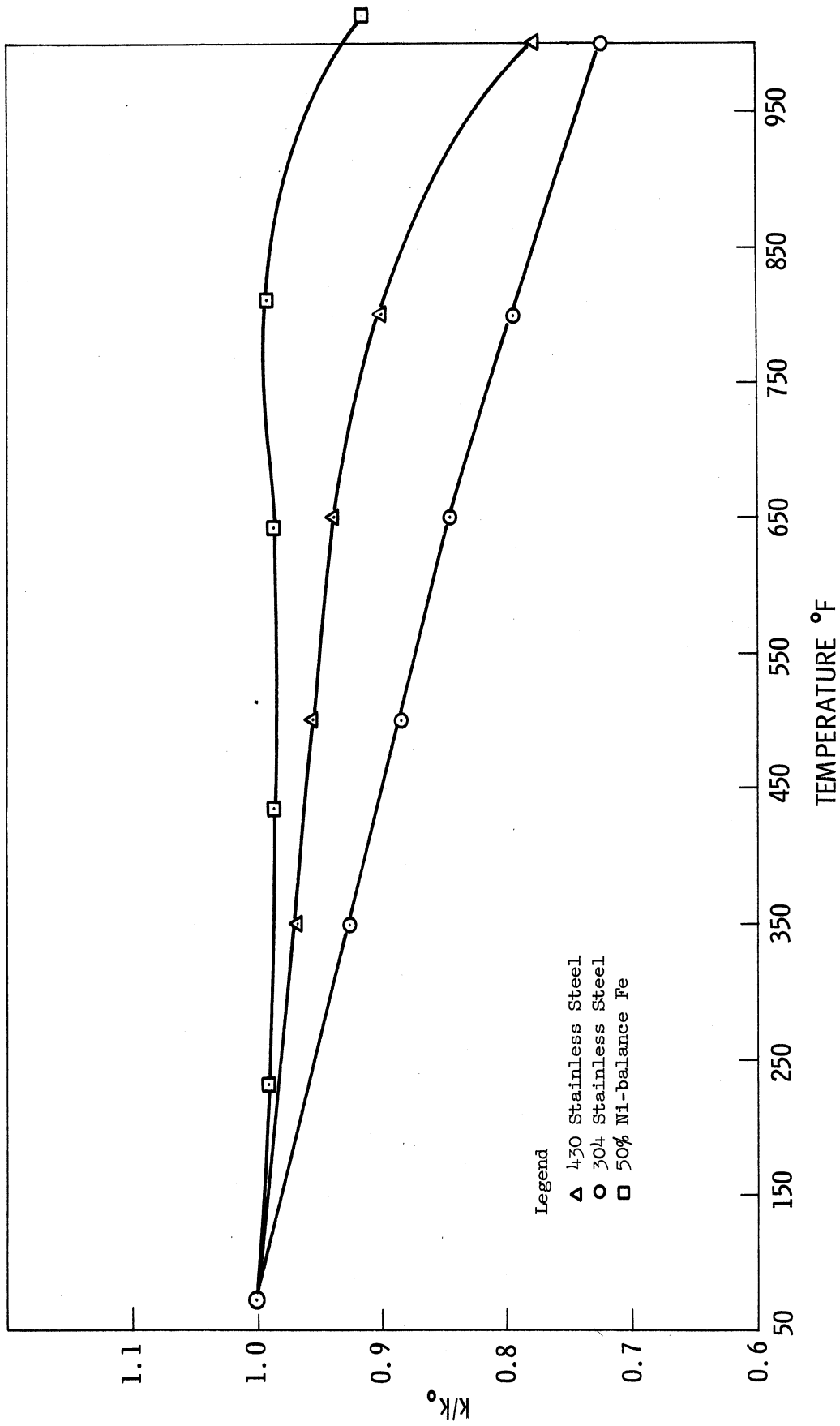
Fig. 33. Elastic modulus versus temperature for 430 stainless steel, 304 stainless steel and 50% nickel-balance iron alloy.
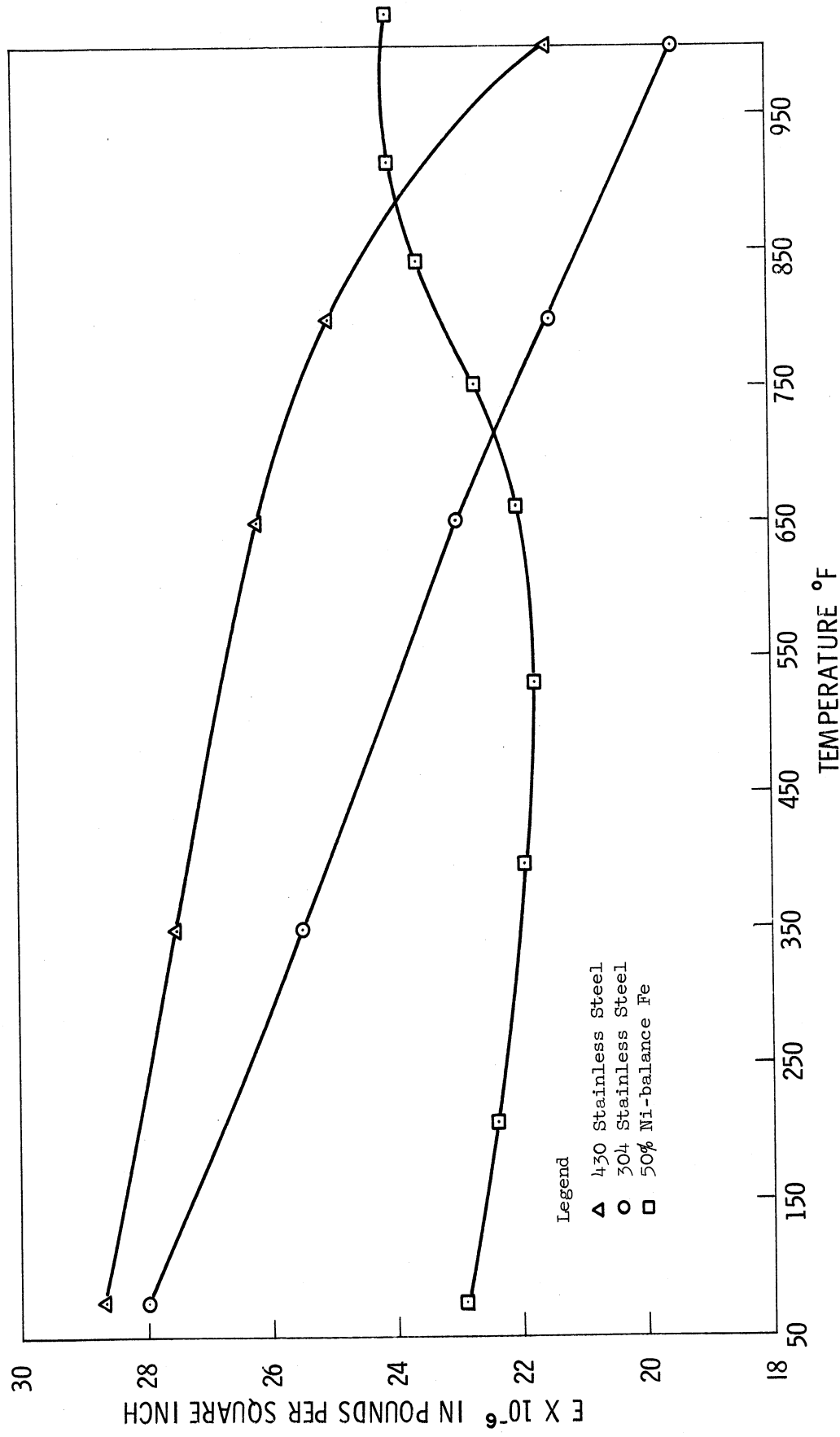
Fig. 34. Dimensionless ratio k/k_0 versus temperature for 430 stainless steel, 304 stainless steel and 50% nickel-balance iron alloy.

67
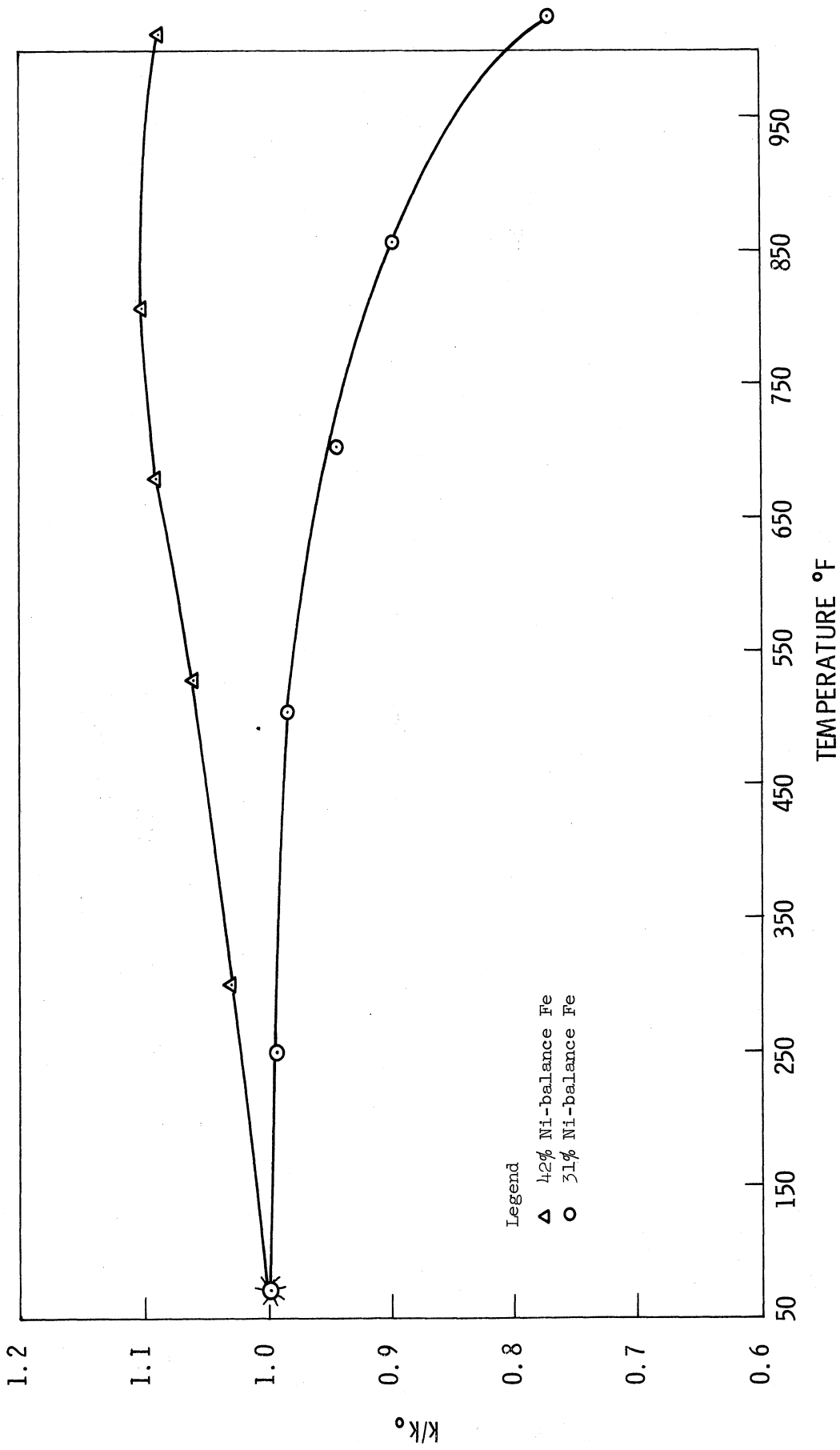
Fig. 35. Dimensionless ratio k/k_o versus temperature for 42% nickel-balance iron and 31% nickel-balance iron alloys.
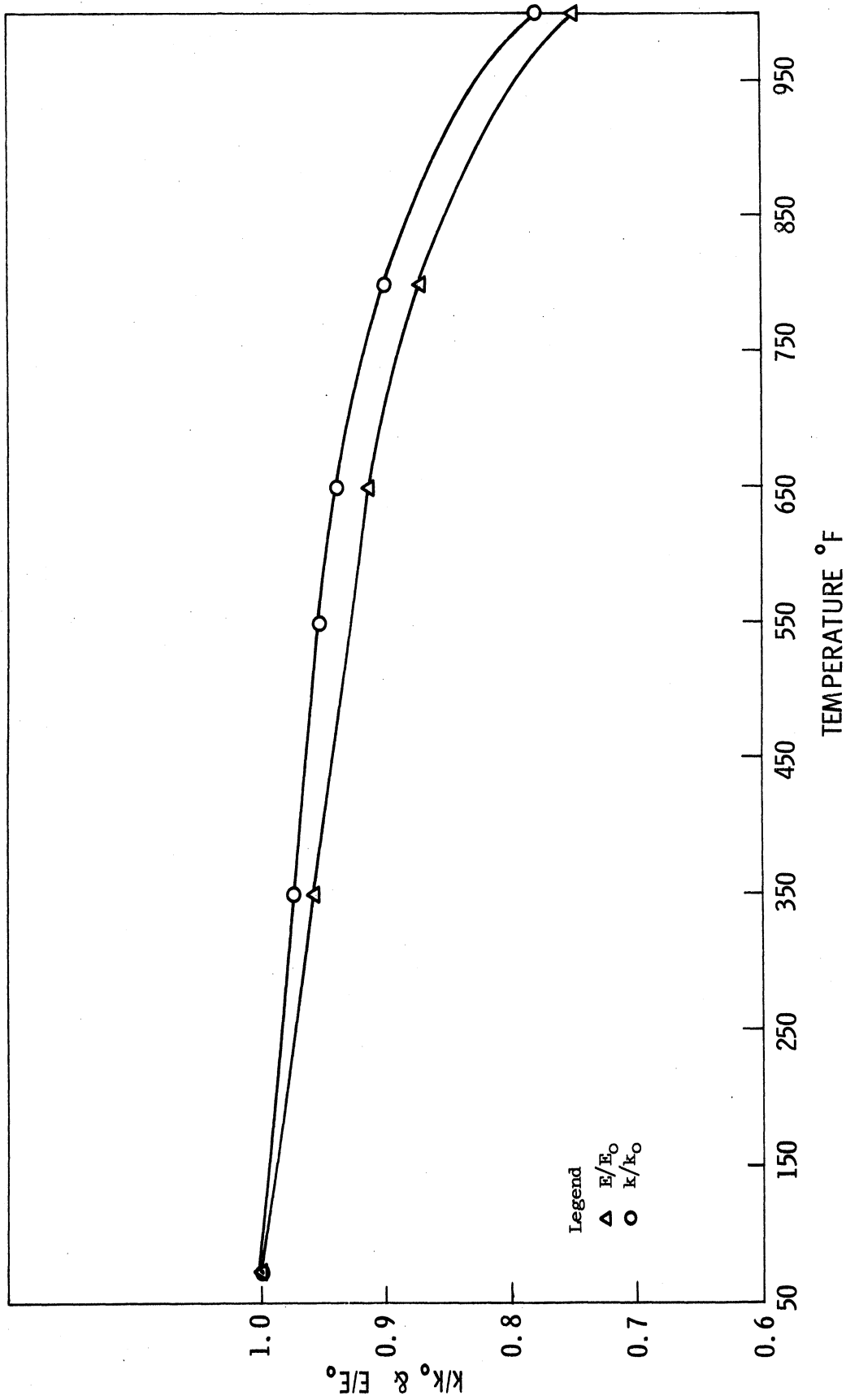
Fig. 36. Dimensionless ratios k/k_o and E/E_o versus temperature for 430 stainless steel where k_o and E_o are values at 70°F.

69
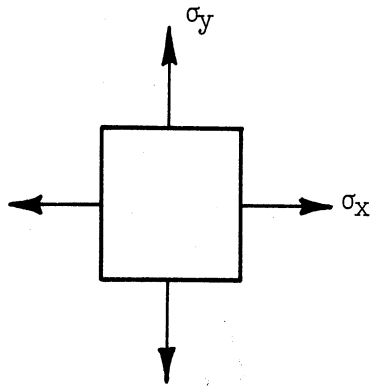
Fig. 37. Biaxial state of stress.

Fig. 38. Load versus deflection for 42% nickel-balance iron alloy washers.

Legend (within plot):

① h/t = 0.871   t = 0.031 in.
② h/t = 2.801   t = 0.031 in.
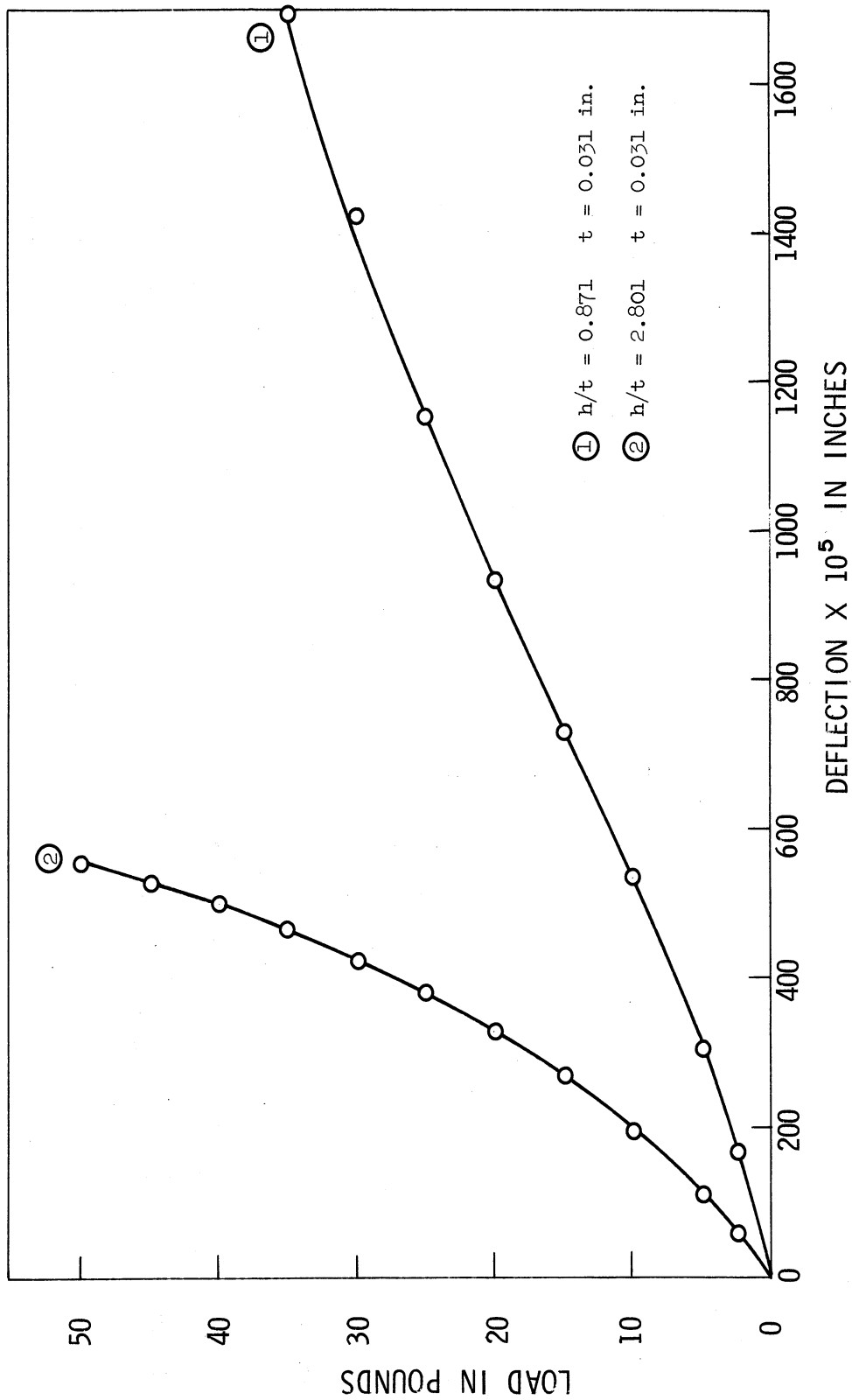
Axis labels:
DEFLECTION X 10^5 IN INCHES
LOAD IN POUNDS
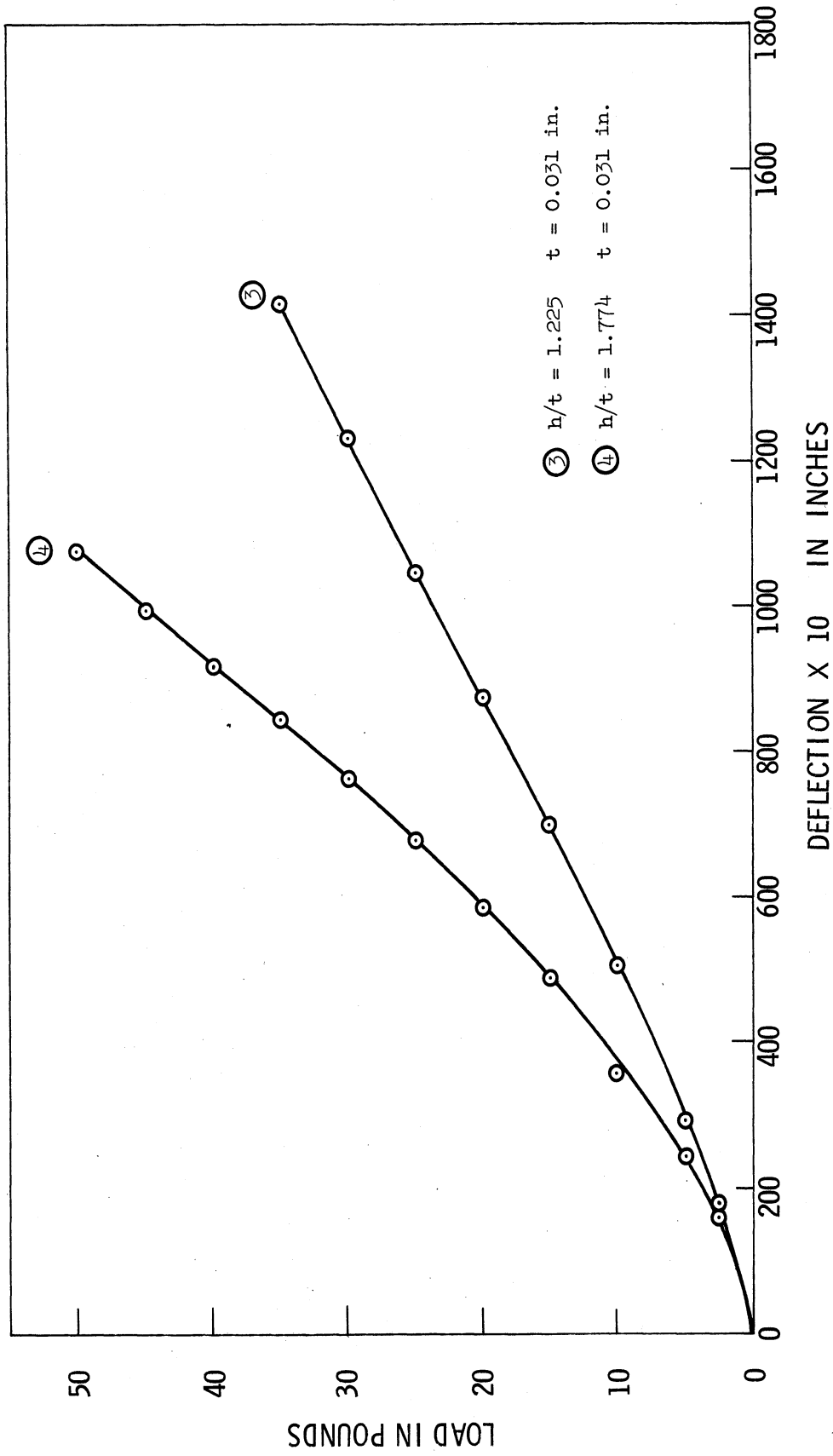
Fig. 39. Load versus deflection for 42% nickel-balance iron alloy washers.
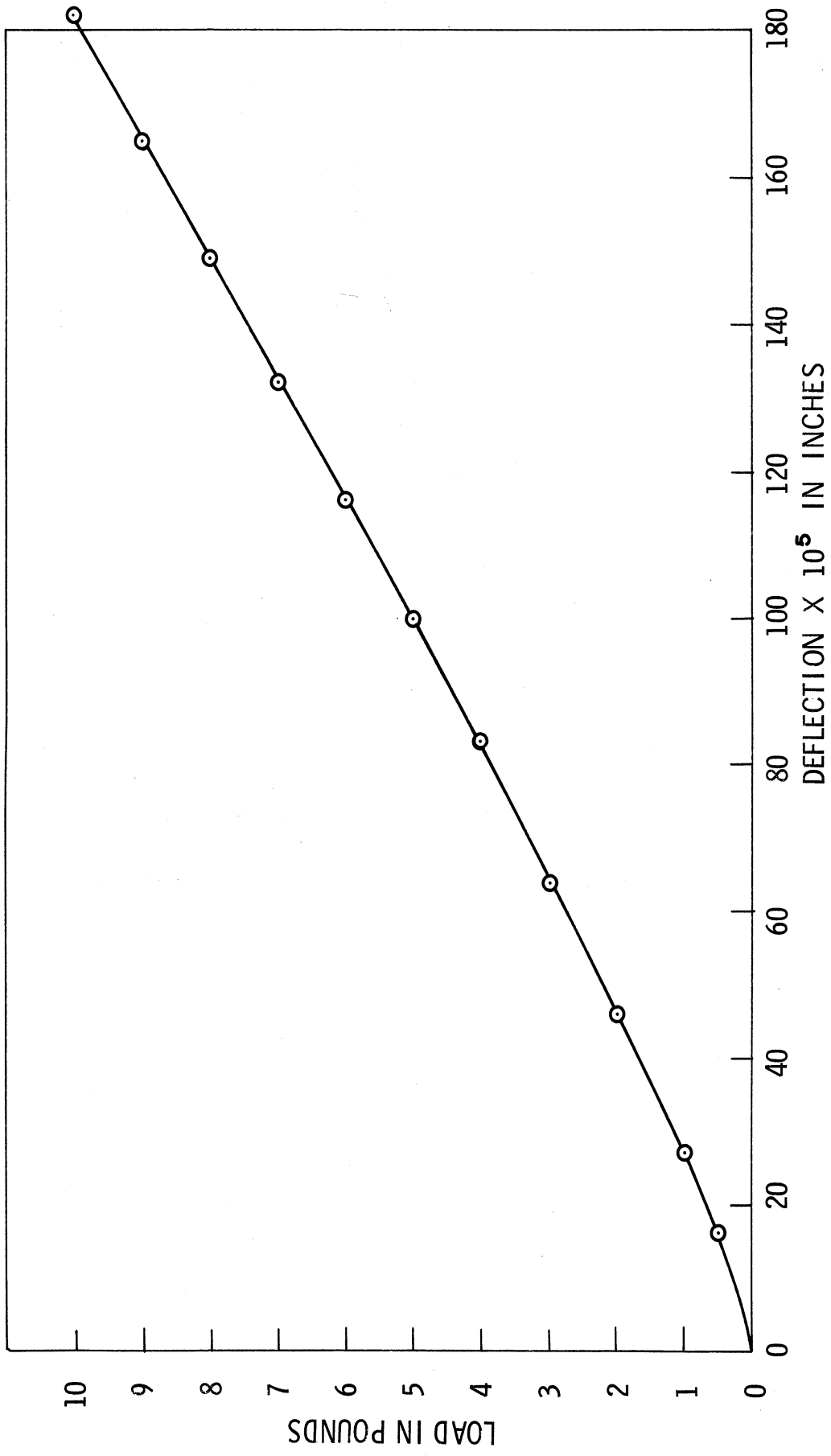
Fig. 40. Test load versus test fixture deflection for 5/16-in.-diameter pull rod, load cell "C."
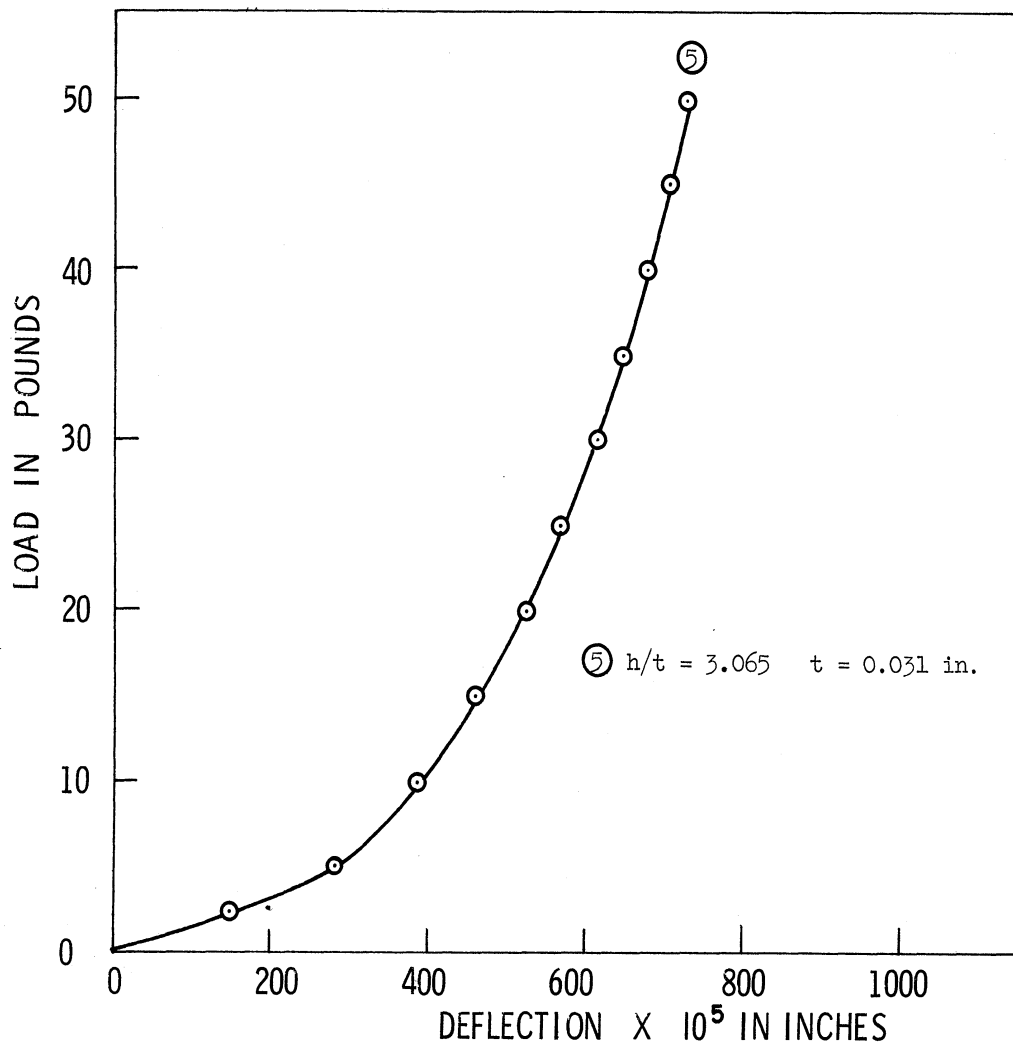
Fig. 41. Load versus deflection for 430 stainless steel washer at 70°F.
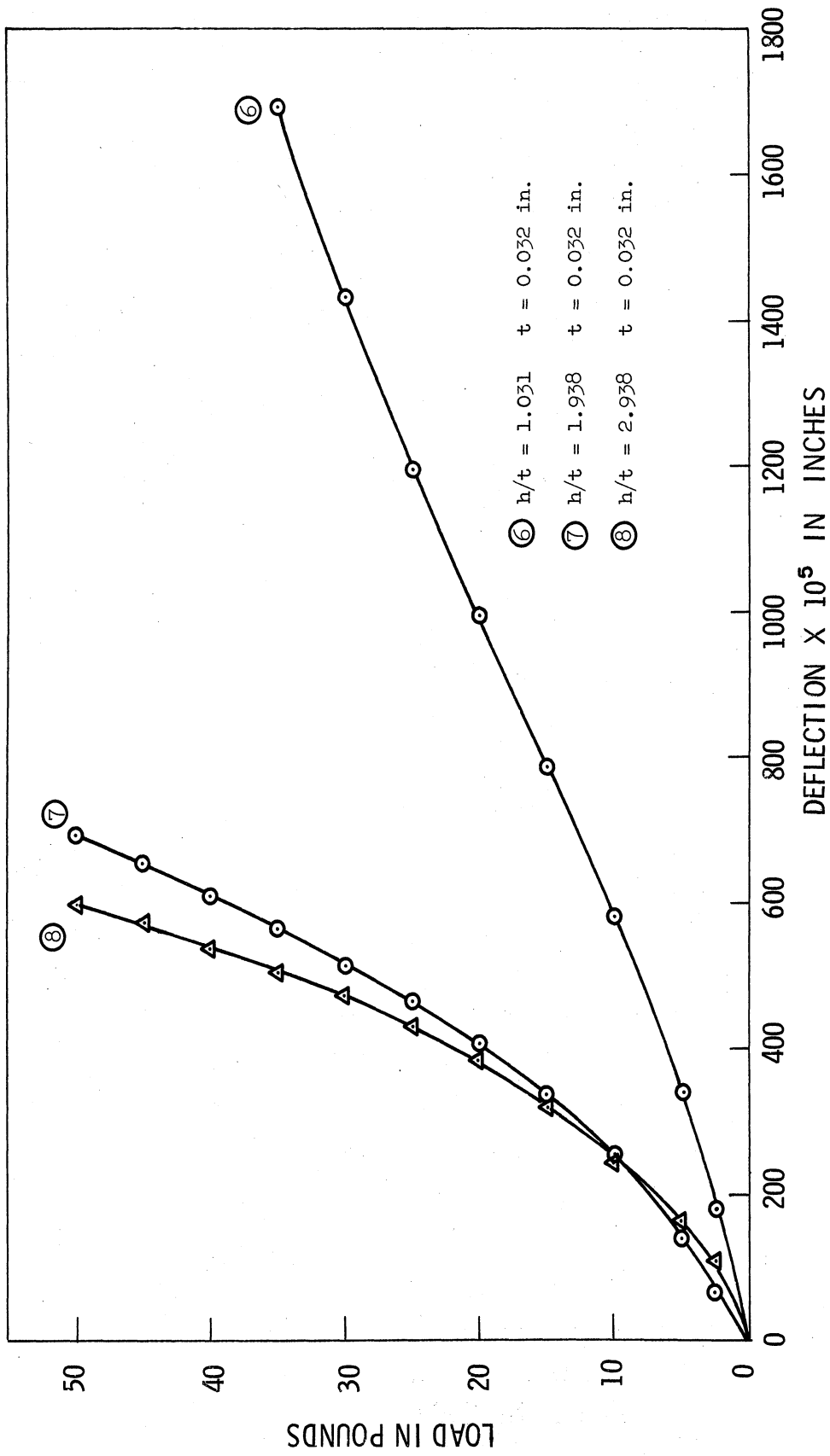
Chart labels:
- Y-axis: LOAD IN POUNDS (0, 10, 20, 30, 40, 50)
- X-axis: DEFLECTION X 10^5 IN INCHES (0, 200, 400, 600, 800, 1000)
- Legend: ⑤ h/t = 3.065 t = 0.031 in.

Fig. 42. Load versus deflection for 50% nickel-balance iron alloy washers at 70°F.

Legend (within figure):

⑥ h/t = 1.031   t = 0.032 in.
⑦ h/t = 1.938   t = 0.032 in.
⑧ h/t = 2.938   t = 0.032 in.

Axis labels:
DEFLECTION X 10^5 IN INCHES
LOAD IN POUNDS

Fig. 43. Load versus deflection for 304 stainless steel washers at 70°F.

9   h/t = 1.032   t = 0.031 in.

10   h/t = 1.871   t = 0.031 in.
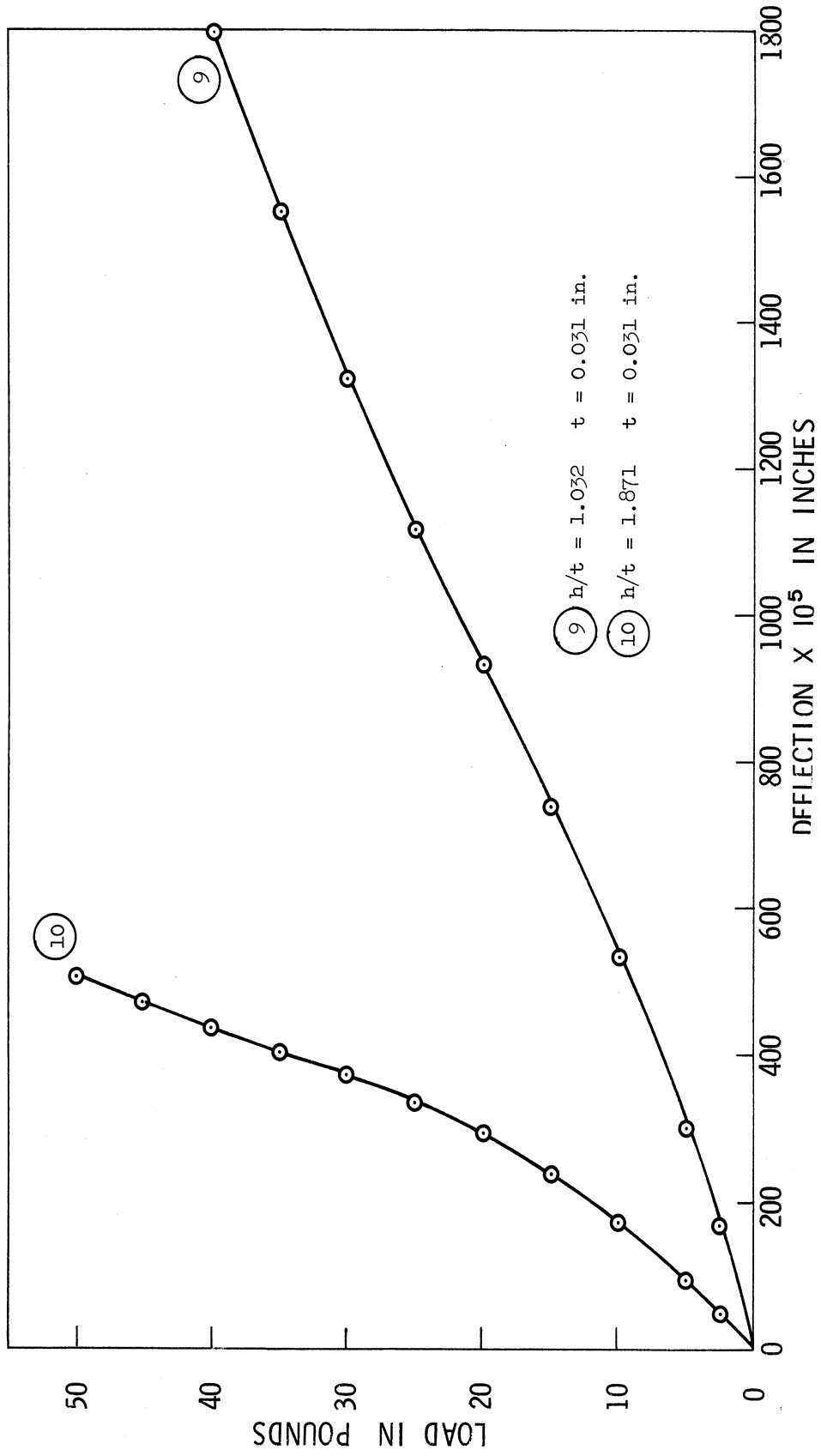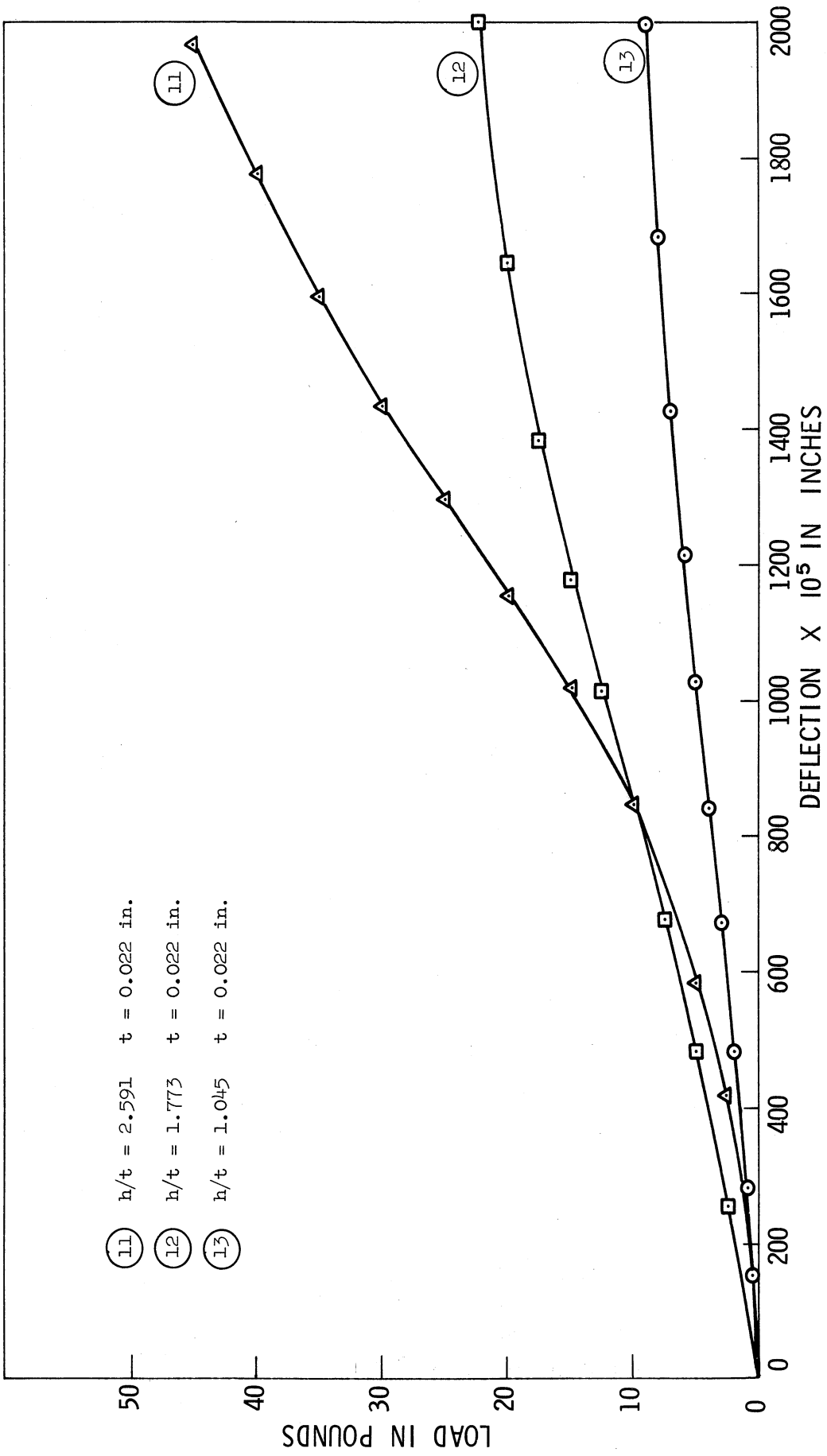
Fig. 44. Load versus deflection for 31% nickel-balance iron alloy washers at 70°F.

77
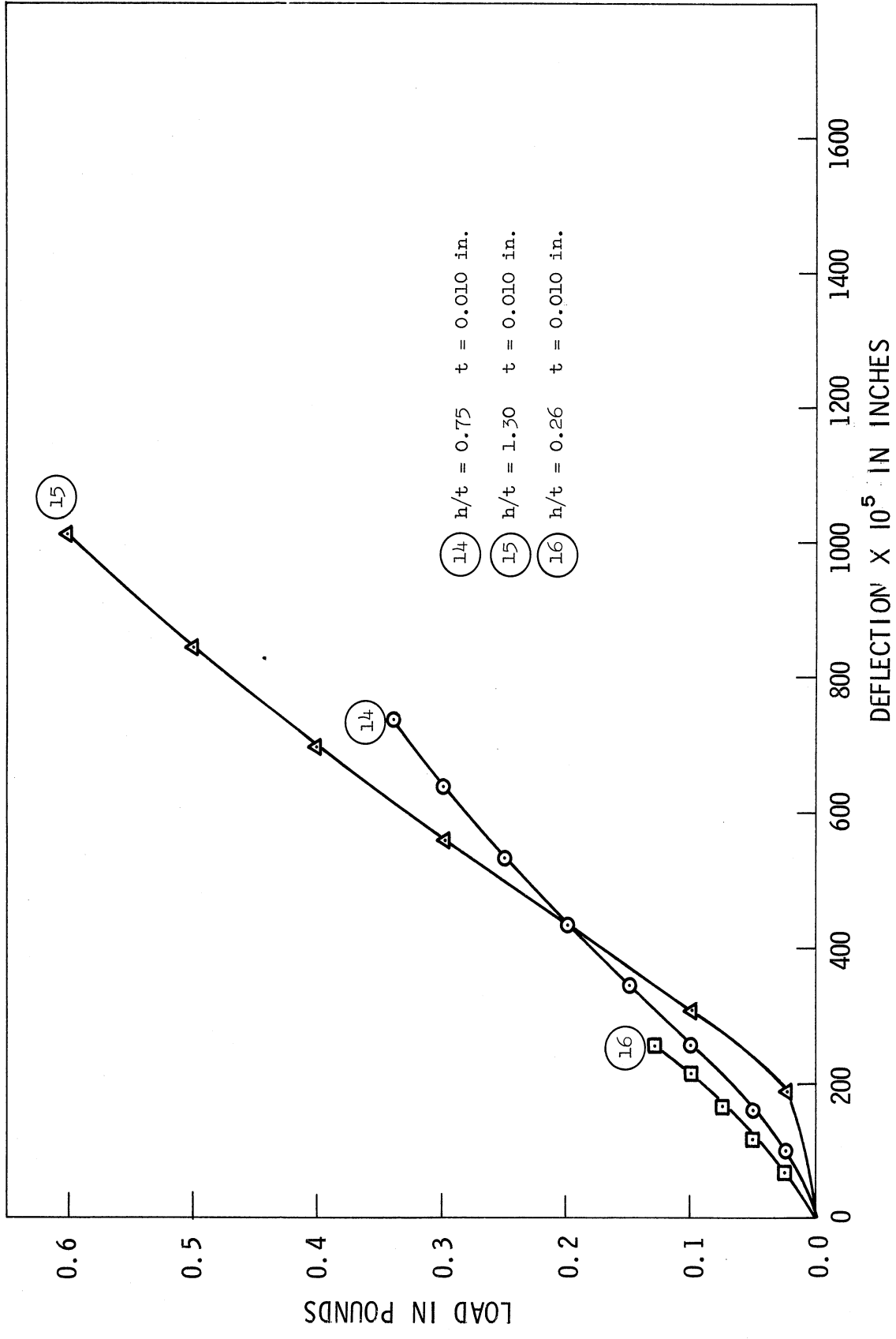
Fig. 45. Load versus deflection for 42% nickel-balance iron alloy washers at 70°F.
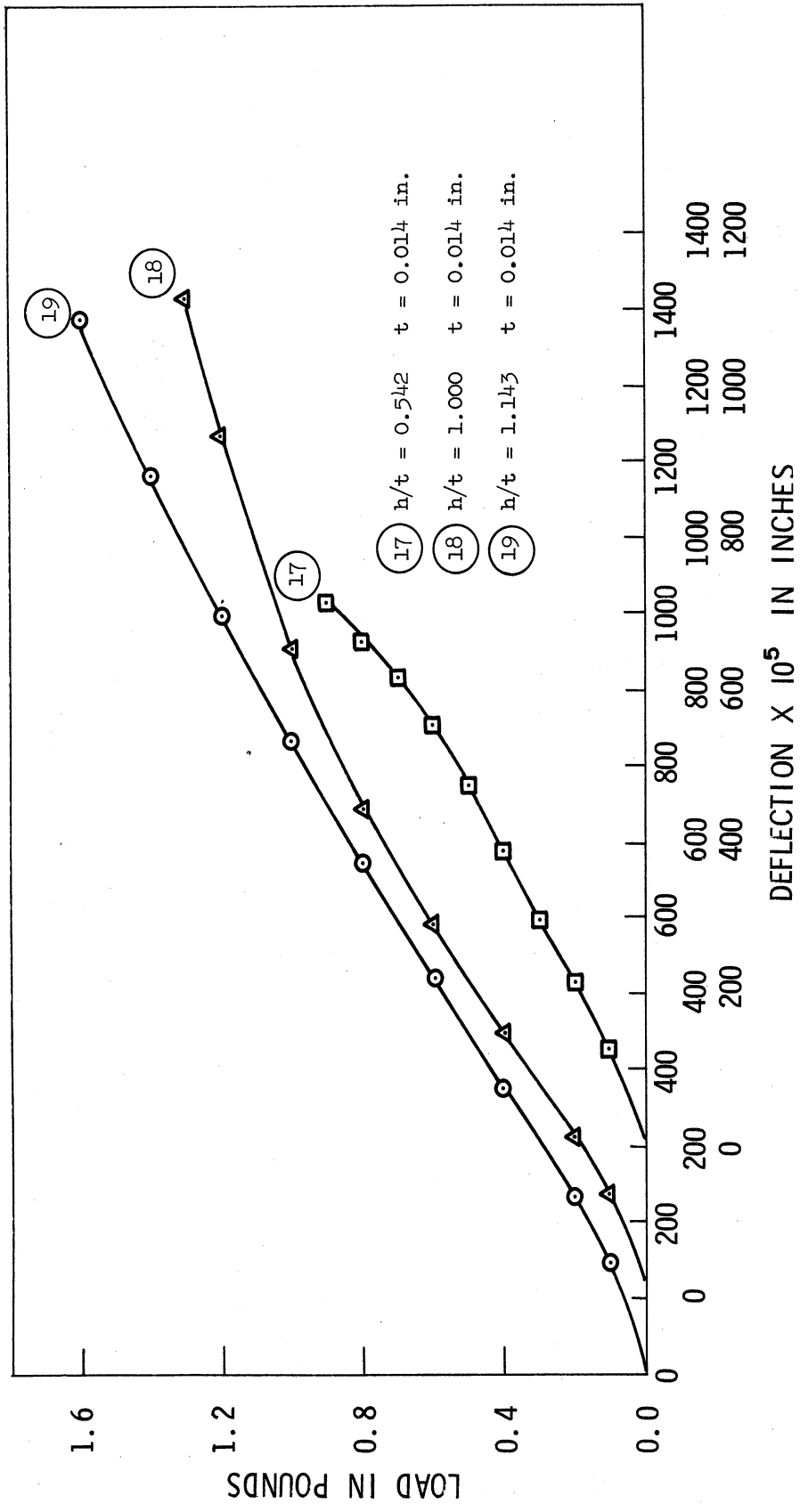
Fig. 46. Load versus deflection for 50% nickel-balance iron alloy washers at 70°F.
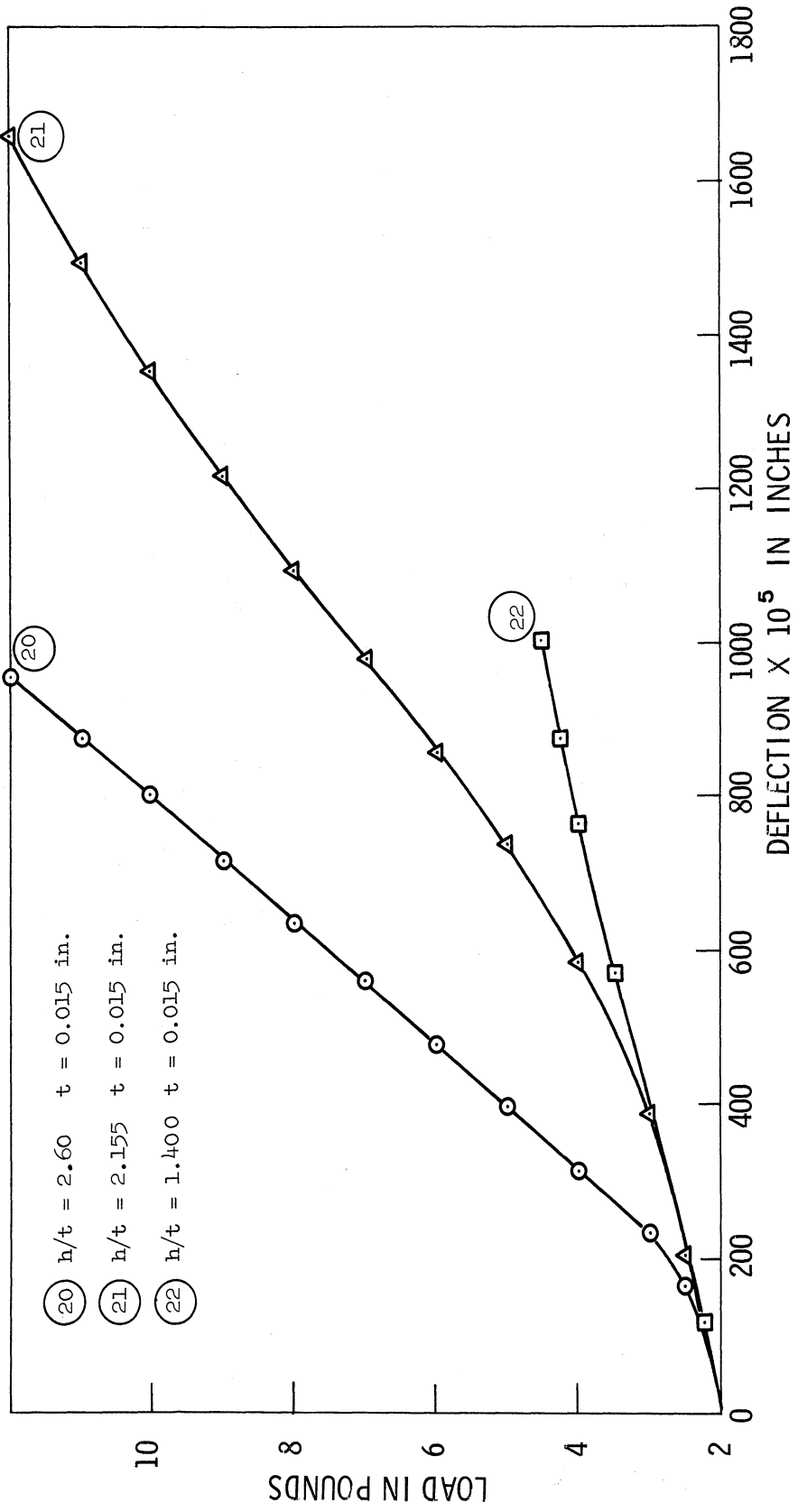
Fig. 47. Load versus deflection for 304 stainless steel washers at 70°F.

20	h/t = 2.60	t = 0.015 in.
21	h/t = 2.155	t = 0.015 in.
22	h/t = 1.400	t = 0.015 in.

DEFLECTION X 10^5 IN INCHES

LOAD IN POUNDS
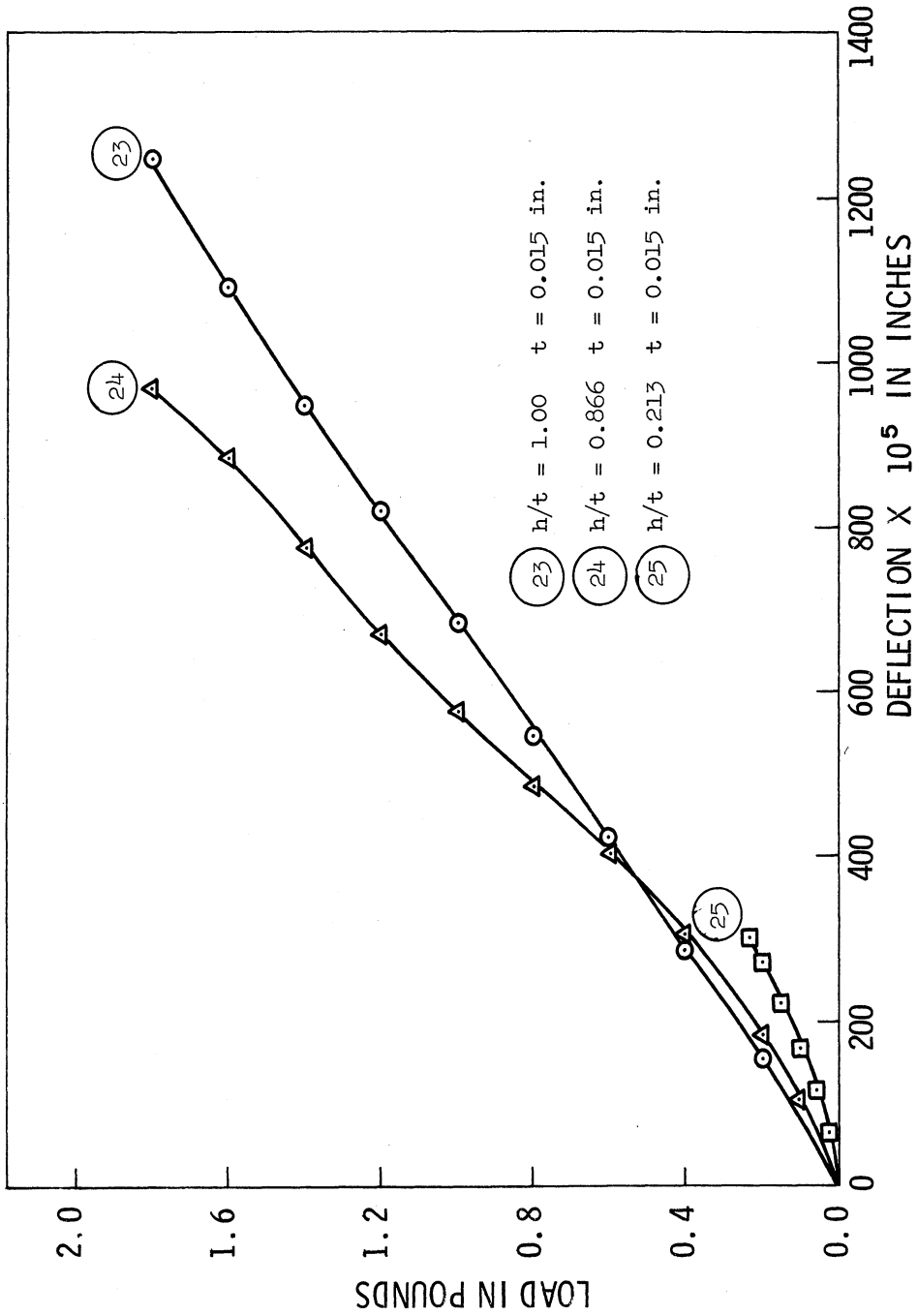
Fig. 48. Load versus deflection for 304 stainless steel washers at 70°F.
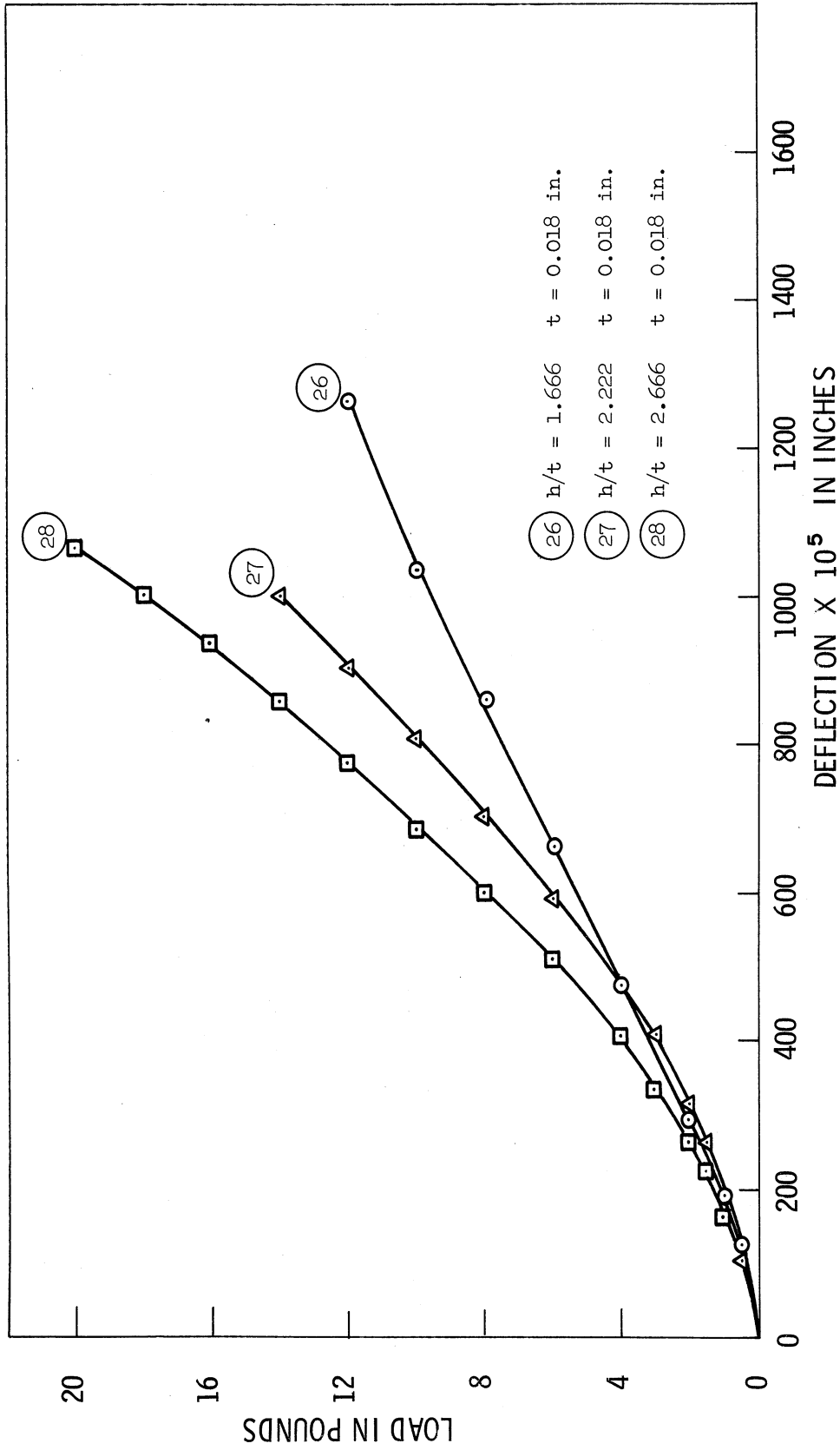
Fig. 49.   Load versus deflection for 430 stainless steel washers at 70°F.
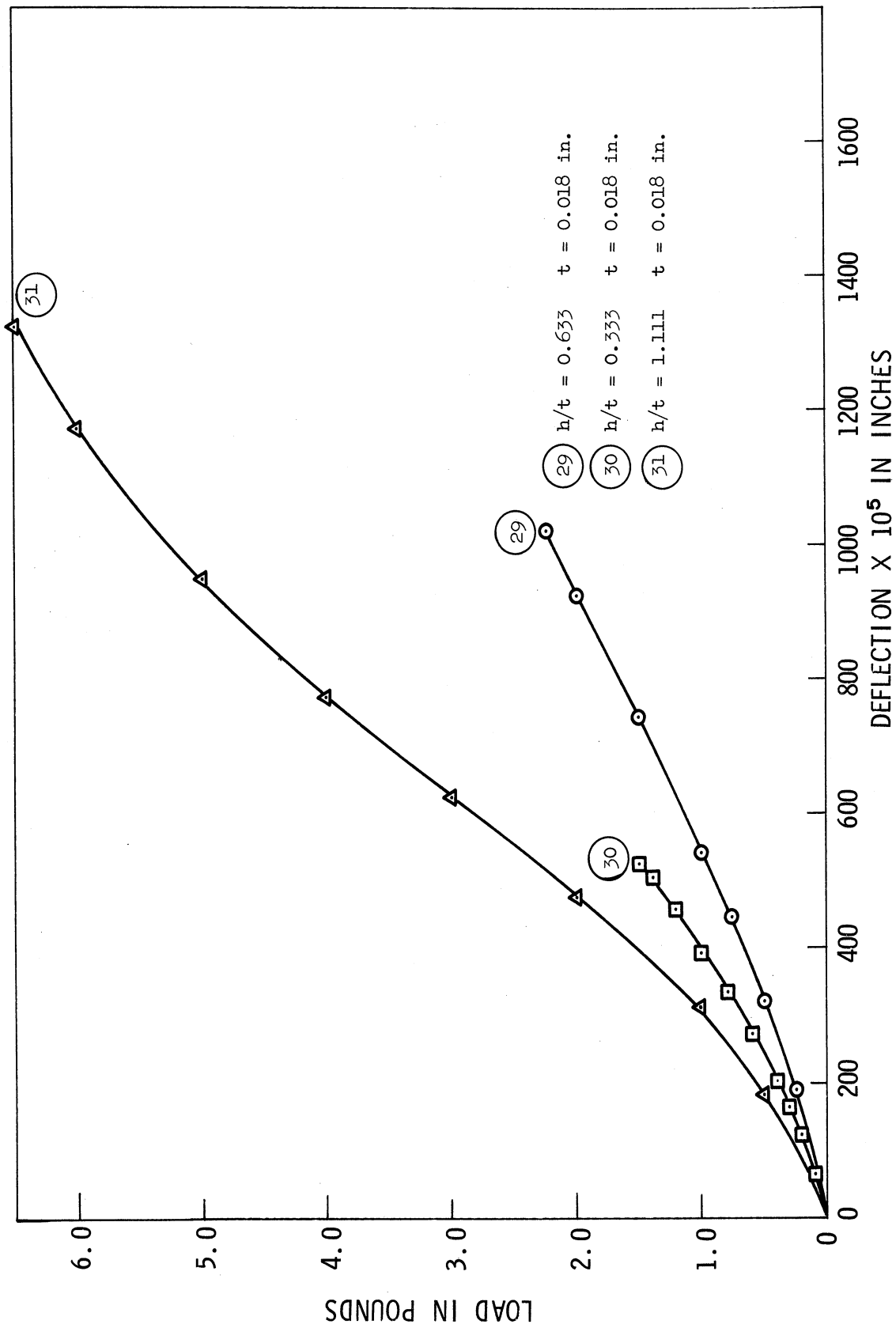
Fig. 50. Load versus deflection for 430 stainless steel washers at 70°F.
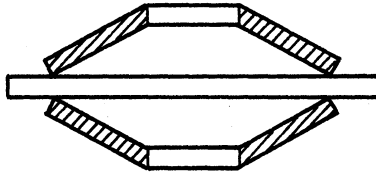
Fig. 51. Belleville spring washers stacked using spacer plates.
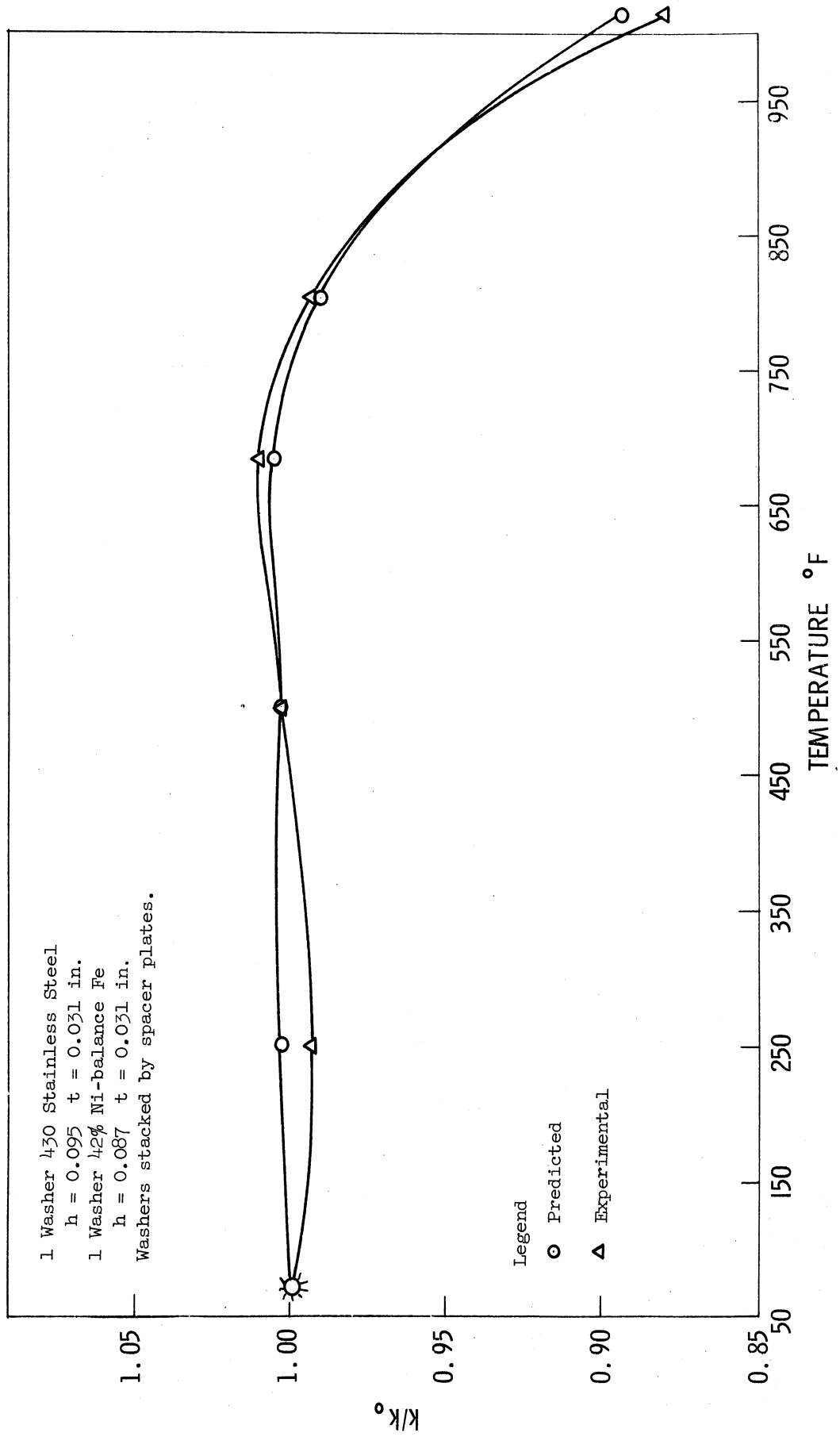
Fig. 52. k/k_O versus temperature for washer combinations using spacer plates.
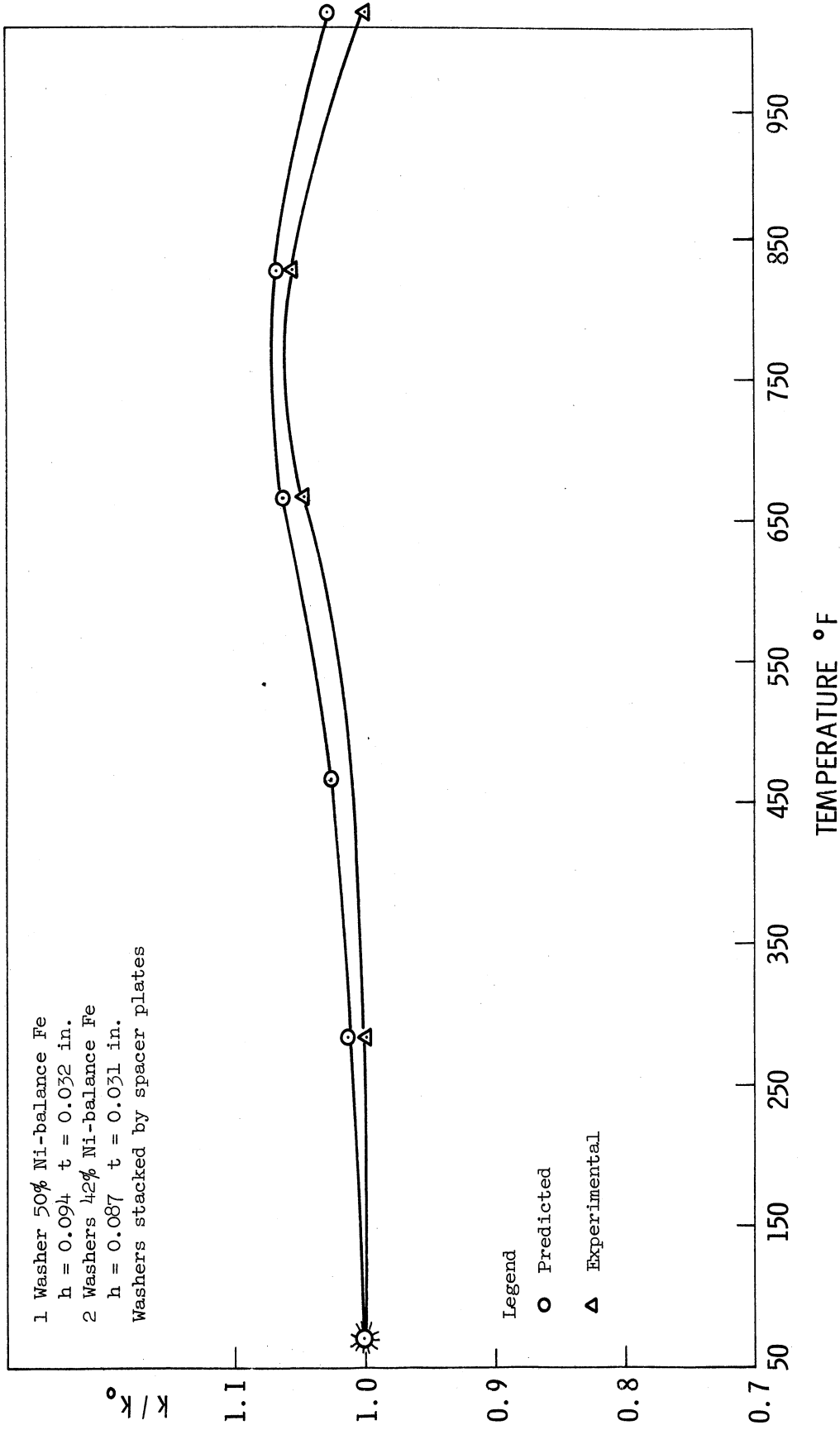
1 Washer 430 Stainless Steel
    h = 0.095   t = 0.031 in.
1 Washer 42% Ni-balance Fe
    h = 0.087   t = 0.031 in.
Washers stacked by spacer plates.

Legend
⊙ Predicted
◁ Experimental

TEMPERATURE °F

k/k_o

85

Fig. 53. k/k_0 versus temperature for washer combinations using spacer plates.

1 Washer 50% Ni-balance Fe
  h = 0.094 t = 0.032 in.
2 Washers 42% Ni-balance Fe
  h = 0.087 t = 0.031 in.
Washers stacked by spacer plates

Legend
O Predicted
△ Experimental

TEMPERATURE °F

k / k_0

86
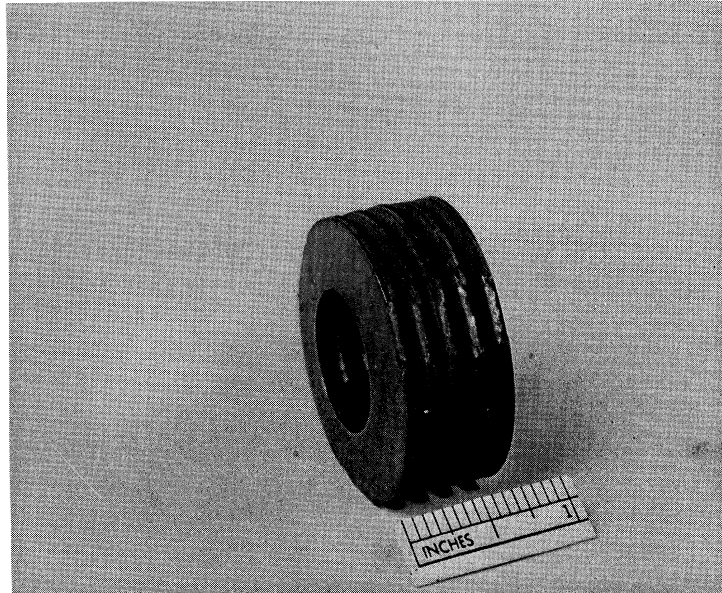
Fig. 54. Belleville spring washers stacked by means of welding.
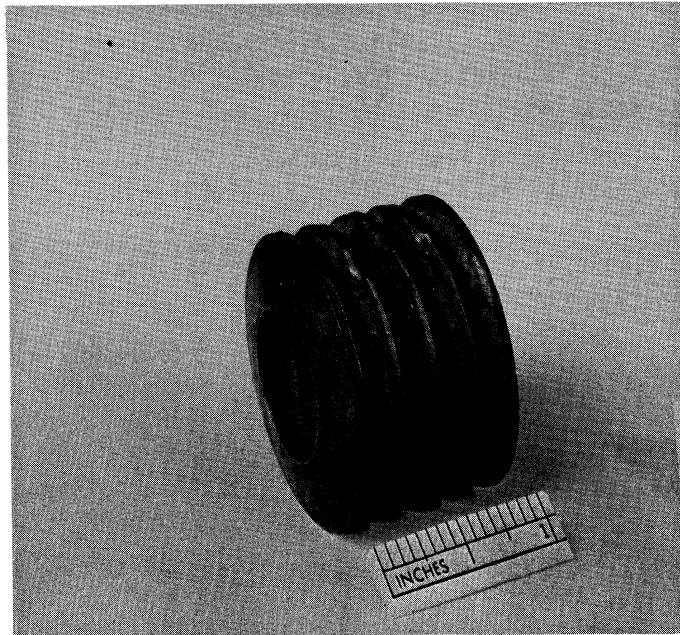
Fig. 55. Belleville spring washers stacked by means of welding.

6 Washers 42% Ni-balance Fe
  h = 0.087 t = 0.031 in.
4 Washers 430 Stainless Steel
  h = 0.095 t = 0.031 in.
All heat-treated 2 hr at 1200°F
Stack height after welding = 1.135 in.
Spot welded 3 places
Series stacked

Legend

○ Experimental

△ Predicted

k_O = 1678 lb/in. at 72°F
Max. deviation from room temperature value = 3.5%
Bimetal effect on two OD joints

k/k_O

TEMPERATURE °F

Fig. 56. k/k_O versus temperature for washer combinations stacked by means of welding.

5 Washers 42% Ni-balance Fe
  h = 0.087   t = 0.031 in.
4 Washers 430 Stainless Steel
  h = 0.095 t = 0.031 in.
1 Washer 50% Ni-balance Fe
  h = 0.094 t = 0.032 in.
All heat-treated 2 hr at 1200°F
Stack height after welding = 0.795 in.
Spot welded 3 places
Series stacked

k_0 = 1256 lb/in. at 72°F
Max. deviation from room temperature value = 3%
Bimetal effects on two OD joints

Fig. 57. k/k_0 versus temperature for washer combinations stacked by means of welding.

89

6 Washers 42% Ni-balance Fe
  h = 0.087 t = 0.031 in.
4 Washers 304 Stainless Steel
  h = 0.093 t = 0.031 in.
All heat-treated 2 hr at 1200°F
Stack height after welding = 0.805 in.
Spot welded 3 places
Series stacked

k_o = 1591 lb/in at 72°F
Max. deviation from room temperature value = 4.0%
No bimetal effect

Fig. 58. k/k_o versus temperature for washer combinations stacked by means of welding.

4 Washers 42% Ni-balance Fe
    h = 0.087 t = 0.031 in.
4 Washers 50% Ni-balance Fe
    h = 0.094 t = 0.032 in.
All heat-treated 1 hr at 1000°F
Stack height after welding = 0.860 in.
Continuous welding joints
Series stacked

k_O = 4192 lb/in. at 72°F
Max. deviation from room temperature value = 7.8%
No bimetal effect
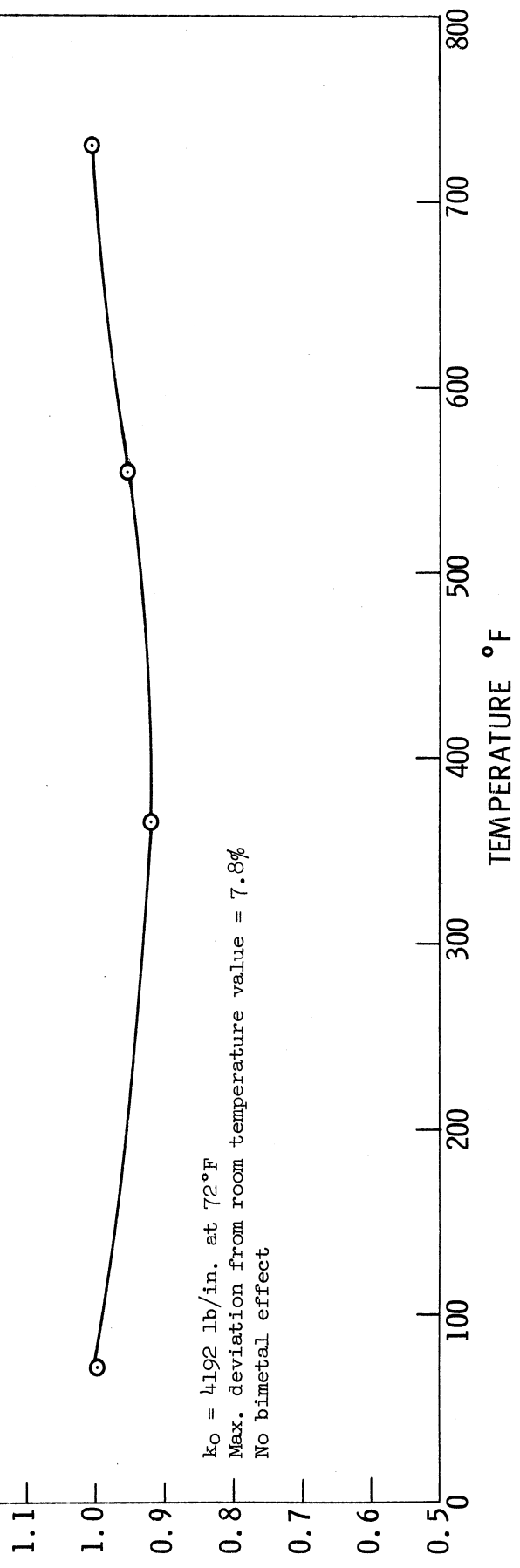
TEMPERATURE °F

Fig. 59. k/k_O versus temperature for washer combinations stacked by means of welding.
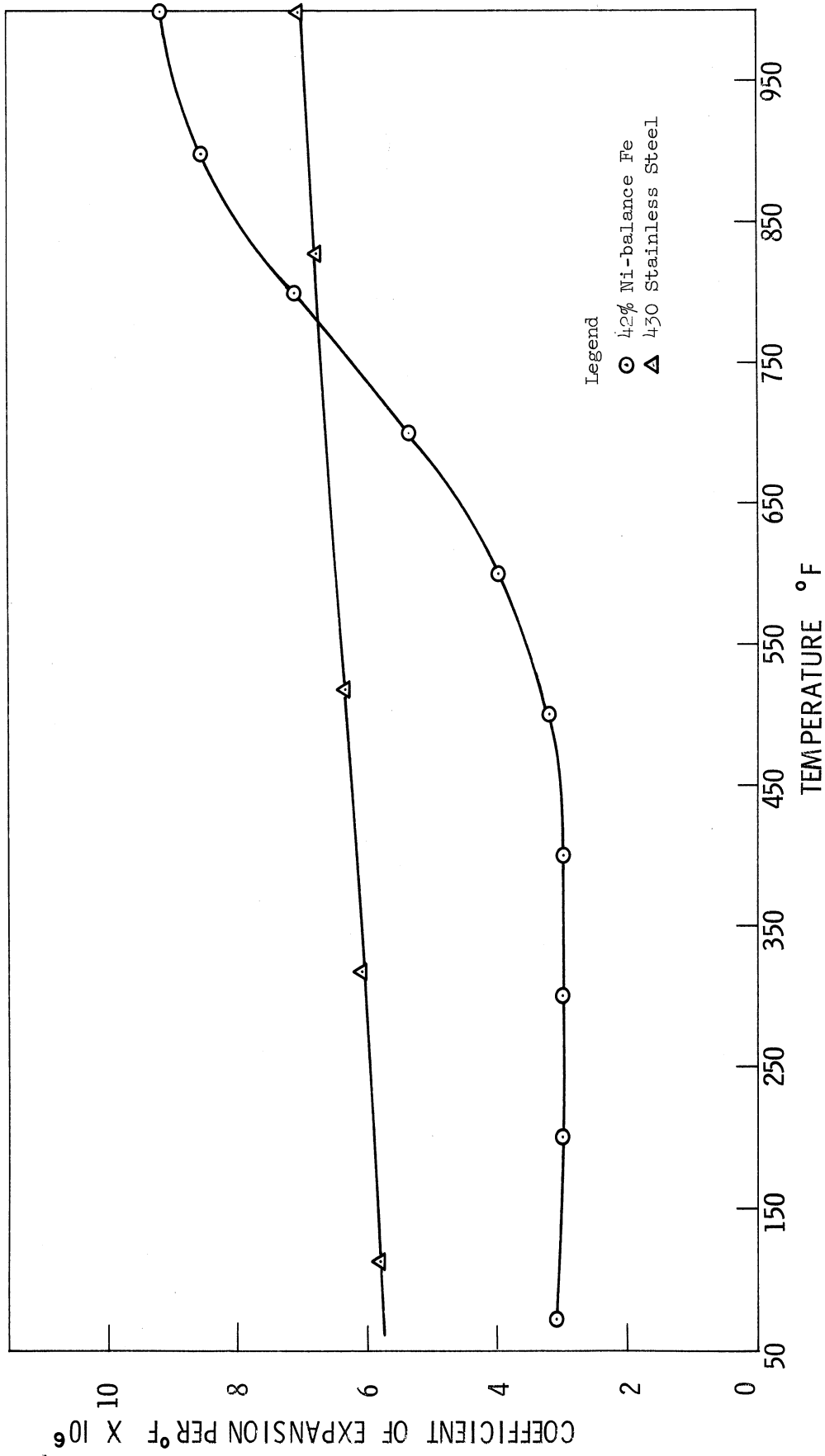
Fig. 60. Coefficients of thermal expansion versus temperature for 430 stainless steel and 42% nickel-balance iron alloy.

Fig. 61. Bimetal system composed of Inconel X thin-walled tubing 0.09375 in. ID, 0.119 in. OD with core 40% nickel-balance iron alloy 0.09375 in. diameter. Outside diameter 1.0 in., n = 9-1/2. View before test.
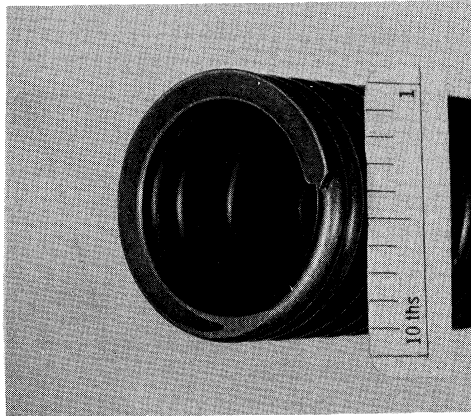
Fig. 62. End detail of Inconel X—40% nickel-balance iron alloy bimetal tube-core configuration. Note core and jacket.
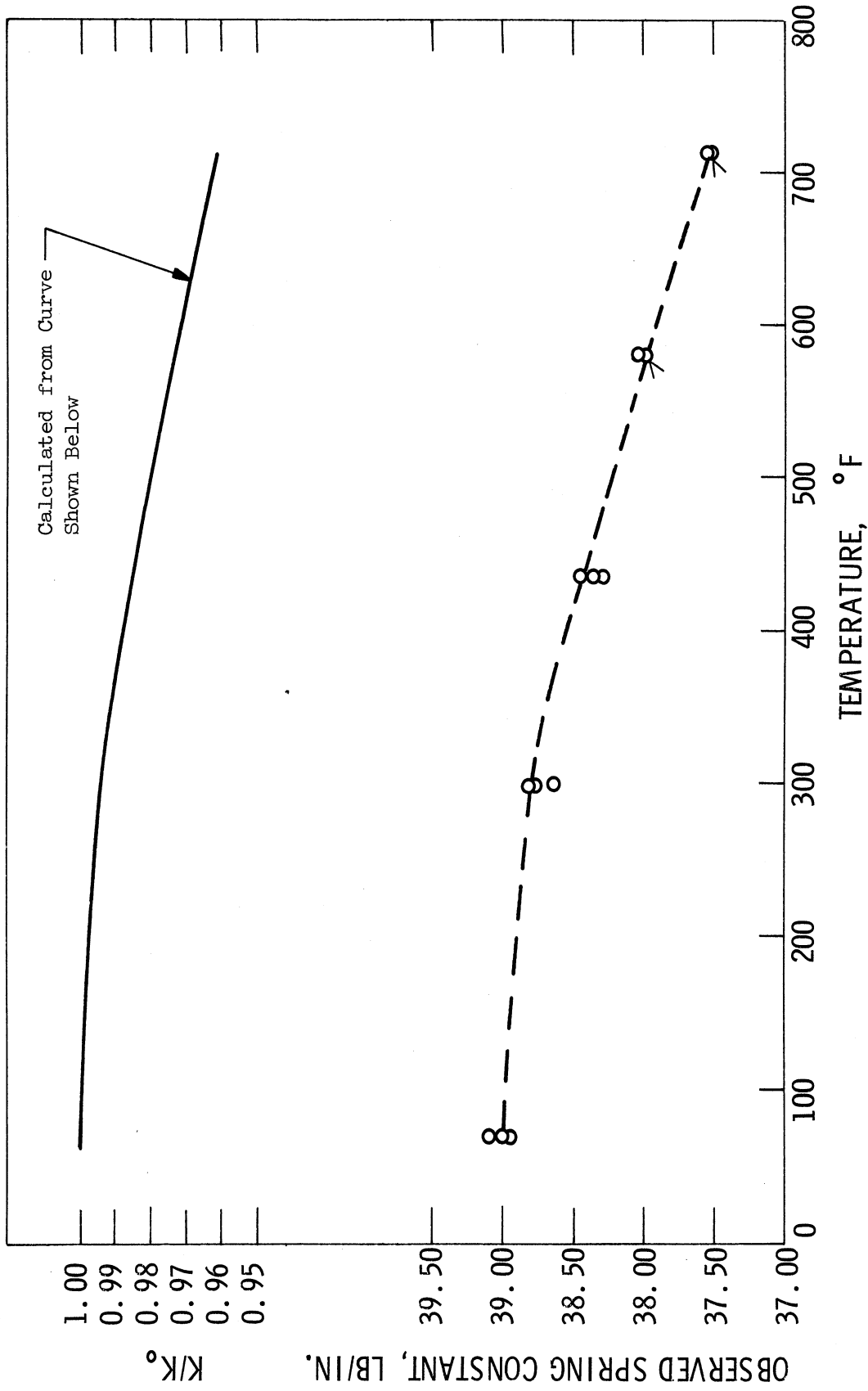
Fig. 63. Spring constant versus temperature for Inconel X—40% nickel-balance iron alloy tube-core configuration coil spring. Initial heat treatment at 1200°F for 2 hours.

O. D. - OUTSIDE DIAMETER
D   - MEAN COIL DIAMETER
I. D. -. INSIDE DIAMETER
d   - WIRE DIAMETER
p   - PITCH
L   - FREE LENGTH
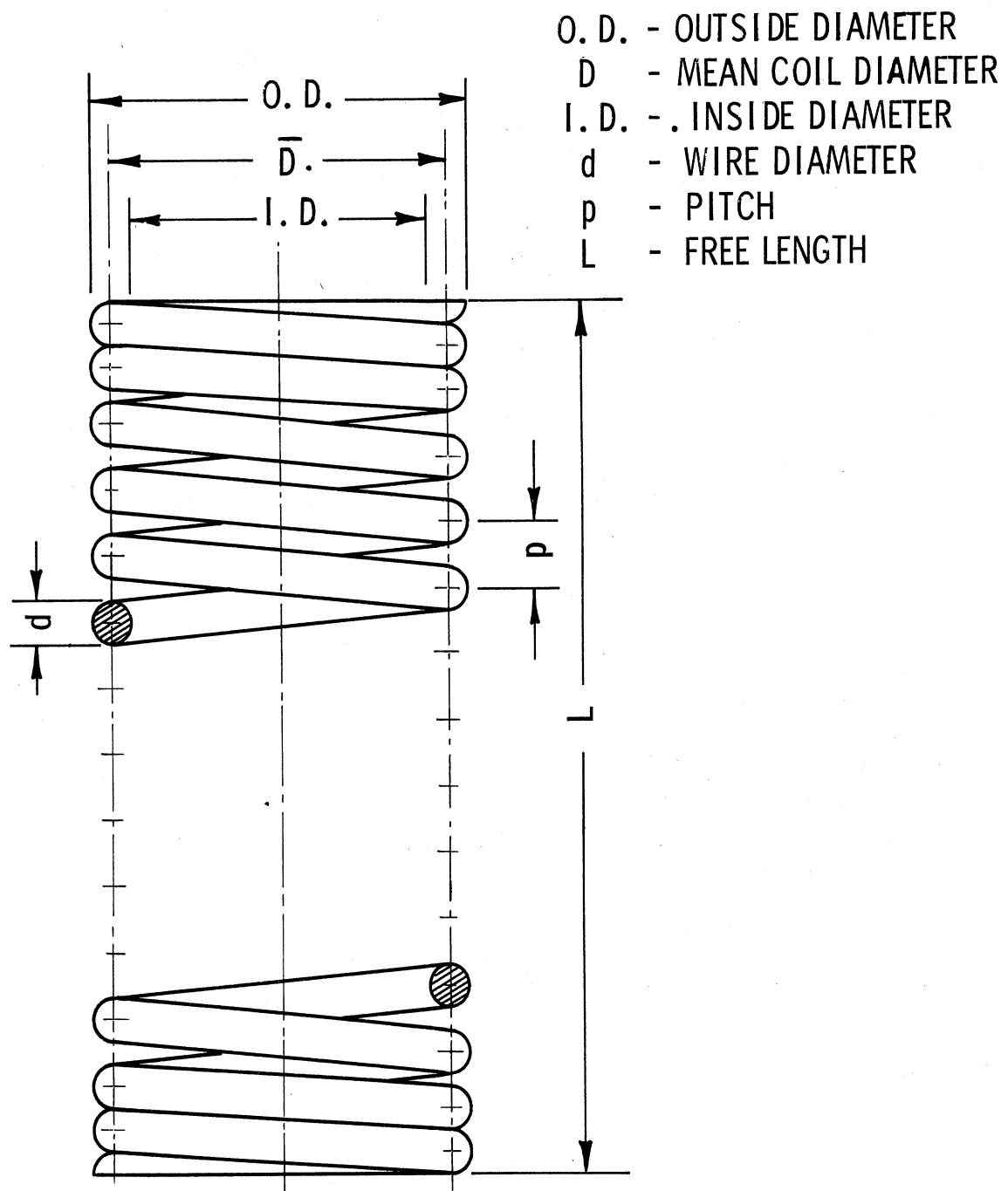
Fig. 64. Coil spring definition sketch.

Fig. 66. Shear modulus testing at -110°F.
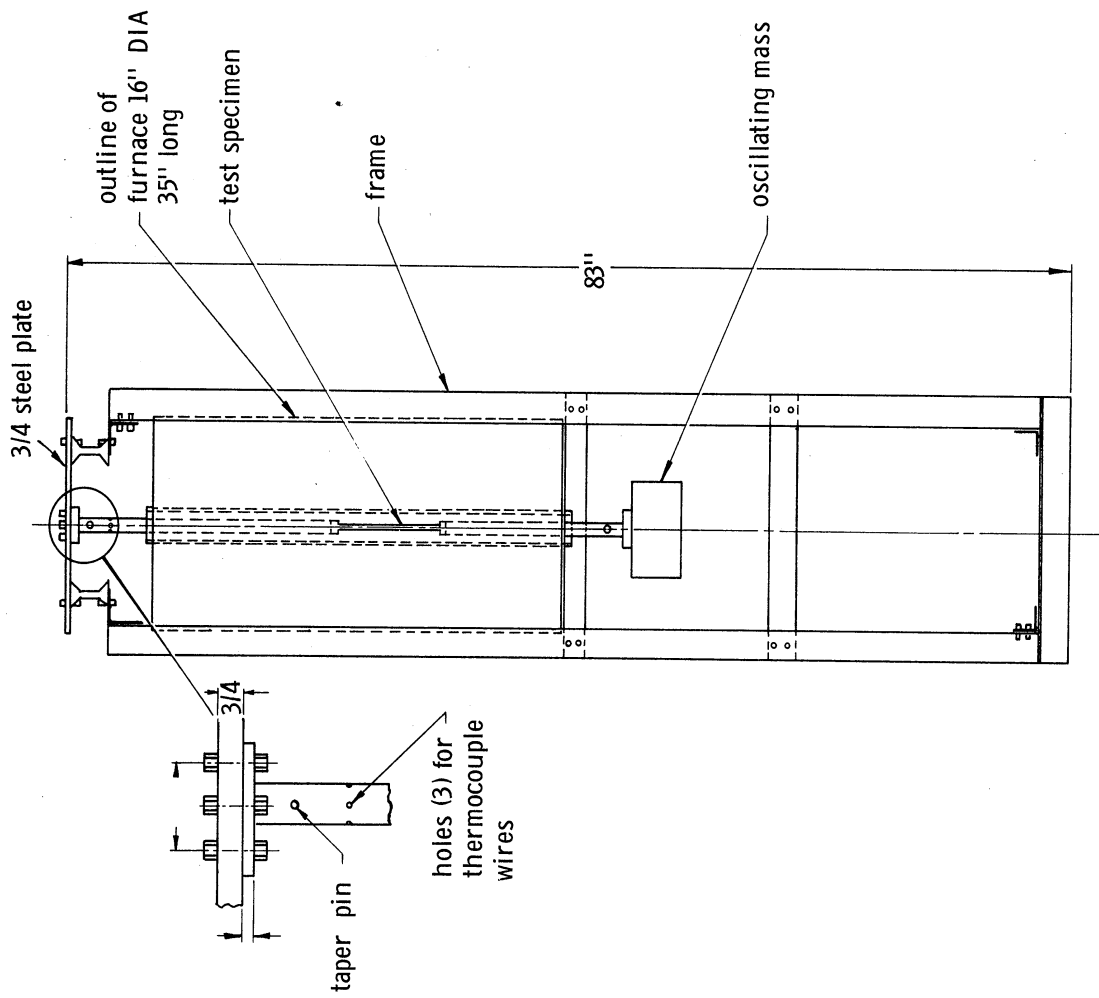
Fig. 65. Schematic diagram of torsion pendulum apparatus.

96

THE UNIVERSITY OF MICHIGAN, Ann Arbor, Michigan. WIDE-RANGE-TEMPERATURE SPRINGS, by J. Ormondroyd, H.E. Gascoigne, J.H. Enns, and P. G. Kessel. 97 p. incl. figs., tables, and refs. (Project 9-(8-7360); (Task 73605)(ASD TR 61-566)(Contract No. AF 33(616)-6284).

UNCLASSIFIED REPORT

Bimetallic spring systems of 40% nickel-60% iron alloy combined with Inconel-X and type 304 stainless steel exhibit characteristics suitable for applications from -65°F to 600°F. In this range the spring constant is held within +0.25%.

The general theory of bimetallic, temperature independent helical coil and Belleville type springs is presented. The bimetallic

(over)

systems tested show that a temperature independent spring is feasible although working stresses must be maintained at relatively low levels.

AF-WP-B-JUL 61 1M

THE UNIVERSITY OF MICHIGAN, Ann Arbor, Michigan. WIDE-RANGE-TEMPERATURE SPRINGS, by J. Ormondroyd, H.E. Gascoigne, J.H. Enns, and P. G. Kessel. 97 p. incl. figs., tables, and refs. (Project 9-(8-7360); (Task 73605)(ASD TR 61-566)(Contract No. AF 33(616)-6284).

UNCLASSIFIED REPORT

Bimetallic spring systems of 40% nickel-60% iron alloy combined with Inconel-X and type 304 stainless steel exhibit characteristics suitable for applications from -65°F to 600°F. In this range the spring constant is held within $\pm 0.25\%$.

The general theory of bimetallic, temperature independent helical coil and Belleville type springs is presented. The bimetallic

(over)

systems tested show that a temperature independent spring is feasible although working stresses must be maintained at relatively low levels.

AF-WP-B-JUL 61 1M

THE UNIVERSITY OF MICHIGAN, Ann Arbor, Michigan. WIDE-RANGE-TEMPERATURE SPRINGS, by J. Ormondroyd, H.E. Gascoigne, J.H. Enns, and P. G. Kessel. 97 p. incl. figs., tables, and refs. (Project 9-(8-7360); (Task 73605)(ASD TR 61-566)(Contract No. AF 33(616)-6284).

UNCLASSIFIED REPORT

Bimetallic spring systems of 40% nickel-60% iron alloy combined with Inconel-X and type 304 stainless steel exhibit characteristics suitable for applications from -65°F to 600°F. In this range the spring constant is held within +0.25%.

The general theory of bimetallic, temperature independent helical coil and Belleville type springs is presented. The bimetallic

(over)

systems tested show that a temperature independent spring is feasible although working stresses must be maintained at relatively low levels.

AF-WP-B-JUL 61 1M

THE UNIVERSITY OF MICHIGAN, Ann Arbor, Michigan. WIDE-RANGE-TEMPERATURE SPRINGS, by J. Ormondroyd, H.E. Gascoigne, J.H. Enns, and P. G. Kessel. 97 p. incl. figs., tables, and refs. (Project 9-(8-7360); (Task 73605)(ASD TR 61-566)(Contract No. AF 33(616)-6284).

UNCLASSIFIED REPORT

. Bimetallic spring systems of 40% nickel-60% iron alloy combined with Inconel-X and type 304 stainless steel exhibit characteristics suitable for applications from -65°F to 600°F. In this range the spring constant is held within +0.25%.

The general theory of bimetallic, temperature independent helical coil and Belleville type springs is presented. The bimetallic

(over)

systems tested show that a temperature independent spring is feasible although working stresses must be maintained at relatively low levels.

AF-WP-B-JUL 61 1M